J. F. JAMES

A Student's Guide to
Fourier Transforms

With Applications in
Physics and Engineering

THIRD EDITION
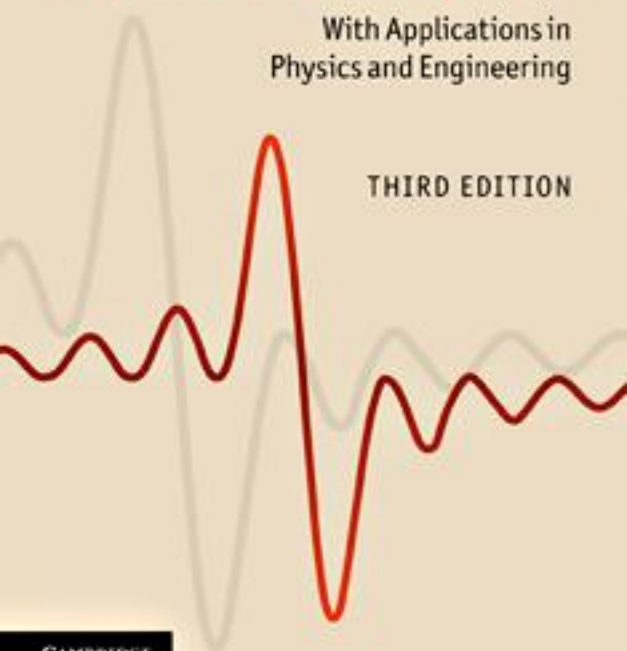
This page intentionally left blank

A Student's Guide to Fourier Transforms

Fourier transform theory is of central importance in a vast range of applications in physical science, engineering and applied mathematics. Providing a concise introduction to the theory and practice of Fourier transforms, this book is invaluable to students of physics, electrical and electronic engineering and computer science.

After a brief description of the basic ideas and theorems, the power of the technique is illustrated through applications in optics, spectroscopy, electronics and telecommunications. The rarely discussed but important field of multi-dimensional Fourier theory is covered, including a description of Computerized Axial Tomography (CAT) scanning. The book concludes by discussing digital methods, with particular attention to the Fast Fourier Transform and its implementation.

This new edition has been revised to include new and interesting material, such as convolution with a sinusoid, coherence, the Michelson stellar interferometer and the van Cittert–Zernike theorem, Babinet's principle and dipole arrays.

J. F. JAMES is a graduate of the University of Wales and the University of Reading. He has held teaching positions at the University of Minnesota, The Queen's University, Belfast and the University of Manchester, retiring as Senior Lecturer in 1996. He is a Fellow of the Royal Astronomical Society and a member of the Optical Society of America and the International Astronomical Union. His research interests include the invention, design and construction of astronomical instruments and their use in astronomy, cosmology and upper-atmosphere physics. Dr James has led eclipse expeditions to Central America, the central Sahara and the South Pacific Islands. He is the author of about 40 academic papers, co-author with R. S. Sternberg of *The Design of Optical Spectrometers* (Chapman & Hall, 1969) and author of *Spectrograph Design Fundamentals* (Cambridge University Press, 2007).

A Student's Guide to Fourier Transforms

with Applications in Physics and Engineering

Third Edition

J. F. JAMES

Contents

Preface to the first edition

Showing a Fourier transform to a physics student generally produces the same reaction as showing a crucifix to Count Dracula. This may be because the subject tends to be taught by theorists who themselves use Fourier methods to solve otherwise intractable differential equations. The result is often a heavy load of mathematical analysis.

This need not be so. Engineers and practical physicists use Fourier theory in quite another way: to treat experimental data, to extract information from noisy signals, to design electrical filters, to 'clean' TV pictures and for many similar practical tasks. The transforms are done digitally and there is a minimum of mathematics involved.

The chief tools of the trade are the theorems in Chapter 2, and an easy familiarity with these is the way to mastery of the subject. In spite of the forest of integration signs throughout the book there is in fact very little integration done and most of that is at high-school level. There are one or two excursions in places to show the breadth of power that the method can give. These are not pursued to any length but are intended to whet the appetite of those who want to follow more theoretical paths.

The book is deliberately incomplete. Many topics are missing and there is no attempt to explain everything: but I have left, here and there, what I hope are tempting clues to stimulate the reader into looking further; and of course, there is a bibliography at the end.

Practical scientists sometimes treat mathematics in general, and Fourier theory in particular, in ways quite different from those for which it was invented.[1] The late E. T. Bell, mathematician and writer on mathematics, once described mathematics in a famous book title as 'The Queen and Servant of Science'.

---

[1] It is a matter of philosophical disputation whether mathematics is invented or discovered. Let us compromise by saying that theorems are discovered; proofs are invented.

The queen appears here in her role as servant and is sometimes treated quite roughly in that role, and furthermore, without apology. We are fairly safe in the knowledge that mathematical functions which describe phenomena in the real world are 'well-behaved' in the mathematical sense. Nature abhors singularities as much as she does a vacuum.

When an equation has several solutions, some are discarded in a most cavalier fashion as 'unphysical'. This is usually quite right.[2] Mathematics is after all only a concise shorthand description of the world and if a position-finding calculation based, say, on trigonometry and stellar observations, gives two results, equally valid, that you are either in Greenland or Barbados, you are entitled to discard one of the solutions if it is snowing outside. So we use Fourier transforms as a guide to what is happening or what to do next, but we remember that for solving practical problems the blackboard-and-chalk diagram, the computer screen and the simple theorems described here are to be preferred to the precise tedious calculations of integrals.

Manchester, January 1994   J. F. James

---

[2] But Dirac's equation, with its positive and negative roots, predicted the positron.

Preface to the second edition

This edition follows much advice and constructive criticism which the author has received from all quarters of the globe, in consequence of which various typos and misprints have been corrected and some ambiguous statements and anfractuosities have been replaced by more clear and direct derivations. Chapter 7 has been largely rewritten to demonstrate the way in which Fourier transforms are used in CAT scanning, an application of more than usual ingenuity and importance: but overall this edition represents a renewed effort to rescue Fourier transforms from the clutches of the pure mathematicians and present them as a working tool to the horny-handed toilers who strive in the fields of electronic engineering and experimental physics.

Glasgow, January 2001   J. F. James

Preface to the third edition

Fourier transforms are eternal. They have not changed their nature since the last edition ten years ago: but the intervening time has allowed the author to correct errors in the text and to expand it slightly to cover some other interesting applications. The van Cittert–Zernike theorem makes a belated appearance, for example, and there are hints of some aspects of radio aerial design as interesting applications.

I also take the opportunity to thank many people who have offered criticism, often anonymously and therefore frankly, which has (usually) been acted upon and which, I hope, has improved the appeal both of the writing and of the contents.

Kilcreggan, August 2010   J. F. James

1

Physics and Fourier transforms

1.1 The qualitative approach

Ninety percent of all physics is concerned with vibrations and waves of one sort or another. The same basic thread runs through most branches of physical science, from acoustics through engineering, fluid mechanics, optics, electromagnetic theory and X-rays to quantum mechanics and information theory. It is closely bound to the idea of a *signal* and its *spectrum*. To take a simple example: imagine an experiment in which a musician plays a steady note on a trumpet or a violin, and a microphone produces a voltage proportional to the instantaneous air pressure. An oscilloscope will display a graph of pressure against time, $F(t)$, which is periodic. The reciprocal of the period is the frequency of the note, 440 Hz, say, for a well-tempered middle A – the tuning-up frequency for an orchestra.

The waveform is not a pure sinusoid, and it would be boring and colourless if it were. It contains 'harmonics' or 'overtones': multiples of the fundamental frequency, with various amplitudes and in various phases,[1] depending on the timbre of the note, the type of instrument being played and on the player. The waveform can be *analysed* to find the amplitudes of the overtones, and a list can be made of the amplitudes and phases of the sinusoids which it comprises. Alternatively a graph, $A(\nu)$, can be plotted (the sound-spectrum) of the amplitudes against frequency (Fig. 1.1).

$A(\nu)$ **is the Fourier transform of** $F(t)$.

Actually it is the *modular* transform, but at this stage that is a detail.

Suppose that the sound is not periodic – a squawk, a drumbeat or a crash instead of a pure note. Then to describe it requires not just a set of overtones

---

[1] 'Phase' here is an angle, used to define the 'retardation' of one wave or vibration with respect to another. One wavelength retardation, for example, is equivalent to a phase difference of 2π. Each harmonic will have its own phase, ϕ_m, indicating its position within the period.
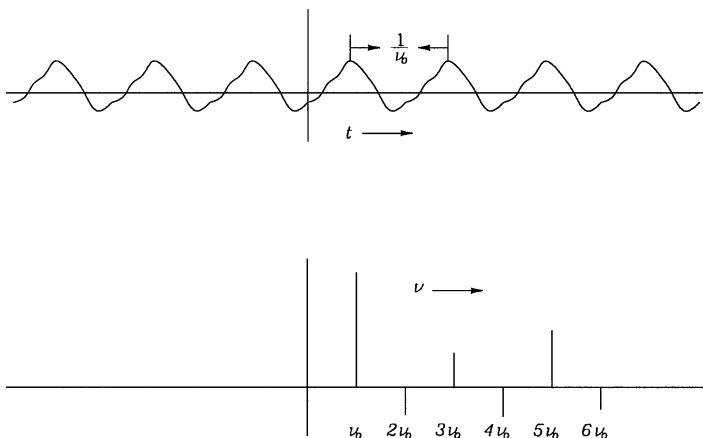
Fig. 1.1. The spectrum of a steady note: fundamental and overtones.

with their amplitudes, but a continuous range of frequencies, each present in an infinitesimal amount. The two curves would then look like Fig. 1.2.

The uses of a Fourier transform can be imagined: the identification of a valuable violin; the analysis of the sound of an aero-engine to detect a faulty gear-wheel; of an electrocardiogram to detect a heart defect; of the light curve of a periodic variable star to determine the underlying physical causes of the variation: all these are current applications of Fourier transforms.

1.2 Fourier series

For a steady note the description requires only the fundamental frequency, its amplitude and the amplitudes of its harmonics. A discrete sum is sufficient. We could write

$$F(t) = a_0 + a_1 \cos(2\pi v_0 t) + b_1 \sin(2\pi v_0 t) + a_2 \cos(4\pi v_0 t)$$
$$+ b_2 \sin(4\pi v_0 t) + a_3 \cos(6\pi v_0 t) + \cdots,$$

where v_0 is the fundamental frequency of the note. Sines as well as cosines are required because the harmonics are not necessarily 'in step' (i.e. 'in phase') with the fundamental or with each other.

More formally:

$$F(t) = \sum_{n=-\infty}^{\infty} a_n \cos(2\pi n v_0 t) + b_n \sin(2\pi n v_0 t) \qquad (1.1)$$

and the sum is taken from $-\infty$ to ∞ for the sake of mathematical symmetry.
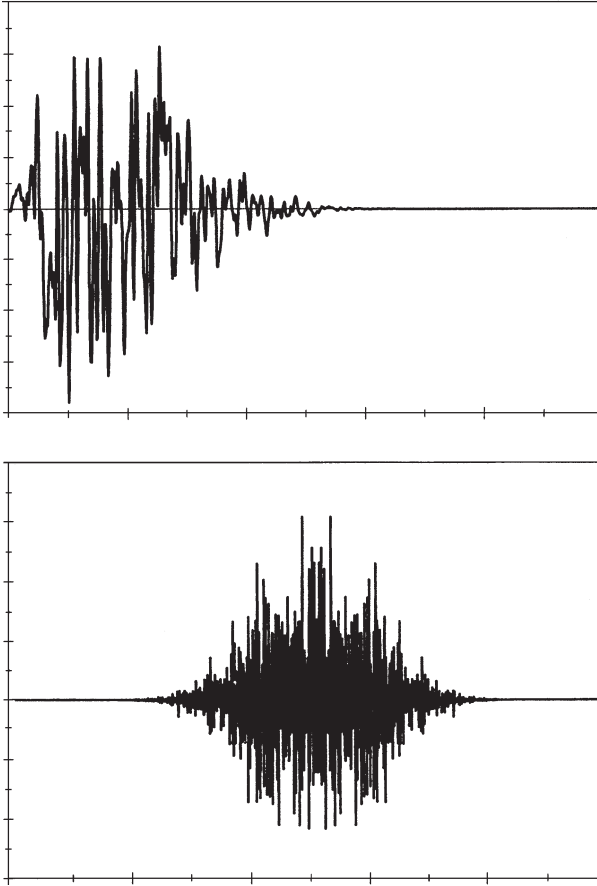
Fig. 1.2. The spectrum of a crash: all frequencies are present.

This process of constructing a waveform by adding together a fundamental frequency and overtones or harmonics of various amplitudes is called Fourier synthesis.

There are alternative ways of writing this expression: since $\cos x = \cos(-x)$ and $\sin x = -\sin(-x)$ we can write

$$F(t) = A_0/2 + \sum_{n=1}^{\infty} A_n \cos(2\pi n v_0 t) + B_n \sin(2\pi n v_0 t) \qquad (1.2)$$

and the two expressions are identical, provided that we set $A_n = a_{-n} + a_n$ and $B_n = b_n - b_{-n}$. A_0 is divided by two to avoid counting it twice: as it is, A_0 can be found by the same formula that will be used to find all the A_n's.

Mathematicians and some theoretical physicists write the expression as

$$F(t) = A_0/2 + \sum_{n=1}^{\infty} A_n \cos(n\omega_0 t) + B_n \sin(n\omega_0 t)$$

and there are entirely practical reasons, which are discussed later, for *not* writing it this way.

1.3 The amplitudes of the harmonics

The alternative process – of extracting from the signal the various frequencies and amplitudes that are present – is called *Fourier analysis* and is much more important in its practical physical applications. In physics, we usually find the curve $F(t)$ experimentally and we want to know the values of the amplitudes A_m and B_m for as many values of m as necessary. To find the values of these amplitudes, we use the *orthogonality* property of sines and cosines. This property is that, if you take a sine and a cosine, or two sines or two cosines, each a multiple of some fundamental frequency, multiply them together and integrate the product over one period of that frequency, the result is always zero except in special cases.

If $P = 1/\nu_0$ is one period, then

$$\int_{t=0}^{P} \cos(2\pi n\nu_0 t) \cdot \cos(2\pi m\nu_0 t) dt = 0$$

and

$$\int_{t=0}^{P} \sin(2\pi n\nu_0 t) \cdot \sin(2\pi m\nu_0 t) dt = 0$$

unless $m = \pm n$, and

$$\int_{t=0}^{P} \sin(2\pi n\nu_0 t) \cdot \cos(2\pi m\nu_0 t) dt = 0$$

always.

The first two integrals are both equal to $1/(2\nu_0)$ if $m = n$.

We multiply the expression (1.2) for $F(t)$ by $\sin(2\pi m\nu_0 t)$ and the product is integrated over one period, P:

$$\int_{t=0}^{P} F(t)\sin(2\pi m\nu_0 t) dt = \frac{A_0}{2} \int_{t=0}^{P} \sin(2\pi m\nu_0 t) dt$$

$$+ \int_{t=0}^{P} \sum_{n=1}^{\infty} \{A_n \cos(2\pi n\nu_0 t) + B_n \sin(2\pi n\nu_0 t)\}\sin(2\pi m\nu_0 t) dt \quad (1.3)$$

and all the terms of the sum vanish on integration except

$$\int_0^P B_m \sin^2(2\pi m\nu_0 t)dt = B_m \int_0^P \sin^2(2\pi m\nu_0 t)dt$$
$$= B_m/(2\nu_0) = B_m P/2$$

so that

$$B_m = (2/P)\int_0^P F(t)\sin(2\pi m\nu_0 t)dt \qquad (1.4)$$

and, provided that $F(t)$ is known in the interval $0 \to P$, the coefficient B_m can be found. If an analytic expression for $F(t)$ is known, the integral can often be done. On the other hand, if $F(t)$ has been found experimentally, a computer is needed to do the integrations.

The corresponding formula for A_m is

$$A_m = (2/P)\int_0^P F(t)\cos(2\pi m\nu_0 t)dt. \qquad (1.5)$$

The integral can start anywhere, not necessarily at $t = 0$, so long as it extends over one period.

Example: Suppose that $F(t)$ is a square-wave of period $1/\nu_0$, so that $F(t) = h$ for $t = -b/2 \to b/2$ and 0 during the rest of the period, as in Fig. 1.3. Then

$$A_m = 2\nu_0 \int_{-1/(2\nu_0)}^{1/(2\nu_0)} F(t)\cos(2\pi m\nu_0 t)dt$$
$$= 2h\nu_0 \int_{-b/2}^{b/2} \cos(2\pi m\nu_0 t)dt$$

and the new limits cover only that part of the cycle where $F(t)$ is different from zero.
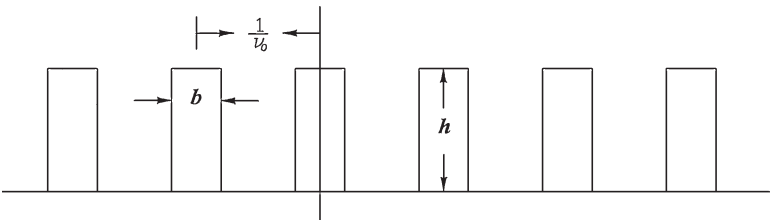

Fig. 1.3. A rectangular wave of period $1/\nu_0$ and pulse-width b.

If we integrate and put in the limits:

$$A_m = \frac{2h\nu_0}{2\pi m \nu_0}\{\sin(\pi m \nu_0 b) - \sin(-\pi m \nu_0 b)\}$$

$$= \frac{2h}{\pi m}\sin(\pi m \nu_0 b)$$

$$= 2h\nu_0 b\{\sin(\pi \nu_0 m b)/(\pi \nu_0 m b)\}.$$

All the B_n's are zero because of the symmetry of the function – we took the origin to be at the centre of one of the pulses.

The original function of time can be written

$$F(t) = h\nu_0 b + 2h\nu_0 b \sum_{m=1}^{\infty}\{\sin(\pi \nu_0 m b)/(\pi \nu_0 m b)\}\cos(2\pi m \nu_0 t) \quad (1.6)$$

or, alternatively,

$$F(t) = \frac{hb}{P} + \frac{2hb}{P} \sum_{m=1}^{\infty}\{\sin(\pi \nu_0 m b)/(\pi \nu_0 m b)\}\cos(2\pi m \nu_0 t). \quad (1.7)$$

Notice that the first term, $A_0/2$, is the *average* height of the function – the area under the top-hat divided by the period; and that the function $\sin(x)/x$, called 'sinc(x)', which will be described in detail later, has the value unity at $x = 0$, as can be shown using de l'Hôpital's rule.[2]

There are other ways of writing the Fourier series. It is convenient occasionally, though less often, to write $A_m = R_m \cos\phi_m$ and $B_m = R_m \sin\phi_m$, so that equation (1.2) becomes

$$F(t) = \frac{A_0}{2} + \sum_{m=1}^{\infty} R_m \cos(2\pi m \nu_0 t + \phi_m) \quad (1.8)$$

and R_m and ϕ_m are the amplitude and phase of the mth harmonic. A single sinusoid then replaces each sine and cosine, and the two quantities needed to define each harmonic are these amplitudes and phases in place of the previous A_m and B_m coefficients. In practice it is usually the amplitude, R_m, which is important, since the energy in an oscillator is proportional to the square of the amplitude of oscillation, and $|R_m|^2$ gives a measure of the power contained in each harmonic of a wave. 'Phase' is a simple and important idea. Two wave trains are 'in phase' if wave crests arrive at a certain point together. They are 'out of phase' if a trough from one arrives at the same time as the crest of the other. (Alternatively, they have 180° phase difference.) In Fig. 1.4 there are two

---

[2] De l'Hôpital's rule is that, if $f(x) \to 0$ as $x \to 0$ and $\phi(x) \to 0$ as $x \to 0$, the ratio $f(x)/\phi(x)$ is indeterminate, but is equal to the ratio $(df/dx)/(d\phi/dx)$ as $x \to 0$.
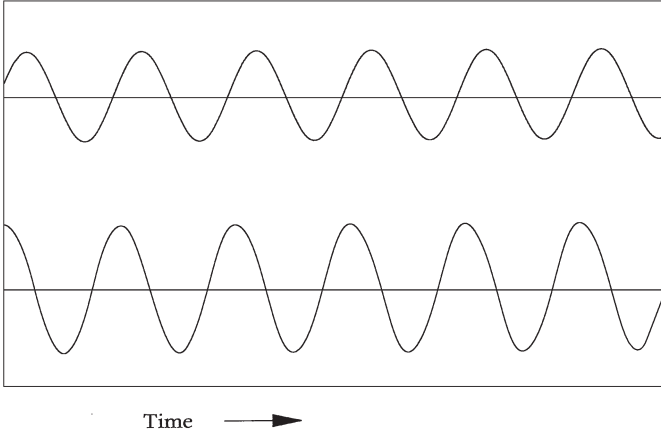
Fig. 1.4. Two wave trains with the same period but different amplitudes and phases. The upper has 0.7 times the amplitude of the lower and there is a phase-difference of 70°.

wave trains. The upper has 0.7 times the amplitude of the other and it *lags* (not *leads*, as it appears to do) the lower by 70°. This is because the horizontal axis of the graph is time, and the vertical axis measures the amplitude at a fixed point as it varies with time. Wave crests from the lower wave train arrive earlier than those from the upper. The important thing is that the 'phase-difference' between the two is 70°.

The most common way of writing the series expansion is with complex exponentials instead of trigonometrical functions. This is because the algebra of complex exponentials is easier to manipulate. The two ways are linked, of course, by de Moivre's theorem. We can write

$$F(t) = \sum_{-\infty}^{\infty} C_m e^{2\pi i m v_0 t},$$

where the coefficients C_m are now complex numbers in general and $C_m = C_{-m}^*$. (The exact relationship is given in detail in Appendix A.3.) The coefficients A_m, B_m and C_m are obtained from the *inversion formulae:*

$$A_m = 2v_0 \int_0^{1/v_0} F(t)\cos(2\pi m v_0 t)dt,$$

$$B_m = 2v_0 \int_0^{1/v_0} F(t)\sin(2\pi m v_0 t)dt,$$

$$C_m = 2v_0 \int_0^{1/v_0} F(t)e^{-2\pi m v_0 t}\, dt$$

(the minus sign in the exponent is important) or, if ω_0 has been used instead of v_0 ($v_0 = \omega_0/(2\pi)$), then

$$A_m = (\omega_0/\pi) \int_0^{2\pi/\omega_0} F(t)\cos(m\omega_0 t)dt,$$

$$B_m = (\omega_0/\pi) \int_0^{2\pi/\omega_0} F(t)\sin(m\omega_0 t)dt,$$

$$C_m = (2\omega_0/\pi) \int_0^{2\pi/\omega_0} F(t)e^{-im\omega_0 t}\, dt.$$

The useful mnemonic form to remember for finding the coefficients in a Fourier series is

$$A_m = \frac{2}{\text{period}} \int_{\text{one period}} F(t)\cos\left\{\frac{2\pi mt}{\text{period}}\right\} dt, \tag{1.9}$$

$$B_m = \frac{2}{\text{period}} \int_{\text{one period}} F(t)\sin\left\{\frac{2\pi mt}{\text{period}}\right\} dt \tag{1.10}$$

and remember that the integral can be taken from any starting point, a, provided that it extends over one period to an upper limit $a + P$. The integral can be split into as many subdivisions as needed if, for example, $F(t)$ has different analytic forms in different parts of the period.

1.4 Fourier transforms

Whether $F(t)$ is periodic or not, a complete description of $F(t)$ can be given using sines and cosines. If $F(t)$ is not periodic it requires all frequencies to be present if it is to be synthesized. A non-periodic function may be thought of as a limiting case of a periodic one, where the period tends to infinity, and consequently the fundamental frequency tends to zero. The harmonics are more and more closely spaced and in the limit there is a continuum of harmonics, each one of infinitesimal amplitude, $a(v)dv$, for example. The summation sign is replaced by an integral sign and we find that

$$F(t) = \int_{-\infty}^{\infty} a(v)dv \cos(2\pi vt) + \int_{-\infty}^{\infty} b(v)dv \sin(2\pi vt) \tag{1.11}$$

or, equivalently,

$$F(t) = \int_{-\infty}^{\infty} r(v)\cos(2\pi vt + \phi(v))dv \tag{1.12}$$

or, again,

$$F(t) = \int_{-\infty}^{\infty} \Phi(v)e^{2\pi ivt}\, dv. \tag{1.13}$$

If $F(t)$ is real, that is to say, if the insertion of any value of t into $F(t)$ yields a real number, then $a(\nu)$ and $b(\nu)$ are real too. However, $\Phi(\nu)$ may be complex and indeed will be if $F(t)$ is asymmetrical so that $F(t) \neq F(-t)$. This can sometimes cause complications, and these are dealt with in Chapter 8: but $F(t)$ is often symmetrical and then $\Phi(\nu)$ is real and $F(t)$ comprises only cosines. We *could* then write

$$F(t) = \int_{-\infty}^{\infty} \Phi(\nu)\cos(2\pi \nu t)d\nu$$

but, because complex exponentials are easier to manipulate, we take equation (1.13) above as the standard form. Nevertheless, for many practical purposes only real and symmetrical functions $F(t)$ and $\Phi(\nu)$ need be considered.

Just as with Fourier series, the function $\Phi(\nu)$ can be recovered from $F(t)$ by inversion. This is the cornerstone of Fourier theory because, astonishingly, the inversion has exactly the same form as the synthesis, and we can write, if $\Phi(\nu)$ is real and $F(t)$ is symmetrical,

$$\Phi(\nu) = \int_{-\infty}^{\infty} F(t)\cos(2\pi \nu t)dt, \tag{1.14}$$

so that not only is $\Phi(\nu)$ the Fourier transform of $F(t)$, but also $F(t)$ is the Fourier transform of $\Phi(\nu)$. The two together are called a 'Fourier pair'.

The complete and rigorous proof of this is long and tedious[3] and it is not necessary here; but the formal definition can be given and this is a suitable place to abandon, for the moment, the physical variables time and frequency and to change to the pair of abstract variables, x and p, which are usually used. The formal statement of a Fourier transform is then

$$\Phi(p) = \int_{-\infty}^{\infty} F(x)e^{2\pi ipx}\, dx, \tag{1.15}$$

$$F(x) = \int_{-\infty}^{\infty} \Phi(p)e^{-2\pi ipx}\, dp \tag{1.16}$$

and this pair of formulae[4] will be used from here on.

---

[3] It is to be found, for example, in E. C. Titchmarsh, *Introduction to the Theory of Fourier Integrals*, Clarendon Press, Oxford, 1962 or in R. R. Goldberg, *Fourier Transforms*, Cambridge University Press, Cambridge, 1965.

[4] Sometimes one finds

$$\Phi(p) = \frac{1}{2\pi} \int_{-\infty}^{\infty} F(x)e^{ipx}\, dx; \qquad F(x) = \int_{-\infty}^{\infty} \Phi(p)e^{-ipx}\, dp$$

as the defining equations, and again symmetry is preserved by some people by defining the transform by

$$\Phi(p) = \left\{\frac{1}{2\pi}\right\}^{1/2} \int_{-\infty}^{\infty} F(x)e^{ipx}\, dx; \qquad F(x) = \left\{\frac{1}{2\pi}\right\}^{1/2} \int_{-\infty}^{\infty} \Phi(p)e^{-ipx}\, dp.$$

Symbolically we write

$$\Phi(p) \rightleftharpoons F(x).$$

One and only one of the integrals must have a minus sign in the exponent. Which of the two you choose does not matter, so long as you keep to the rule. If the rule is broken half way through a long calculation the result is chaos; but if someone else has used the opposite choice, the Fourier pair calculated of a given function will be the complex conjugate of that given by your choice.

When time and frequency are the conjugate variables we shall use

$$\Phi(\nu) = \int_{-\infty}^{\infty} F(t)e^{-2\pi i\nu t}\, dt, \qquad (1.17)$$

$$F(t) = \int_{-\infty}^{\infty} \Phi(\nu)^{2\pi i\nu t}\, d\nu \qquad (1.18)$$

and again, symbolically,

$$\Phi(\nu) \rightleftharpoons F(t).$$

There are two good reasons for incorporating the 2π into the exponent. Firstly the defining equations are easily remembered without worrying where the 2π's go, but, more importantly, quantities like t and ν are actually physically measured quantities – time and frequency – rather than time and *angular* frequency, ω. Angular measure is for mathematicians. For example, when one has to integrate a function wrapped around a cylinder it is convenient to use the angle as the independent variable. Physicists will generally find it more convenient to use t and ν, for example, with the 2π in the exponent.

1.5 Conjugate variables

Traditionally x and p are used when abstract transforms are considered and they are called 'conjugate variables'. Different fields of physics and engineering use different pairs, such as frequency, ν, and time, t, in acoustics, telecommunications and radio; position, x, and momentum divided by Planck's constant, $p/\hbar$, in quantum mechanics; and aperture, x, and the sine of the diffraction angle divided by the wavelength, $p = \sin\theta/\lambda$, in diffraction theory.

In general we will use x and p as abstract entities and give them a physical meaning when an illustration seems called for. It is worth remembering that x and p have inverse dimensionality, as in time, t, and frequency, t^{-1}. The product px, like any exponent, is always a dimensionless number.

One further definition is needed: the 'power spectrum' of a function.[5] This notion is important in electrical engineering as well as in physics. If power

---

[5] Actually the *energy* spectrum; 'power spectrum' is just the conventional term used in most books. This is discussed in more detail in Chapter 4.

is transmitted by electromagnetic radiation (radio waves or light) or by wires or waveguides, the voltage at a point varies with time as $V(t)$. $\Phi(\nu)$, the Fourier transform of $V(t)$, may very well be – indeed usually is – complex. However, the power per unit frequency interval being transmitted is proportional to $\Phi(\nu)\Phi^*(\nu)$, where the constant of proportionality depends on the load impedance. The function $S(\nu) = \Phi(\nu)\Phi^*(\nu) = |\Phi(\nu)|^2$ is called the power spectrum or the spectral power density (SPD) of $F(t)$. This is what an optical spectrometer measures, for example.

1.6 Graphical representations

It frequently happens that greater insight into the physical processes which are described by a Fourier transform can be achieved by use of a diagram rather than a formula. When a real function $F(x)$ is transformed it generally produces a complex function $\Phi(p)$, which needs an Argand diagram to demonstrate it. Three dimensions are required: Re $\Phi(p)$, Im $\Phi(p)$ and p. A perspective drawing will display the function, which appears as a more or less sinuous line. If $F(x)$ is symmetrical, the line lies in the Re p-plane, whereas if it is antisymmetrical, the line lies in the Im p-plane. Figures 8.1 and 8.2 in Chapter 8 illustrate this point.

Electrical engineering students, in particular, will recognize the end-on view along the p-axis as the 'Nyquist diagram' of feedback theory. There will be examples of this graphical representation in later chapters.

1.7 Useful functions

There are some functions which occur again and again in physics, and whose properties should be learned. They are extremely useful in the manipulation and general taming of other functions which would otherwise be almost unmanageable. Chief among these are the following.

1.7.1 The 'top-hat' function[6]

This has the property that

$$\Pi_a(x) = \begin{cases} 0, & -\infty < x < -a/2 \\ 1, & -a/2 < x < a/2 \\ 0, & a/2 < x < \infty \end{cases}$$

and the symbol Π is chosen as an obvious aid to memory.

---

[6] In the USA this is called a 'box-car' or 'rect' function.
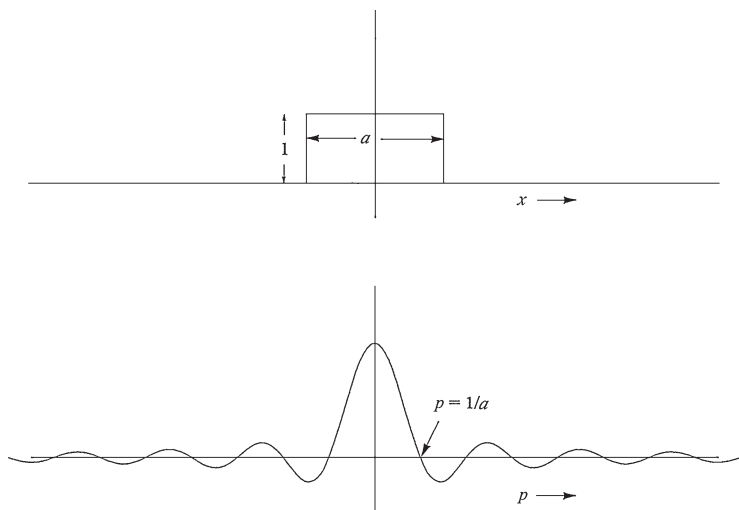
Fig. 1.5. The top-hat function and its transform, the sinc-function.

Its Fourier pair is obtained by integration:

$$\Phi(p) = \int_{-\infty}^{\infty} \Pi_a(x)e^{2\pi ipx}\,dx$$

$$= \int_{-a/2}^{a/2} e^{2\pi ipx}\,dx$$

$$= \frac{1}{2\pi ip}[e^{\pi ipa} - e^{-\pi ipa}]$$

$$= a\left\{\frac{\sin(\pi pa)}{\pi pa}\right\}$$

$$= a\,\text{sinc}(\pi pa)$$

and the 'sinc-function', defined[7] by $\text{sinc}(x) = \sin x/x$, is one which recurs throughout physics (Fig. 1.5). As before, we write symbolically

$$\Pi_a(x) \rightleftharpoons a\,\text{sinc}(\pi pa).$$

1.7.2 The sinc-function

The sinc-function $\text{sinc}(x) = \sin x/x$ has the value unity at $x = 0$, and has zeros whenever $x = n\pi$. The function $\text{sinc}(\pi pa)$ above, the most common form, has zeros when $p = 1/a, 2/a, 3/a, \ldots$

[7] Caution: some people define $\text{sinc}(x)$ as $\sin(\pi x)/(\pi x)$, although without noticeable advantage and with occasional confusion when the argument is complicated.
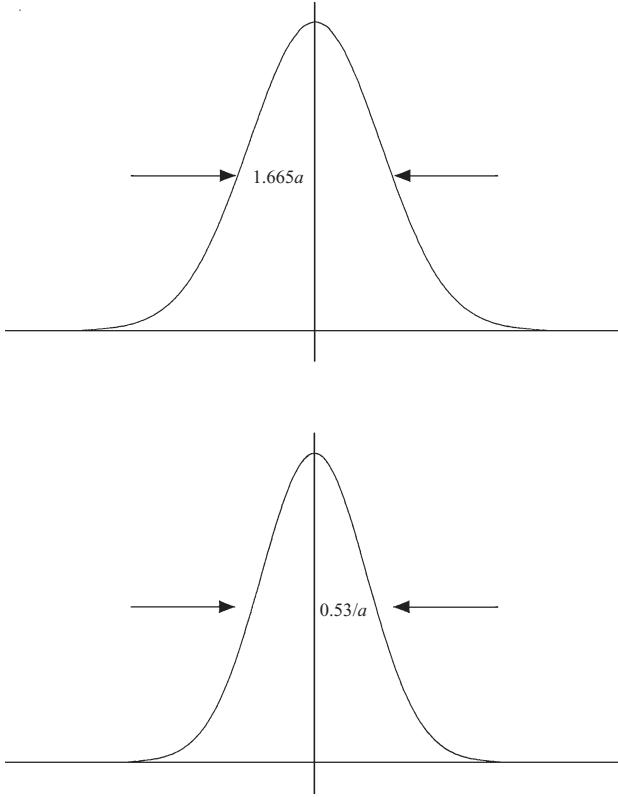
Fig. 1.6. The Gaussian function and its transform, another Gaussian with full width at half maximum inversely proportional to that of its Fourier pair.

1.7.3 The Gaussian function

Suppose $G(x) = e^{-x^2/a^2}$, where a is the 'width parameter' of the function. The value of $G(x) = 1/2$ when $(x/a)^2 = \log_e 2$, or $x = \pm 0.8325a$ so that the full width at half maximum (FWHM) is $1.665a$ and (which every scientist should know!) $\int_{-\infty}^{\infty} e^{-x^2/a^2}\, dx = a\sqrt{\pi}$.

Its Fourier transform is $g(p)$, given by

$$g(p) = \int_{-\infty}^{\infty} e^{-x^2/a^2} e^{2\pi i p x}\, dx$$

(Fig. 1.6). The exponent can be rewritten (by 'completing the square') as

$$-(x/a - \pi i p a)^2 - \pi^2 p^2 a^2$$

and then

$$g(p) = e^{-\pi^2 p^2 a^2} \int_{-\infty}^{\infty} e^{-(x/a - \pi ipa)^2} \, dx.$$

Put $x/a - \pi ipa = z$, so that $dx = a \, dz$. Then

$$g(p) = ae^{-\pi^2 p^2 a^2} \int_{-\infty}^{\infty} e^{-z^2} \, dz$$
$$= a\sqrt{\pi} e^{-\pi^2 a^2 p^2}$$

so that $g(p)$ is another Gaussian function, with width parameter $1/(\pi a)$.

Notice that the wider the original Gaussian, the narrower will be its Fourier pair.

Notice, too, that the value at $p = 0$ of the Fourier pair is equal to the area under the original Gaussian.

1.7.4 The exponential decay

This, in physics, is generally the positive part of the function $e^{-x/a}$. It is asymmetrical, so its Fourier transform is complex:

$$\Phi(p) = \int_0^{\infty} e^{-x/a} e^{2\pi ipx} \, dx$$
$$= \left[\frac{e^{2\pi ipx - x/a}}{2\pi ip - 1/a} \right]_0^{\infty} = \frac{-1}{2\pi ip - 1/a}.$$

Usually, with this function, the power spectrum is the most interesting:

$$|\Phi(p)|^2 = \frac{a^2}{4\pi^2 p^2 a^2 + 1}.$$

This is a bell-shaped curve, similar in appearance to a Gaussian curve, and is generally known as a Lorentz profile.[8] Its FWHM is $1/(\pi a)$.

It is the shape found in spectrum lines when they are observed at very low pressure, when collisions between emitting particles are infrequent compared with the transition probability. If the line profile is taken as a function of frequency, $I(\nu)$, the FWHM, $\Delta \nu$, is related to the 'lifetime of the excited state', the reciprocal of the transition probability in the atom which undergoes the transition. In this example, a and x obviously have dimensions of time. Looked

---

[8] It is also known to mathematicians as the 'Witch of Agnesi' or more accurately as the 'curve of Agnesi', having been studied by the eighteenth-century mathematician Maria Agnesi (1718–1799). The translator confused *versiera* – 'curve' – with *avversiera* – witch.
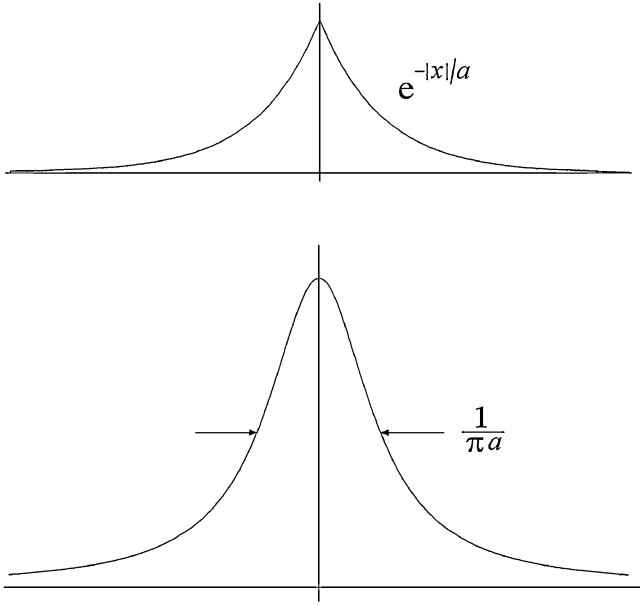
Fig. 1.7. The exponential decay $e^{-|x|/a}$ and its Fourier transform.

at classically, the emitting particle is behaving like a damped harmonic oscillator radiating power at an exponentially decreasing rate. Quantum mechanics yields the same equation through perturbation theory.

There is more discussion of this profile in Chapter 5.

1.7.5 The Dirac 'delta-function'

This has the following properties:

$$\delta(x) = 0 \text{ unless } x = 0,$$
$$\delta(0) = \infty,$$
$$\int_{-\infty}^{\infty} \delta(x)dx = 1.$$

It is an example of a function which disobeys one of Dirichlet's conditions, since it is unbounded at $x = 0$. It can be regarded crudely as the limiting case of a top-hat function $(1/a)\Pi_a(x)$ as $a \to 0$. It becomes narrower and higher, and its area, which we shall refer to as its *amplitude*, is always equal to unity. Its Fourier transform (Fig. 1.7) is $\text{sinc}(\pi p a)$ and, as $a \to 0$, $\text{sinc}(\pi p a)$ stretches

and in the limit is a straight line at unit height above the x-axis. In other words,

the Fourier transform of a delta-function is unity

and we write

$$\delta(x) \rightleftharpoons 1.$$

Alternatively, and more accurately, it is the limiting case of a Gaussian function of unit area as it gets narrower and higher. Its Fourier transform then is another Gaussian of unit height, getting broader and broader until in the limit it is a straight line at unit height above the axis.

Although the function has infinite height, we frequently encounter it multiplied by a constant. In this case it is convenient, if not strictly accurate, to refer to the function $a\delta(x)$ as having a 'height' a.

The following useful properties of the delta-function (or δ-function) should be memorized. They are

$$\delta(x - a) = 0 \text{ unless } x = a$$

and the so-called 'shift theorem':

$$\int_{-\infty}^{\infty} f(x)\delta(x - a)dx = f(a),$$

where the product under the integral sign is zero except at $x = a$, where, on integration, the δ-function has the amplitude $f(a)$.

It is then easy to show, using this shift theorem, that for positive[9] values of a, b, c and d

$$\delta(x/a - 1) = a\delta(x - a).$$

To show this, put $x = au; dx = a\,du$. Then

$$\int_{-\infty}^{\infty} \delta(x/a - 1)f(x)dx = a\int_{-\infty}^{\infty} \delta(u - 1)f(au)du$$

and the integrand is zero except at the point $u = 1$, so that the result is $af(a)$. Compare this with

$$\int_{-\infty}^{\infty} \delta(x - a)f(x)dx = f(a)$$

and the substitution is obvious.

---

[9] For negative values of these quantities a minus sign may be needed, bearing in mind that the integral of a δ-function is always positive, even though a, for example, may be negative. Alternatively, we may write, for example, $\delta(x/a - 1) = |a|\delta(x - a)$.

Similarly, we find

$$\delta(a/b - c/d) = ac\delta(ad - bc)$$
$$= bd\delta(ad - bc)$$
$$\delta(ax) = (1/a)\delta(x).$$

Another important consequence of the shift theorem is that

$$\int_{-\infty}^{\infty} e^{2\pi ipx}\delta(x - a)dx = e^{2\pi ipa}$$

so that we can write

$$\delta(x - a) \rightleftharpoons e^{2\pi ipa},$$
$$\delta(mx - a) \rightleftharpoons (1/m)e^{2\pi ipa/m}$$

and a formula which we shall need in Chapter 7:

$$\frac{1}{n}\delta\left(\frac{p}{l} - \frac{r}{n}\right) = \delta\left(\frac{pn}{l} - r\right) \rightleftharpoons e^{-2\pi i\left(\frac{pn}{l} - r\right)}.$$

1.7.6 A pair of δ-functions

If two δ-functions are equally disposed on either side of the origin, the Fourier transform is a cosine wave:

$$\delta(x - a) + \delta(x + a) \rightleftharpoons e^{2\pi ipa} + e^{-2\pi ipa}$$
$$= 2\cos(2\pi pa).$$

1.7.7 The Dirac comb

This is an infinite set of equally-spaced δ-functions, usually denoted by the Cyrillic letter Ш (shah). Formally, we write

$$Ш_a(x) = \sum_{n=-\infty}^{\infty} \delta(x - na).$$

It is useful because it allows us to include Fourier series in the general theory of Fourier transforms. For example, the *convolution* (to be described later) of $Ш_a(x)$ and $(1/b)\Pi_b(x)$ (where $b < a$) is a square wave similar to that in the earlier example, of period a and width b, and with unit area in each rectangle. The Fourier transform is then a Dirac comb, with 'teeth' of height a_m spaced at intervals $1/a$. The a_m are, of course, the coefficients in the series.

   If the square wave is allowed to become infinitesimally wide and infinitely high so that the area under each rectangle remains unity, then the coefficients a_m
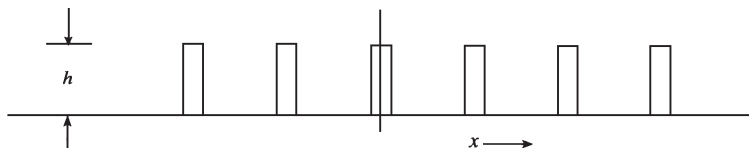
Fig. 1.8. A rectangular pulse-train with a 4 : 1 'mark–space' ratio.

will all become of the same height, $1/a$. In other words, the Fourier transform of a Dirac comb is another Dirac comb:

$$III_a(x) \rightleftharpoons \frac{1}{a} III_{1/a}(p)$$

and again notice that the period in p-space is the reciprocal of the period in x-space.

This is not a formal demonstration of the Fourier transform of a Dirac comb. A rigorous proof is much more elaborate, but is unnecessary here.

1.8 Worked examples

(1) A train of rectangular pulses, as in Fig. 1.8, has a pulse width equal to $1/4$ of the pulse period. Show that the 4th, 8th, 12th etc. harmonics are missing.

Taking zero at the centre of one pulse, the function is clearly symmetrical so that there are only cosine amplitudes:

$$
\begin{aligned}
A_n &= \frac{2}{P} \int_{-P/8}^{P/8} h \cos\left(\frac{2\pi nx}{P}\right) dx \\
&= \left(\frac{h}{\pi n}\right) 2 \sin\left(\frac{2\pi n}{P} \cdot \frac{P}{8}\right) \\
&= \left(\frac{h}{2}\right) \operatorname{sinc}\left(\frac{\pi n}{4}\right)
\end{aligned}
$$

so that $A_n = 0$ if $n = 4, 8, 12, \ldots$

(2) Find the sine-amplitude of a sawtooth waveform as in Fig. 1.9.

By choosing the origin half way up one of the teeth, the function is clearly made antisymmetrical, so that there are no cosine amplitudes:

$$
\begin{aligned}
B_n &= \frac{2}{P} \int_{-P/2}^{P/2} \frac{xh}{P} \sin\left(\frac{2\pi nx}{P}\right) dx \\
&= \frac{2h}{P^2} \left[-x \cos\left(\frac{2\pi nx}{P}\right) \frac{P}{2\pi n} + \frac{P^2}{4\pi^2 n^2} \sin\left(\frac{2\pi nx}{P}\right) \right]_{-P/2}^{P/2} \\
&= [-2h/(\pi n)] \cos(\pi n)
\end{aligned}
$$
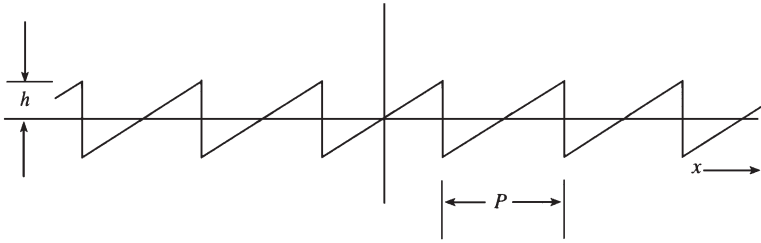
Fig. 1.9. A sawtooth waveform, antisymmetrical about the origin.

since $\sin(\pi n) = 0$, so that

$$B_0 = 0,$$
$$B_n = (-1)^{n+1}[2h/(\pi n)], \quad n \neq 0.$$

As a matter of interest, it is worthwhile calculating the sine-amplitudes when the origin is taken at the tip of a tooth, to see how changing the position of the origin changes the amplitudes. It is also worthwhile doing the calculation for a similar wave, with negative-going slopes instead of positive.

2

Useful properties and theorems

2.1 The Dirichlet conditions

Not all functions can be Fourier-transformed. They are transformable if they fulfil certain conditions, known as the Dirichlet conditions.

The integrals which formally define the Fourier transform in Chapter 1 will exist if the integrands fulfil the following conditions:

- The functions $F(x)$ and $\Phi(p)$ are square-integrable, i.e. $\int_{-\infty}^{\infty} |F(x)|^2 \, dx$ is finite, which implies that $F(x) \to 0$ as $|x| \to \infty$.
- $F(x)$ and $\Phi(p)$ are single-valued. For example, a curve such as that in Fig. 2.1, despite having a respectable-looking Cartesian equation,[1] is not Fourier-transformable.
- $F(x)$ and $\Phi(p)$ are 'piece-wise continuous'. The function can be broken up into separate pieces, so that there can be isolated discontinuities, as many as you like, at the junctions, but the functions must be *continuous*, as defined for instance by Weierstrass, between these discontinuities.[2]
- The functions $F(x)$ and $\Phi(p)$ have upper and lower bounds. This is a condition which is *sufficient* but has not been proved *necessary*. In fact we shall assume that it is not. The Dirac δ-function, for instance, disobeys this condition. Figure 2.2 shows another example. No engineer or physicist has yet lost sleep over this one.

In Nature, all the phenomena that can be described mathematically seem to require only well-behaved functions which obey the Dirichlet conditions. For

---

[1] $y = (x - 1)\sqrt{x}$.
[2] The classical nonconformist example is Dirichlet's function, $W(x)$, which has the property that $W(x) = 1$ if x is rational and $W(x) = 0$ if x is irrational. It looks like a straight line but it is not transformable, since it can be shown that between any two rational numbers, however close, there is at least one irrational number, and between any two irrational numbers there is at least one rational number, so that the function is everywhere discontinuous.
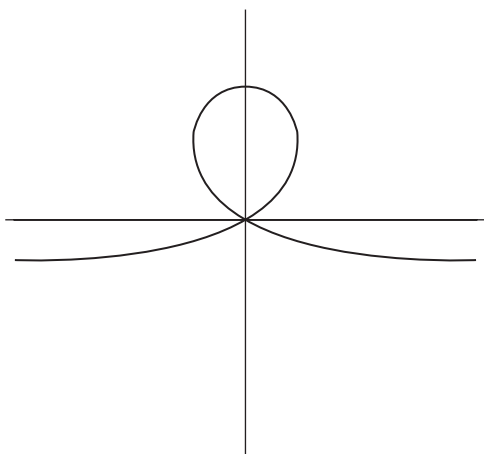
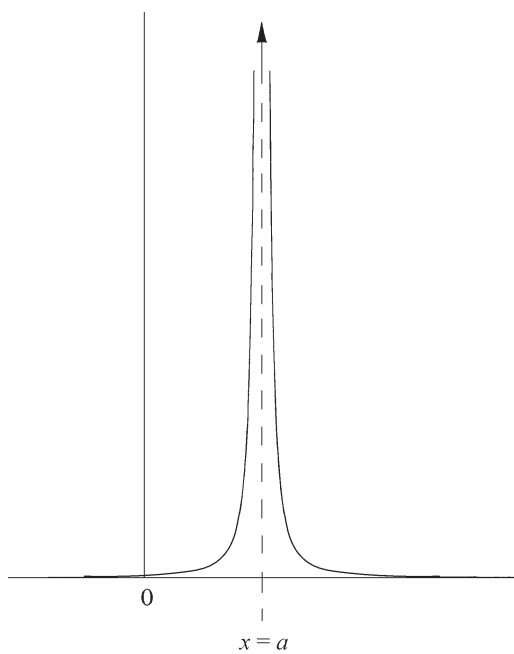Fig. 2.1. A double-valued function like this is not Fourier-transformable.

Fig. 2.2. $F(x) = 1/(x-a)^2$, an unbounded function of x which is not Fourier-transformable.

example, we can describe the electric field of a 'wave-packet' by a function which is continuous, finite and single-valued everywhere, and, since the wave-packet contains only a finite amount of energy, the electric field is square-integrable.

2.2 Theorems

There are several theorems which are of great use in manipulating Fourier pairs, and they should be memorized. For the most part the proofs are elementary. The art of practical Fourier-transforming is in the manipulation of functions using these theorems, rather than in doing extensive and tiresome elementary integrations. It is this, as much as anything, which makes Fourier theory such a powerful tool for the practical working scientist.

In what follows, we assume that

$$F_1(x) \rightleftharpoons \Phi_1(p); \qquad F_2(x) \rightleftharpoons \Phi_2(p),$$

where '$\rightleftharpoons$' implies that F_1 and Φ_1 are a Fourier pair.

The addition theorem states that

$$F_1(x) + F_2(x) \rightleftharpoons \Phi_1(p) + \Phi_2(p). \tag{2.1}$$

The shift theorem already mentioned in Chapter 1 has the following lemmas:

$$F_1(x + a) \rightleftharpoons \Phi_1(p)e^{2\pi ipa},$$
$$F_1(x - a) \rightleftharpoons \Phi_1(p)e^{-2\pi ipa}, \tag{2.2}$$
$$F_1(x - a) + F_1(x + a) \rightleftharpoons 2\Phi_1(p)\cos(2\pi pa).$$

In particular, notice that, if $F_1(x)$ is a δ-function, the lemmas are

$$\delta(x + a) \rightleftharpoons e^{-2\pi ipa},$$
$$\delta(x - a) \rightleftharpoons e^{2\pi ipa},$$
$$\delta(x - a) + \delta(x + a) \rightleftharpoons 2\cos(2\pi pa). \tag{2.3}$$

The third of these is illustrated in Fig. 2.3.

2.3 Convolutions and the convolution theorem

Convolutions are an important concept, especially in practical physics, and the idea of a convolution can be illustrated simply by an example.

Imagine a 'perfect' spectrometer, plotting a graph of intensity against wavelength, of a monochromatic source of light of intensity S and wavelength λ_0.
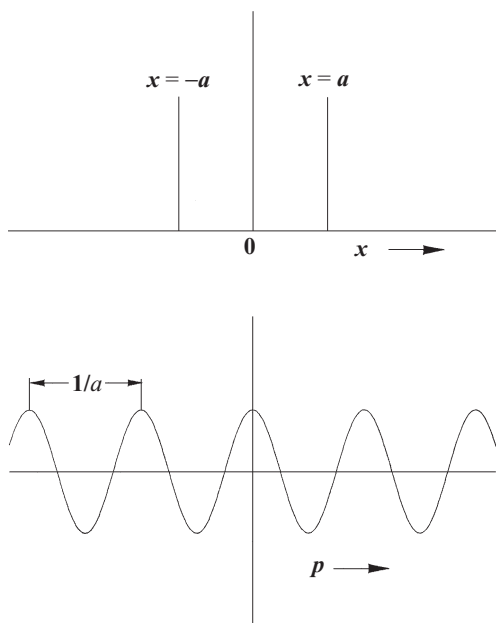
Fig. 2.3. A pair of δ-functions and its transform.

Represent the spectral power density ('the spectrum', see Fig. 2.4) of the source by $S\delta(\lambda - \lambda_0)$. The spectrometer will plot the graph as $kS\delta(\lambda - \lambda_0)$, where k is a factor which depends on the throughput of the spectrometer, its geometry and its detector sensitivity.

No spectrometer is perfect in practice, and what a real instrument will plot in response to a monochromatic input is a continuous curve $kSI(\lambda - \lambda_0)$, where $I(\lambda)$ is called the 'instrumental function' and $\int_{-\infty}^{\infty} I(\lambda)d\lambda = 1$.

Now we inquire what the instrument will plot in response to a continuous spectrum input. Suppose that the intensity of the source as a function of wavelength is $S(\lambda)$. We assume that a monochromatic line at *any* wavelength λ_1 will be plotted as a similarly shaped function $kI(\lambda - \lambda_1)$. Then an infinitesimal interval of the spectrum can be considered as a monochromatic line, at λ_1, say, and of intensity $S(\lambda_1)d\lambda_1$ and it is plotted by the spectrometer as a function of λ:

$$dO(\lambda) = kS(\lambda_1)d\lambda_1 I(\lambda - \lambda_1)$$

and the intensity *apparently* at another wavelength λ_2 is

$$dO(\lambda_2) = kS(\lambda_1)I(\lambda_2 - \lambda_1)d\lambda_1.$$

$$\delta(\lambda-\lambda_0)$$

$$I(\lambda-\lambda_0)$$
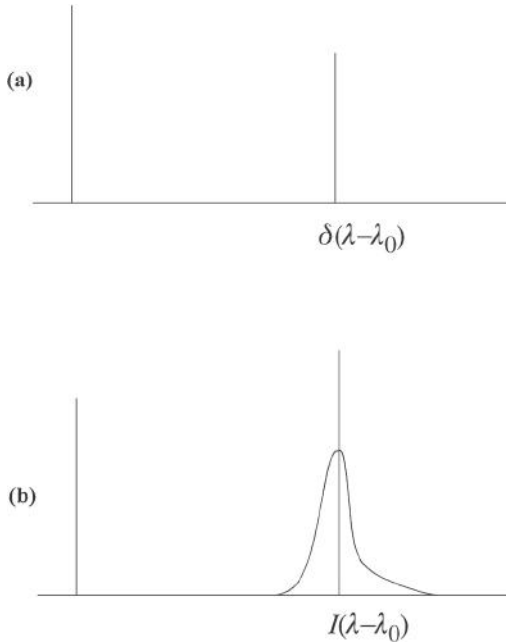
Fig. 2.4. The spectrum of a monochromatic wave (a) entering and (b) leaving a spectrometer. The area under curve (b) must be unity – the same as the 'area' under the δ-function – in order to preserve the idea of an 'instrumental function'.

The total power apparently at λ_2 is got by integrating this over all wavelengths:

$$O(\lambda_2) = k \int_{-\infty}^{\infty} S(\lambda_1)I(\lambda_2 - \lambda_1)d\lambda_1$$

or, dropping unnecessary subscripts,

$$O(\lambda) = k \int_{-\infty}^{\infty} S(\lambda_1)I(\lambda - \lambda_1)d\lambda_1,$$

and the output curve, $O(\lambda)$, is said to be the convolution of the spectrum $S(\lambda)$ with the instrumental function $I(\lambda)$.

It is the idea of an instrumental function, $I(\lambda)$, which is important here. We assume that the same shape $I(\lambda)$ is given to any monochromatic line input. The idea extends to all sorts of measuring instruments and has various names, such as 'impulse response', 'point-spread function', 'Green's function' and so on, depending on which branch of physics or electrical engineering is being discussed. In an electronic circuit, for example, it answers the question 'if you put in a sharp pulse, what comes out?'. Most instruments have no fixed

unique 'instrumental function', but the function often changes slowly enough (with wavelength, in the spectrometer example) that the idea can be used for practical calculations.

The same idea can be envisaged in two dimensions: a point object – a distant star for instance – is imaged by a camera lens as a small smear of light, the 'point-spread function' of the lens. Even a 'perfect' lens has a diffraction pattern, so that the best that can be done is to convert a point object into an 'Airy-disc' – a spot, $1.22 f\lambda/d$ in diameter, where f is the focal length and d the diameter of the lens. The lens in general, when taking a photograph, gives an image which is the convolution, in two dimensions, of its point-spread function with the object.

The formal definition of a convolution of two functions is then

$$C(x) = \int_{-\infty}^{\infty} F_1(x')F_2(x - x')dx' \qquad (2.4)$$

and we write this symbolically as

$$C(x) = F_1(x) * F_2(x).$$

Convolutions obey various rules of arithmetic, and can be manipulated using them.

- The commutative rule:

$$C(x) = F_1(x) * F_2(x) = F_2(x) * F_1(x)$$

 or

$$C(x) = \int_{-\infty}^{\infty} F_2(x')F_1(x - x')dx'$$

 as can be shown by a simple substitution.
- The distributive rule:

$$F_1(x) * [F_2(x) + F_3(x)] = F_1(x) * F_2(x) + F_1(x) * F_3(x).$$

- The associative rule: the idea of a convolution can be extended to three or more functions, and the *order* in which the convolutions are done does not matter:

$$F_1(x) * [F_2(x) * F_3(x)] = [F_1(x) * F_2(x)] * F_3(x)$$

and usually the convolution of three functions is written without the square brackets:

$$C(x) = F_1(x) * F_2(x) * F_3(x)$$
$$= \int_{-\infty}^{\infty}\int_{-\infty}^{\infty} F_1(x - x')F_2(x' - x'')F_3(x'')dx'\,dx''.$$

In fact a whole algebra of convolutions exists and is very useful in taming some of the more fearsome-looking functions that are found in physics. For example,

$$[F_1(x) + F_2(x)] * [F_3(x) + F_4(x)] = F_1(x) * F_3(x) + F_1(x) * F_4(x)$$
$$+ F_2(x) * F_3(x) + F_2(x) * F_4(x).$$

There is a way of visualizing a convolution. Draw the graph of $F_1(x)$. Draw, on a piece of transparent paper, the graph of $F_2(x)$. Turn the transparent graph over about a vertical axis and lay this mirror-image of F_2 on top of the graph of F_1. When the two y-axes are displaced by a distance x', integrate the product of the two functions. The result is one point on the graph of $C(x')$.

2.3.1 The convolution theorem

With the exception of Fourier's inversion theorem, the convolution theorem is the most astonishing result in Fourier theory. It is as follows.

If $C(x)$ is the convolution of $F_1(x)$ with $F_2(x)$ then its Fourier pair, $\Gamma(p)$, is the *product* of $\Phi_1(p)$ and $\Phi_2(p)$, the Fourier pairs of $F_1(x)$ and $F_2(x)$. Symbolically:

$$F_1(x) * F_2(x) \rightleftharpoons \Phi_1(p) \cdot \Phi_2(p). \tag{2.5}$$

The applications of this theorem are manifold and profound. Its proof is elementary:

$$C(x) = \int_{-\infty}^{\infty} F_1(x')F_2(x - x')dx'$$

by definition.

Fourier transform both sides (and note that, because the limits are $\pm\infty$, x' is a dummy variable and can be replaced by any other symbol not already in use):

$$\Gamma(p) = \int_{-\infty}^{\infty} C(x)e^{2\pi ipx}\,dx = \int_{-\infty}^{\infty}\int_{-\infty}^{\infty} F_1(x')F_2(x - x')e^{2\pi ipx}\,dx'\,dx. \tag{2.6}$$

Introduce a new variable $y = x - x'$. Then, during the x-integration, x' is held constant and $dx = dy$:

$$\Gamma(p) = \int_{-\infty}^{\infty}\int_{-\infty}^{\infty} F_1(x')F_2(y)e^{2\pi ip(x'+y)}\,dx'\,dy,$$

which can be separated to give

$$\Gamma(p) = \int_{-\infty}^{\infty} F_1(x')e^{2\pi i px'}\, dx' \cdot \int_{-\infty}^{\infty} F_2(y)e^{2\pi i py}\, dy$$
$$= \Phi_1(p) \cdot \Phi_2(p).$$

2.3.2 Examples of convolutions

One of the chief uses of convolutions is to generate new functions which are easy to transform using the convolution theorem.

Convolution of a function with a δ-function, $\delta(x - a)$, gives

$$C(x) = \int_{-\infty}^{\infty} F(x - x')\delta(x' - a)dx' = F(x - a)$$

by virtue of the properties of δ-functions. This can be written symbolically as

$$F(x) * \delta(x - a) = F(x - a).$$

Applying the convolution theorem to this is instructive since it yields the shift theorem:

$$F(x) \rightleftharpoons \Phi(p); \qquad \delta(x - a) \rightleftharpoons e^{-2\pi i pa}$$

so that $F(x - a) = F(x) * \delta(x - a) \rightleftharpoons \Phi(p)e^{-2\pi i pa}$.

More interesting is the convolution of a pair of δ-functions with another function:

$$[\delta(x - a) + \delta(x + a)] \rightleftharpoons 2\cos(2\pi pa).$$

Hence

$$[\delta(x - a) + \delta(x + a)] * F(x) \rightleftharpoons 2\cos(2\pi pa) \cdot \Phi(p) \qquad (2.7)$$

and this is illustrated in Fig. 2.5.

The Fourier transform of a Gaussian $g(x) = e^{-x^2/a^2}$ is, from Chapter 1, $a\sqrt{\pi}e^{-\pi^2 p^2 a^2}$. The convolution of two unequal Gaussian curves, $e^{-x^2/a^2} * e^{-x^2/b^2}$, can then be done, either as a tiresome exercise in elementary calculus, or by application of the convolution theorem:

$$e^{-x^2/a^2} * e^{-x^2/b^2} \rightleftharpoons ab\pi e^{-\pi^2 p^2 (a^2 + b^2)}$$
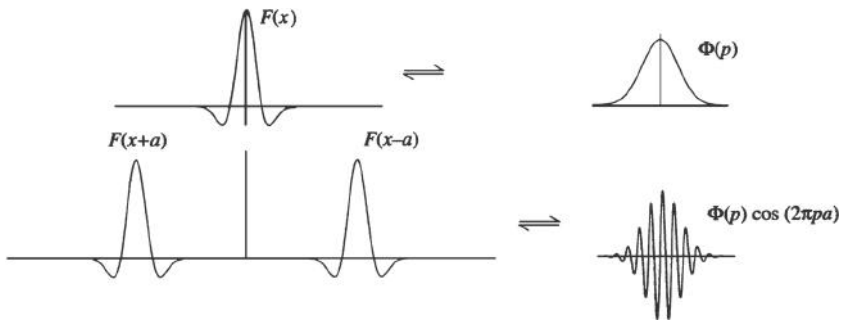
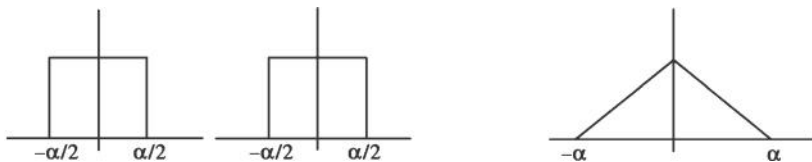Fig. 2.5. Convolution of a pair of δ-functions with $F(x)$, and its transform.

Fig. 2.6. The triangle function, $\Lambda_a(x)$, as the convolution of two top-hat functions.

and the Fourier transform of the right-hand side is

$$\frac{ab\sqrt{\pi}}{\sqrt{a^2 + b^2}}e^{-x^2/(a^2+b^2)} \tag{2.8}$$

so that we arrive at a useful practical result:

**the convolution of two Gaussians of width parameters a and b
is another Gaussian of width parameter $\sqrt{a^2 + b^2}$**

or, to put it another way, the resulting half-width is the Pythagorean sum of the two component half-widths.

The convolution of two equal top-hat functions (Fig. 2.6) is a good example of the power of the convolution theorem. It can be seen by inspection that the convolution of two top-hat functions, each of height h and width a, is going to be a triangle, usually called the 'triangle function' and denoted by $\Lambda_a(x)$, with height $h^2 a$ and base length $2a$.

The Fourier transform of this triangle function can be done by elementary integration, splitting the integral into two parts: $x = -a \to 0$ and $x = 0 \to a$. This, too, is tiresome. On the other hand, it is trivial to see that if $h\Pi_a(x) \rightleftharpoons ah\operatorname{sinc}(\pi pa)$ then $h^2 a\Lambda_a(x) \rightleftharpoons a^2 h^2 \operatorname{sinc}^2(\pi pa)$ or, more usefully,

$$h\Lambda_a(x) \rightleftharpoons ah\operatorname{sinc}^2(\pi pa)$$

since the height of the sinc^2-function is the area under the triangle.

2.3.3 The autocorrelation theorem

This is superficially similar to the convolution theorem but it has a different physical interpretation. This will be mentioned later in connection with the Wiener–Khinchine theorem. The autocorrelation function of a function $F(x)$ is defined as

$$A(x) = \int_{-\infty}^{\infty} F(x')F(x + x')dx'.$$

The process of autocorrelation can be thought of as a multiplication of every point of a function by another point at distance x' further on, and then summing all the products; or like a convolution as described earlier, but with identical functions and without taking the mirror-image of one of the two.

There is a theorem similar to the convolution theorem. Beginning with the definition

$$A(x) = \int_{-\infty}^{\infty} F(x')F(x + x')dx'$$

Fourier transform both sides:

$$\Gamma(p) = \int_{-\infty}^{\infty} A(x)e^{2\pi ipx}\,dx = \int_{-\infty}^{\infty}\int_{-\infty}^{\infty} F(x')F(x + x')e^{2\pi ipx}\,dx'\,dx.$$

Let $x + x' = y$. Then, if x' is held constant, $dx = dy$:

$$\Gamma(p) = \int_{-\infty}^{\infty}\int_{-\infty}^{\infty} F(x')F(y)e^{2\pi ip(y-x')}\,dx'\,dy,$$

which can be separated into

$$\Gamma(p) = \int_{-\infty}^{\infty} F(x)e^{-2\pi ipx'}\,dx' \cdot \int_{-\infty}^{\infty} F(y)e^{2\pi ipy}\,dy$$
$$= \Phi^{\star}(p) \cdot \Phi(p)$$

so that

$$A(x) \rightleftharpoons |\Phi(p)|^2.$$

It is worth noting that, since $\Phi^{\star}(p) \cdot \Phi(p)$ is real, an autocorrelation is automatically a symmetrical function of x. This is something which may be intuitively obvious anyway.

The Wiener–Khinchine theorem, to be described in Chapter 4, may be thought of as a physical version of this theorem. It says that, if $F(t)$ represents a signal, then its autocorrelation is (apart from a constant of proportionality) the Fourier transform of its power spectrum, $|\Phi(\nu)|^2$.

2.4 The algebra of convolutions

You can think of convolution as a mathematical operation analogous to addition, subtraction, multiplication, division, integration and differentiation. There are rules for combining convolution with the other operations. It cannot be associated with multiplication for example, and in general

$$[A(x) * B(x)] \cdot C(x) \neq A(x) * [B(x) \cdot C(x)].$$

But convolution signs and multiplication signs can be exchanged across a Fourier transform symbol, and this is very useful in practice. For example,

$$[A(x) * B(x)] \cdot [C(x) * D(x)] \rightleftharpoons [a(p) \cdot b(p)] * [c(p) \cdot d(p)].$$

(Obviously upper-case and lower-case letters have been used to associate Fourier pairs.)

As further examples:

$$A(x) * [B(x) \cdot C(x)] \rightleftharpoons a(p) \cdot [b(p) * c(p)],$$
$$[A(x) + B(x)] * [C(x) + D(x)] \rightleftharpoons [a(p) + b(p)] \cdot [c(p) + d(p)],$$
$$[A(x) * B(x) + C(x) \cdot D(x)] \cdot E(x) \rightleftharpoons [a(p) \cdot b(p) + c(p) * d(p)] * e(p).$$

Insofar as we use Fourier transforms in physics and engineering, we are concerned mostly with functions and manipulations like this to solve problems, and fluency in this relatively easy algebra is the key to success. Computation, rather than calculation, is involved, and there is much software available to compute Fourier transforms digitally. However, most computation is done using complex exponentials and these involve the full complex transform. A later chapter deals with this subject.

2.4.1 Convolution of two δ-functions

The convolution of two δ-functions can be regarded as the limiting case of the convolution of two Gaussians: in other words it is another δ-function,

$$A\delta(x) * B\delta(x) = AB\delta(x),$$

and this follows, after a few lines of algebra, from the definition of the δ-function as

$$\lim_{a \to 0} \frac{1}{a\sqrt{\pi}} \cdot e^{-x^2/a^2}.$$

2.5 Other theorems

2.5.1 The derivative theorem

If $\Phi(p)$ and $F(x)$ are a Fourier pair $F(x) \rightleftharpoons \Phi(p)$, then

$$dF/dx \rightleftharpoons -2\pi i p \Phi(p).$$

Proofs are elementary. You can integrate dF/dx by parts or you can differentiate[3] $F(x)$:

$$F(x) = \int_{-\infty}^{\infty} \Phi(p) e^{-2\pi i px} \, dp.$$

Differentiate with respect to x:

$$dF/dx = \int_{-\infty}^{\infty} -2\pi i p \Phi(p) e^{-2\pi i px} \, dp$$

$$= -2\pi i \int_{-\infty}^{\infty} p \Phi(p) e^{-2\pi i px} \, dp \qquad (2.9)$$

and the right-hand side is $-2\pi i$ times the Fourier transform of $p\Phi(p)$.

> *Example 1:* The top-hat function $\Pi_a(x) \rightleftharpoons a \operatorname{sinc}(\pi pa)$. If the top-hat function is differentiated with respect to x, the result is a pair of δ-functions at the points where the slope was infinite:
>
> $$\frac{d\Pi_a(x)}{dx} = \delta(x + a/2) - \delta(x - a/2).$$
>
> Transforming both sides gives
>
> $$\delta(x + a/2) - \delta(x - a/2) \rightleftharpoons e^{-\pi i pa} - e^{\pi i pa} = -2i \sin(\pi pa)$$
> $$= -2\pi i p[a \operatorname{sinc}(\pi pa)].$$

The theorem extends to further derivatives:

$$d^n F(x)/dx^n \rightleftharpoons (-2\pi i p)^n \Phi(p)$$

and much use is made of this in mathematics.

> *Example 2:* If the moment of inertia about the y-axis of a symmetrical curve is infinite, its Fourier transform has a cusp at the origin. Because
>
> $$\int_{\infty}^{\infty} f(x)dx = \phi(0),$$

---

[3] A word of caution: this works only if $F(x)$ is an analytic function obeying the Dirichlet conditions. Do not try it with a δ-function or a Heaviside step-function, for instance.

if

$$\left(\frac{\partial^2 f}{\partial x^2}\right)_{x=0} = -4\pi^2 \int_{-\infty}^{\infty} p^2 \phi(p) dp = \infty$$

there is a discontinuity in $(\partial f/\partial x)$ at the origin.

Example 3: The differential equation of simple harmonic motion is

$$m d^2 F(t)/dt^2 + k F(t) = 0,$$

where $F(t)$ is the displacement of the oscillator from equilibrium at time t. If we Fourier-transform this equation, $F(t)$ becomes $\Phi(\nu)$ and $d^2 F/dt^2$ becomes $-4\pi^2 \nu^2 \Phi(\nu)$. The equation then becomes

$$\Phi(\nu)(k/m - 4\pi^2 \nu^2) = 0,$$

which, apart from the trivial solution $\Phi(\nu) = 0$, requires

$$\nu = \pm\frac{1}{2\pi}\sqrt{\frac{k}{m}}$$

– and this is just a small taste of the power which is available for the solution of differential equations using Fourier transforms.

2.5.2 The convolution derivative theorem

$$\frac{d}{dx}[F_1(x) * F_2(x)] = F_1(x) * \frac{dF_2(x)}{dx} = \frac{dF_1(x)}{dx} * F_2(x). \qquad (2.10)$$

The derivative of the convolution of two functions is the convolution of either of the two with the derivative of the other. The proof is simple and is left as an exercise.

2.5.3 Parseval's theorem

This is met under various guises. It is sometimes called 'Rayleigh's theorem' or simply the 'power theorem'. In general it states that

$$\int_{-\infty}^{\infty} F_1(x) F_2^*(x) dx = \int_{-\infty}^{\infty} \Phi_1(p) \Phi_2^*(p) dp, \qquad (2.11)$$

where the superscript * denotes a complex conjugate. The proof of the theorem is given in Appendix A.1.
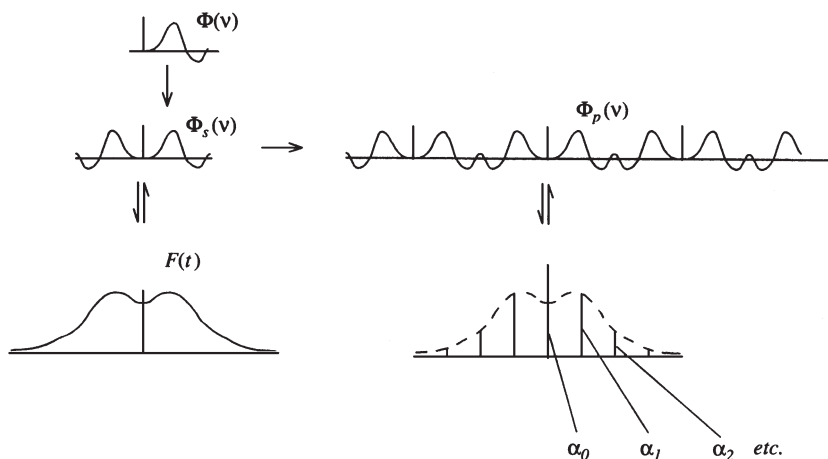
Fig. 2.7. The sampling theorem.

Two special cases of particular interest are

$$\frac{1}{P} \int_0^P |F(x)|^2\, dx = \sum_{-\infty}^{\infty} (a_n^2 + b_n^2) = \frac{A_0^2}{4} + \frac{1}{2} \sum_1^{\infty} [A_n^2 + B_n^2], \qquad (2.12)$$

which is used for finding the power in a periodic waveform, and

$$\int_{-\infty}^{\infty} |F(x)|^2\, dx = \int_{-\infty}^{\infty} |\Phi(p)|^2\, dp \qquad (2.13)$$

for non-periodic Fourier pairs.

2.5.4 The sampling theorem

This is also known as the 'cardinal theorem' of interpolary function theory, and originated with Whittaker,[4] who asked and answered the following question: how often must a signal be measured (sampled) in order that all the frequencies present should be detected? The answer is that the sampling interval must be the reciprocal of twice the highest frequency present.

The theorem is best illustrated with a diagram (Fig. 2.7). The highest frequency is sometimes called the 'folding frequency', or alternatively the 'Nyquist' frequency, and is given the symbol ν_f.

Suppose that the frequency spectrum, $\Phi(\nu)$, of the signal is symmetrical about the origin and stretches from $-\nu_f$ to ν_f. The convolution of this with a Dirac comb of period $2\nu_0$ provides a periodic function and the Fourier transform

[4] J. M. Whittaker, *Interpolary Function Theory*, Cambridge University Press, Cambridge, 1935.

of this periodic function is the *product* of a Dirac comb with the original signal (and, to be strict, its reflection in the origin): in other words it is the set of Fourier coefficients in the series representing the periodic function. The periodic function is known, provided that the coefficients are known, and the coefficients are the values of the original signal $F(t)$, at intervals $1/(2\nu_f)$, multiplied by a suitable constant. The more coefficients are known, the more harmonics can be added to make the spectrum, and the more detail can be seen in the function when it is reconstructed. With the help of the interpolation theorem (below) all the points between the sample points can be filled in.

Formally, the process can be written with $F(t)$ and $\Phi(\nu)$ a Fourier pair as usual. The Fourier transform of $F(t)\text{III}_a(t)$ is

$$\int_{-\infty}^{\infty} F(t)\text{III}_a(t)e^{-2\pi i\nu t}\,dt = \Phi(\nu) * \text{III}_{1/a}(\nu).$$

Rewrite the left-hand side as

$$\int_{-\infty}^{\infty} F(t)\sum_{n=-\infty}^{\infty}\delta(t-na)e^{-2\pi i\nu t}\,dt = \sum_{n=-\infty}^{\infty}\int_{-\infty}^{\infty}F(t)\delta(t-na)e^{-2\pi i\nu t}\,dt$$

$$= \sum_{n=-\infty}^{\infty}F(na)e^{-2\pi i\nu na} = \Phi'(\nu).$$

The left-hand side is now a Fourier series, so that $\Phi'(\nu)$ is a periodic function, namely the convolution of $\Phi(\nu)$ with a Dirac comb of period $1/a$. The constraint is that $\Phi(\nu)$ must occupy the interval $-1/(2a)$ to $1/(2a)$ only; in other words, $1/a$ is twice the highest frequency in the function $F(t)$, in accordance with the sampling theorem.

2.6 Aliasing

In the sampling theorem it is strictly necessary that the signal should contain no power at frequencies above the folding frequency. If it does, this power will be 'folded' back into the spectrum and will appear to be at a lower frequency. If the frequency is $\nu_f + \nu_a$ it will appear to be at $\nu_f - \nu_a$ in the spectrum. If it is at twice the folding frequency, it will appear to be at zero frequency. For example, a sine-wave sampled at intervals $a, 2\pi + a, 4\pi + a, \dots$ will give a set of samples which are identical. There are, in effect, 'beats' between the frequency and the sampling rate. It is always necessary to take precautions when examining a signal in order to be sure that a given 'spike' corresponds to the apparent frequency. This can be done either by deliberate filtering of the incoming signal, or by making several measurements at different sampling
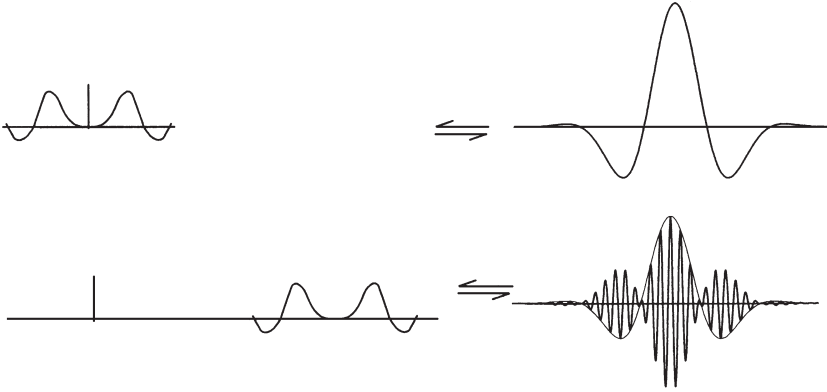
Fig. 2.8. A signal occupying a high alias of a fundamental in frequency space, and its recovery by deliberate undersampling or 'demodulating'.

frequencies. The former is the obvious method but not necessarily the best: if the signal is in the form of a pulse and is in a noisy environment, a lot of the power can be lost by filtering.

Aliasing can be put to good use. If the frequency band stretches from ν_0 to ν_1, the empty frequency band between ν_0 and 0 can be divided into a number of equal frequency intervals each less than $2(\nu_1 - \nu_0)$. The sampling interval then need be only $1/[2(\nu_1 - \nu_0)]$ instead of $1/(2\nu_1)$. This is a way of demodulating the signal, and the spectrum that is recovered appears to occupy the first alias even though the original occupied a possibly much higher one. The process is illustrated in Fig. 2.8.

2.6.1 The interpolation theorem

This too comes from Whittaker's interpolary function theory. If the signal samples are recorded, the values of the signal in between the sample points can be calculated. The spectrum of the signal can be regarded as the product of the periodic function with a top-hat function of width $2\nu_f$. In the signal, each sample is replaced by the convolution of the sinc-function with the corresponding δ-function. Each sample, $a_n \delta(t - t_n)$, is replaced by the sinc-function, $a_n \text{sinc}(\pi \nu_f)$, and each sinc-function conveniently has zeros at the positions of all the other samples (this is hardly a coincidence, of course) so that the signal can be reconstructed from a knowledge of its samples, which are the coefficients of the Fourier series which form its spectrum.

This is much used in practical physics, where digital recording of data is common, and generally the signal at a point can be well enough recovered by a

sum of sinc-functions over twenty or thirty samples on either side. The reason for this is that, unless there is a very large amplitude to a sample at some distant point, the sinc-function at a distance of 30π from the sample has fallen to such a low value that it is lost in the noise. It depends obviously on practical details such as the signal-to-noise ratio in the original data and, more importantly, on the absence of any power at frequencies higher than the folding frequency.

Stated formally, the signal $F(t)$ sampled at times $0, t_0, 2t_0, 3t_0, 4t_0, 5t_0, \ldots$ can be computed at any intermediate point t as the sum

$$F(nt_0 + t) = \sum_{m=-N}^{N} F\{(n+m)t_0\}\mathrm{sinc}[\pi(m - t/t_0)],$$

where N, infinite in theory, is about 20–30 in practice. The sum cannot be computed accurately near the ends of the data stream and there is a loss of N samples at each end unless fewer samples are taken there.

2.6.2 The similarity theorem

This is fairly obvious: if you stretch $F(x)$ so that it is twice as wide, then $\Phi(p)$ will be only half as wide, but twice as high as it was. Formally,

$$\text{if } F(x) \rightleftharpoons \Phi(p) \text{ then } F(ax) \rightleftharpoons |(1/a)|\Phi(p/a).$$

The proof is trivial, and it is done by substituting $x = ay, dx = a\,dy; p = z/a, dp = (1/a)dz$. Because the integrals are between $-\infty$ and ∞, the variables for integration are 'dummy' variables and can be replaced by any other symbol not already in use.

2.7 Worked examples

2.7.1 An arithmetical result using Parseval's theorem

The sawtooth used in Chapter 1 shows an interesting result using Parseval's theorem. The nth sine-coefficient, as we saw, is $(-1)^{n+1}2h/(n\pi)$. The sum to infinity of the squares is

$$\sum_{n=1}^{\infty} \frac{4h^2}{\pi^2 n^2} = \frac{2}{P} \int_{-P/2}^{P/2} \left[\frac{2hx}{P}\right]^2 dx$$

$$= \frac{8h^2}{P^3} \left[\frac{x^3}{3}\right]_{-P/2}^{P/2}$$

$$= \frac{2h^2}{3} = \frac{4h^2}{\pi^2} \sum_{n=1}^{\infty} \frac{1}{n^2}$$

so that finally

$$\sum_{n=1}^{\infty} \frac{1}{n^2} = \frac{\pi^2}{6}.$$

This is an example of an arithmetical result coming from a purely analytic calculation. As a way of computing π it is not very efficient: it is accurate to only six significant figures (3.14159) after one million terms. Using the fact that $\pi = 6 \sin^{-1}(1/2)$, with $\sin^{-1}$ obtained by integrating $1/\sqrt{1-x^2}$ term-by-term, is much more efficient.

2.7.2 Alternating pulse-heights

In a rectangular waveform with pulses of length $a/4$ separated by spaces of length $a/4$ and with alternate rectangles twice the height of their neighbours, the amplitude of the second harmonic is greater than the fundamental amplitude.

The waveform can be represented by

$$F(t) = h\,\Pi_{a/4}(t) * [\text{III}_a(t) + \text{III}_{a/2}(t)].$$

The Fourier transform is

$$\Phi(\nu) = (ah/4)\text{sinc}(\pi\nu a/4) \cdot [(1/a)\text{III}_{1/a}(\nu) + (2/a)\text{III}_{2/a}(\nu)]$$

and the teeth of this Dirac comb are at $\nu = 1/a, 2/a, \ldots$, with heights

$$(h/4)\text{sinc}(\pi/4), (3h/4)\text{sinc}(\pi/2), (h/4)\text{sinc}(3\pi/4)\ldots$$

and the ratio of heights of the first and second harmonics is $\sqrt{2} : 3$.

This effect can be seen in astronomy or radioastronomy when searching for pulsars using a real-time Fourier transformer. The 'interpulses' between the main pulses generate extra power in the second harmonic and can make it larger than the fundamental (Fig. 2.9).
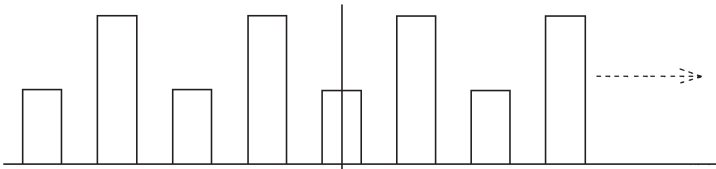

Fig. 2.9. A square-wave with alternating pulse heights. The Fourier transform will show more power in the second harmonic than in the fundamental.
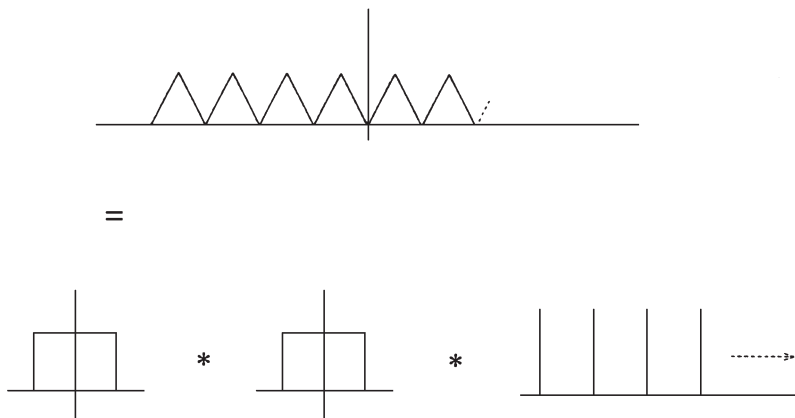
Fig. 2.10. The double-sawtooth waveform.

2.7.3 The double-sawtooth waveform

This cannot be regarded as the convolution of two rectangular waveforms of equal mark–space[5] ratio, since the effect of integration is to give an embarrassing infinity. Instead it is the convolution of a top-hat of width a with another identical top-hat and with a Dirac comb of period $2a$. Thus

$$\Pi_a(t) * \Pi_a(t) * \amalg_{2a}(t) \rightleftharpoons (a/2)\mathrm{sinc}^2(\pi \nu a) \cdot \amalg_{1/(2a)}(\nu).$$

So the amplitudes, which occur at $\nu = 1/(2a), 1/a, 3/(2a), \dots$, are $2a/\pi^2, 0, 2a/(9\pi^2), 0, 2a/(25\pi^2), \dots$

2.7.4 Convolution with a sinusoid

Consider an ordinary analytic function of x which obeys the Dirichlet conditions and is neither symmetrical nor antisymmetrical. Its convolution with a cosine of unit amplitude and period $1/r$ is formally

$$C(x) = f(x) * \cos(2\pi r x).$$

To calculate this convolution, first split the function $f(x)$ into its symmetrical and antisymmetrical parts (see Fig. 8.1 for how to do this). Then

$$C(x) = [f_s(x) + f_a(x)] * \cos(2\pi r x).$$

The Fourier transform of this is

$$\Gamma(p) = [\phi_s(p) + i\phi_a(p)] \cdot [\delta(p - r) + \delta(p + r)]/2.$$

---

[5] The term 'equal mark–space ratio' comes from radio jargon, and implies that the signal is zero for the same interval as that during which it is not.
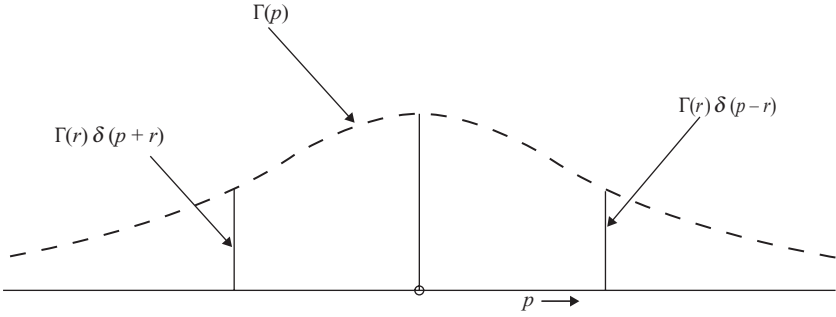
Fig. 2.11. Convolution of a function with a sinusoid. $\Gamma(p)$ is the Fourier transform of $f(x)$ and the two δ-functions are the Fourier transform of $\cos(2\pi r x)$, the other partner in the convolution. The product is the pair of δ-functions modified in height by the appropriate Fourier component of $\Gamma(p)$.

Notice that the product of a function with a δ-function is still a δ-function, i.e.

$$\phi(p) \cdot \delta(p - r) = \phi(r)\delta(p - r).$$

Thus

$$\Gamma(p) = \frac{1}{2}[\phi_s(r)\delta(p - r) + \phi_s(-r)\delta(p + r)$$
$$+ i\phi_a(r)\delta(p - r) + i\phi_a(-r)\delta(p + r)]$$

and, since $\phi_s(r) = \phi_s(-r)$ and $\phi_a(r) = -\phi_a(-r)$, we have

$$\Gamma(p) = \frac{1}{2}\{\phi_s(r)[\delta(p - r) + \delta(p + r)] + i\phi_a(r)[\delta(p - r) - \delta(p + r)]\}$$

and on transforming back we find

$$C(x) = \phi_s(r)\cos(2\pi r x) + \phi_a(r)\sin(2\pi r x)$$

so that $C(x)$ is a sinusoid of amplitude $\sqrt{\phi_s(r)^2 + \phi_a(r)^2}$ and phase-shifted by comparison with the original sinusoid by an angle α, given by

$$\alpha = \tan^{-1}[\phi_a(r)/\phi_s(r)].$$

This result (see Fig. 2.11) is important in the next chapter when we consider the Michelson stellar interferometer and the van Cittert–Zernike theorem.

3

Applications 1: Fraunhofer diffraction

3.1 Fraunhofer diffraction

The application of Fourier theory to Fraunhofer diffraction problems, and to interference phenomena generally, was hardly recognized before the late 1950s. Consequently, only textbooks written since then mention the technique. Diffraction theory, of which interference is only a special case, derives from Huygens' principle: that every point on a wavefront which has come from a source can be regarded as a secondary source; and that all the wavefronts from all these secondary sources combine and interfere to form a new wavefront.

Some precision can be added by using calculus. In Fig. 3.1, suppose that at O there is a source of 'strength' q, defined by the fact that at A, a distance r from O, there is a 'field', E, of strength $E = q/r$. Huygens' principle is now as follows:

> If we consider an area dS on the surface S we can regard it as a source of strength $E\,dS$ giving at B, a distance r' from A, a field $E' = q\,dS/(rr')$. All these elementary fields at B, summed over the transparent part of the surface S, each with its proper phase,[1] give the resultant field at B. This is quite general – and vague.

In elementary Fraunhofer diffraction theory we simplify. We assume the following.

- That only two dimensions need be considered. All apertures bounding the transparent part of the surface S are rectangular and of length unity perpendicular to the plane of the diagram.

---

[1] Remember: phase change $= (2\pi/\lambda) \times$ path change and the paths from different points on the surface S (which, being a wavefront, is a surface of constant phase) to B are all different.
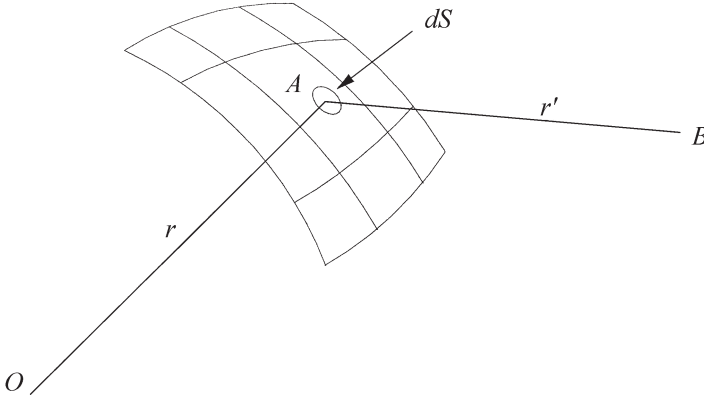
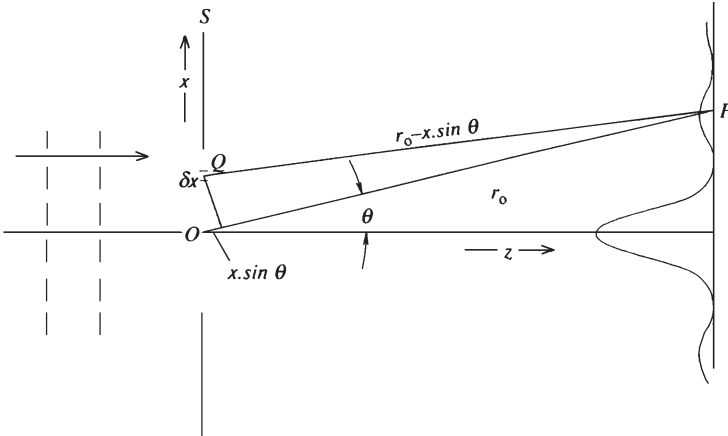Fig. 3.1. Secondary sources in Fraunhofer diffraction.

Fig. 3.2. Fraunhofer diffraction by a plane aperture.

- That the dimensions of the aperture are small compared with r'.
- That r is very large so that the field E has the same magnitude at all points on the transparent part of S, and a slowly varying or constant phase. (Another way of putting it is to say that plane wavefronts arrive at the surface S from a source at $-\infty$.)
- That the aperture S lies in a plane.

To begin, suppose that the source, O, lies on a line perpendicular to the surface S, the diffracting aperture. Use Cartesian coordinates, x in the plane of S, and z perpendicular to this (x and z are traditional here; see Fig. 3.2). Then the magnitude of the field E at P can be calculated.

Consider an infinitesimal strip at Q, of unit length perpendicular to the x, z-plane, of width dx and distance x above the z-axis. Let the field strength[2] there be $E = E_0 e^{2\pi i v t}$. Then the field strength at P from this source will be

$$d\overline{E}(P) = E_0 e^{2\pi i v t} e^{-2\pi i r'/\lambda}\, dx,$$

where r' is the distance QP. The exponent in this last factor is the *phase difference* between Q and P.

For convenience, choose a time t so that the phase of the wavefront is zero at the plane S, i.e. $t = 0$. Then at P

$$\overline{E}(P) = \int_{\text{aperture}, S} E_0 e^{-2\pi i r'/\lambda}\, dx$$

and the aperture S may have opaque spots or partially transmitting spots, so that E_0 is generally a function of x.

This is not yet a useable expression.

Now, because $r' \gg x$ (the condition for Fraunhofer diffraction), we can write

$$r' \approx r_0 - x \sin\theta$$

and then the field $\overline{E}$ at P is obtained by summing all the infinitesimal contributions from the secondary sources like that at Q, and remembering to include the phase-factor for each. The result is

$$\overline{E} = E_0 e^{-2\pi i r_0/\lambda} \int_{\text{aperture}} e^{2\pi i x \sin\theta/\lambda}\, dx$$

and if we write $\sin\theta/\lambda = p$ we have, finally,

$$\overline{E} = E_0 e^{-2\pi i r_0/\lambda} \int_{-\infty}^{\infty} A(x) e^{2\pi i p x}\, dx,$$

where $A(x)$ is the 'aperture function' which describes the transparent and opaque parts of the screen S. The result of the Fourier transform is to give the *amplitude* diffracted through an angle θ. Where it appears on a screen depends on the distance to the screen, and on whether the screen is perpendicular to the z-direction and other geometrical factors.[3]

The important thing to remember is this: that diffraction of a certain wavelength at a certain aperture is always *through an angle*: the variable p conjugate

---

[2] As usual, we use complex variables to represent *real* quantities – in this case the electric field strength. This complex variable is called the 'analytic' signal and the real part of it represents the actual physical quantity at any time at any place.

[3] This is all an approximation: in fact the field *outside* the diffracting aperture is not exactly zero and depends in practice on whether the opaque part of the screen is conducting or insulating and on the direction of polarization of the passing light. These are subtleties which can safely be left to post-graduate students.
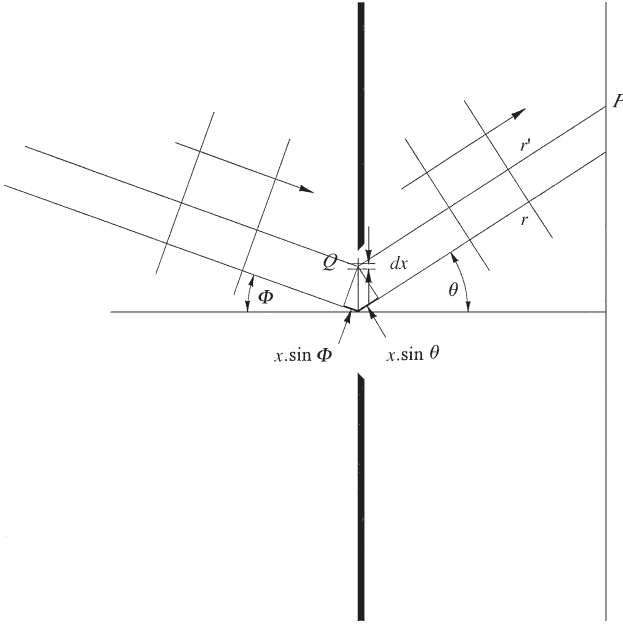
Fig. 3.3. Oblique incidence from a source not on the z-axis.

to x is $\sin\theta/\lambda$ and it is θ which matters. Diffraction theory alone says nothing about the size of the pattern: that depends on geometry.

Very often, in practice, the diffracting aperture is followed by a lens, and the pattern is observed at the focal plane of this lens. The approximation that $r' = r_0 - x\sin\theta$ is now exact, since the image of the focal plane, seen from the diffracting aperture, is at infinity.

Problems in Fraunhofer diffraction can thus be reduced to writing down the aperture function, $A(x)$, and taking its Fourier transform. The result gives the amplitude in the diffraction pattern on a screen at a large distance from the aperture. For example, for a simple parallel-sided slit of width a, the aperture function, $A(x)$, is $\Pi_a(x)$. For two parallel-sided slits of width a separated by a distance b between their centres, $A(x) = \Pi_a(x) * [\delta(x - b/2) + \delta(x + b/2)]$, and so on. Apertures of various sizes are now encompassed by the same formula and the amplitude of the light (or sound, or radio waves or water waves) diffracted by the aperture through an angle θ can be calculated. The *intensity* of the wave is given by the r.m.s. value of the amplitude multiplied by its complex conjugate and the factor $e^{2\pi i r_0/\lambda}$ disappears when this is done.

If the original source is not on the z-axis, then the amplitude of E at $z = 0$ contains a phase factor, as in Fig. 3.3.
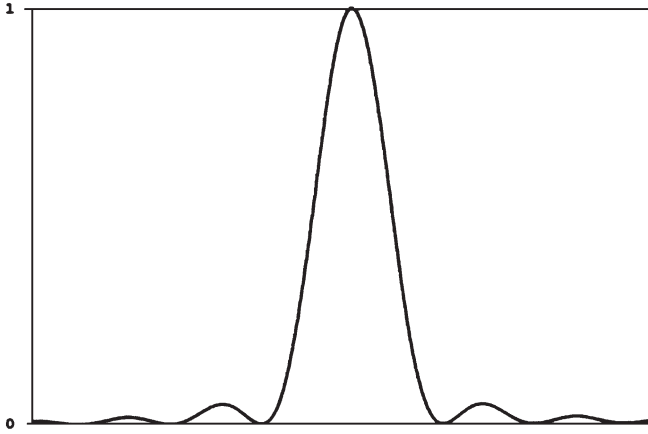
Fig. 3.4. The intensity pattern, $\mathrm{sinc}^2(\pi a \sin\theta/\lambda)$, from diffraction at a single slit.

$W - W'$ is a wavefront (a surface of constant phase) and, if we choose a moment when the phase is zero at the origin, the phase at x at that moment is given by $(2\pi/\lambda)x \cdot \sin\phi$, and the phase factor that must multiply E_0 is $e^{(-2\pi/\lambda)x\sin\phi}$.

The magnitude at P is then

$$\overline{E} = E_0 e^{2\pi i r_0/\lambda} \int_{-\infty}^{\infty} A(x) e^{(-2\pi i/\lambda)x(\sin\theta + \sin\phi)} \, dx$$

and when the Fourier transform is done, the oblique incidence is accounted for by remembering that $p = (\sin\theta + \sin\phi)/\lambda$.

3.2 Examples

3.2.1 Single-slit diffraction, normal incidence

For a single slit with parallel sides, of width a, the aperture function is $A(x) = \Pi_a(x)$. Then

$$\overline{E} = k \cdot \mathrm{sinc}(\pi a p) = k \cdot \mathrm{sinc}(\pi a \sin\theta/\lambda)$$

(where k is the constant[4] $E_0 a e^{-2\pi i r_0/\lambda}$), and the intensity is this multiplied by its complex conjugate:

$$\overline{EE^*} = I(\theta) = |k|^2 \cdot \mathrm{sinc}^2(\pi a \sin\theta/\lambda). \tag{3.1}$$

See Fig. 3.4.

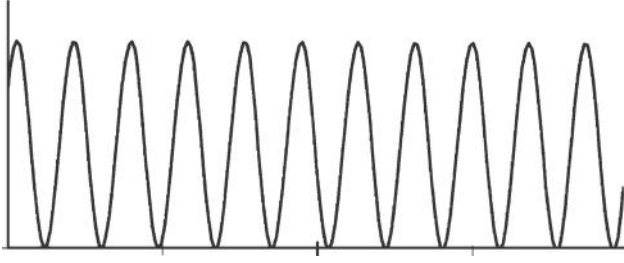[4] For most practical purposes, the *unimportant* constant.

Fig. 3.5. The intensity pattern from interference between two point sources.

3.2.2 Two point sources at $\pm b/2$ (for example, two antennae, transmitting in phase from the same oscillator)

We have

$$A(x) = \delta(x - b/2) + \delta(x + b/2)$$

and the Fourier transform of this is (Chapter 1, equation (1.19))

$$\overline{E} = 2k \cdot \cos(\pi b \sin \theta / \lambda)$$

and the intensity is this amplitude multiplied by its complex conjugate:

$$\begin{aligned} I(\theta) &= 4|k|^2 \cdot \cos^2(\pi b \sin \theta / \lambda) \\ &= 2|k|^2[1 + \cos(2\pi b \sin \theta / \lambda)]. \end{aligned}$$

See Fig. 3.5.

3.2.3 Two slits, each of width a, with centres separated by a distance b (Young's slits, Fresnel's biprism, Lloyd's mirror, Rayleigh's refractometer, Billet's split-lens)

We have

$$A(x) = \Pi_a(x) * [\delta(x - b/2) + \delta(x + b/2)].$$

Then, applying the convolution theorem,

$$I(\theta) = 4k^2 \, \text{sinc}^2(\pi a \sin \theta / \lambda) \cos^2(\pi b \sin \theta / \lambda).$$
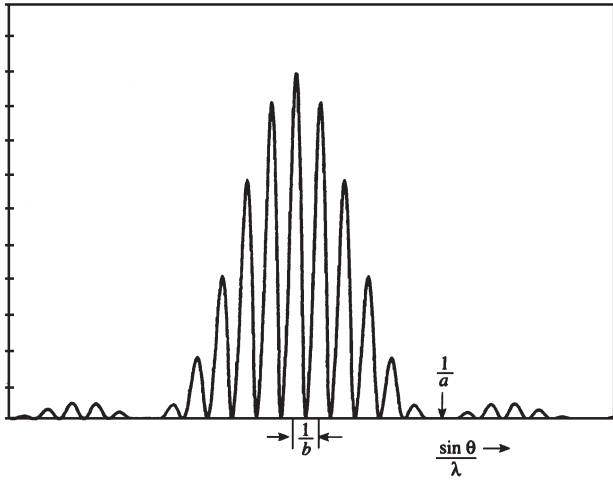
See Fig. 3.6.

Fig. 3.6. The intensity pattern from interference between two slits of width a separated by a distance b.

3.2.4 Three parallel slits, each of width a, with centres separated by a distance b

To simplify the algebra, put $\sin \theta / \lambda = p$:

$$A(x) = \Pi_0(x) * [\delta(x - b) + \delta(x) + \delta(x + b)],$$
$$\overline{A}(p) = k \operatorname{sinc}(\pi p a)[e^{2\pi i b p} + 1 + e^{-2\pi i p b}]$$
$$= k \operatorname{sinc}(\pi p a)[2 \cos(2\pi p b) + 1]$$

and the intensity diffracted at angle θ is

$$I(p) = k^2 \operatorname{sinc}^2(\pi p a)[2 \cos(4\pi p b) + 4 \cos(2\pi p b) + 3]$$
$$= k^2 \operatorname{sinc}^2(\pi a \sin \theta / \lambda)[2 \cos(4\pi b \sin \theta / \lambda) + 4 \cos(2\pi b \sin \theta / \lambda) + 3].$$

See Fig. 3.7.

3.2.5 The transmission diffraction grating

There are two obvious ways of representing the aperture function. In either case we assume that there are N slits, each of width w, each separated from its neighbours by a, the grating constant, and that N is a large number $(10^4 – 10^5)$.

Then, since $A(x) = \Pi_w(x) * \text{III}_a(x)$ represents an infinitely wide grating, its width can be restricted by multiplying it by $\Pi_{Na}(x)$, so that the aperture
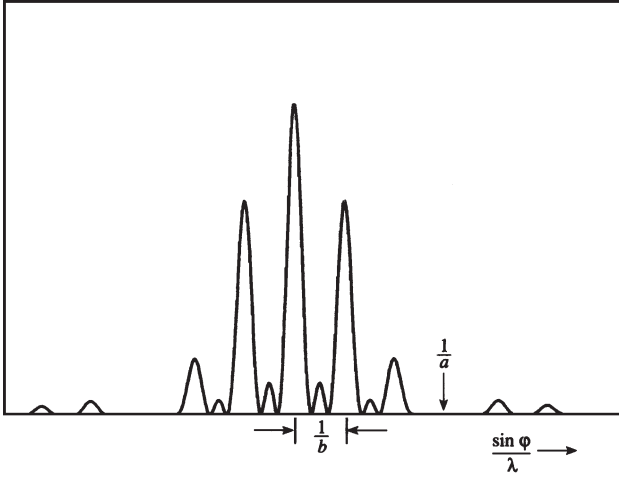
Fig. 3.7. The intensity pattern from interference between three slits of width a, separated by b.

function is

$$A(x) = \Pi_{Na}(x) \cdot [\Pi_w(x) * III_a(x)].$$

Then the diffraction amplitude is

$$\overline{E}(\theta) = Na \cdot \text{sinc}(\pi Na \sin\theta/\lambda) * [w \cdot \text{sinc}(\pi w \sin\theta/\lambda) \cdot (1/a)III_{1/a}(\sin\theta/\lambda)]$$
$$= Nw \cdot \text{sinc}(\pi Na \sin\theta/\lambda) * [\text{sinc}(\pi w \sin\theta/\lambda) \cdot III_{1/a}(\sin\theta/\lambda)].$$

(N.B. The convolution is with respect to $\sin\theta/\lambda$.)

A diagram here is helpful, see Fig. 3.8: the second factor (in the square brackets) is the product of a Dirac comb and a very broad (because w is very small) sinc-function; and the convolution of this with the first factor, a very narrow sinc-function, represents the diffraction produced by the whole aperture of the grating. Since the narrow sinc-function is reduced to insignificance by the time it has reached as far as the next tooth in the Dirac comb, the intensity distribution is this very narrow line profile $\text{sinc}^2(\pi Na \sin\theta/\lambda)$, reproduced at each tooth position with its intensity reduced by the factor $\text{sinc}^2(\pi wa \sin\theta/\lambda)$.

This is not precise, but is close enough for all practical purposes. To be precise, fastidious and pedantic, the aperture function, as described in the older optics textbooks, is

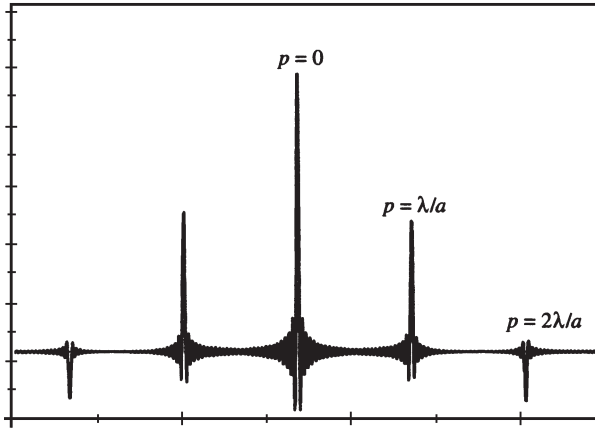$$A(x) = \sum_{n=0}^{N-1} \delta(x - na) * \Pi_w(x)$$

Fig. 3.8. The amplitude transmitted by a diffraction grating.

and since $\delta(x - na) \rightleftharpoons e^{2\pi inpa}$ the diffracted amplitude is

$$\bar{E}(\theta) = k \cdot \mathrm{sinc}(\pi wp) \sum_{n=0}^{N-1} e^{2\pi inpa},$$

where $k = w \cdot E_0 e^{-2\pi ir_0/\lambda}$. The third factor in the equation is the sum of a geometrical progression of common ratio $e^{2\pi ipa}$ and, after a few lines of algebra, the equation becomes

$$\bar{E}(\theta) = k \cdot \mathrm{sinc}(\pi wp)e^{\pi i(N-1)pa} \sin(\pi Npa)/\sin(\pi pa)$$

with $p = \sin\theta/\lambda$ as usual.

The intensity is given by $\bar{E}(\theta)\bar{E}(\theta)^*$. The exponential factor disappears together with its own complex conjugate and if we write I_0 for E_0^2 the intensity distribution is

$$I(\theta) = I_0 \cdot \left(\frac{\sin(\pi Npa)}{\sin(\pi pa)}\right)^2 \mathrm{sinc}^2(\pi wp). \tag{3.2}$$

If N is large, the first factor is very similar to a sinc^2-function, especially near the origin, where $\sin(\pi pa) \simeq \pi pa$, and although it is exact it yields no more information about the diffraction pattern details than the previous approximate derivation. Either way, the factor in the first bracket gives details about the line shape and the resolution to be obtained, and the third factor, the broad sinc^2-function, gives information about the intensities of the various diffraction maxima in the pattern.

In particular, if a maximum for one wavelength λ falls at the same diffraction angle θ as the first zero of an adjacent wavelength $\lambda + \delta\lambda$ (the usual
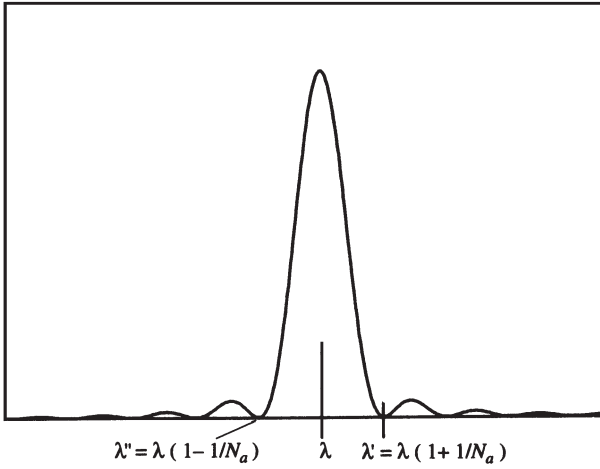
Fig. 3.9. The shape of a spectrum line from a grating. The profile has the form $\text{sinc}^2(\pi Nap)$.

criterion for resolution in a grating spectrometer), the two values of p can be compared:

$$\text{for } \lambda \text{ at maximum, } \sin\theta \sim \theta = m\lambda/a;$$
$$\text{for } \lambda \text{ at first zero, } \theta = m\lambda/a + \lambda/(Na),$$

which is the same angle as for $\lambda + \delta\lambda$ at maximum, i.e. $m(\lambda + \delta\lambda)/a$, whence

$$\delta\lambda = \lambda/(mN),$$

which gives the theoretical resolution of the grating.

Two points are worth noting.

(1) No one expects to get the full theoretical resolution from a grating. Manufacturing imperfections may reduce it in practice to ∼70% of the theoretical value.

(2) Although this is the closest spacing for which two wavelengths can still produce separate images, more closely spaced wavelengths can be disentangled if the combined shape is known. The process of *deconvolution* can be used to enhance resolution if need be, although the improvement can be disappointing.

The sinc^2-function in Fig. 3.9 represents the radiation intensity near the diffraction image of a monochromatic spectrum line. Although the diffraction intensity corresponds to a *direction*, θ, in practice a lens or a mirror will focus
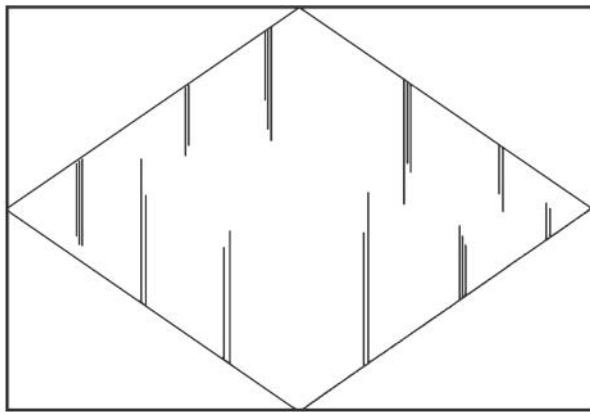
Fig. 3.10. A diffraction grating with a diamond-shaped apodizing mask.

all the radiation that comes from the grating at that angle θ to a place on its focal surface where the CCD or other photo-sensitive detector is located.

The intensity distribution in the image will be the square modulus of the amplitude distribution, in this case a sinc^2-function, which has its width[5] determined by the width Na of the grating.

The minima at λ' and λ'' are at a wavelength difference $\pm 1/(Na)$, from the properties of the sinc^2-function.

Interesting things can be done to the amplitude of the radiation transmitted (or reflected) by the grating by covering the grating with a mask. A diamond-shaped mask, for example (Fig. 3.10), will change the aperture function from $\Pi_a(x)$ to $\Lambda_a(x)$ and the Fourier transform of the aperture function is then

$$\overline{E}(\theta) = k \cdot \text{sinc}^2(\pi(aN/2)\sin\theta/\lambda) * [\text{sinc}(\pi w \sin\theta/\lambda) \cdot (1/a)\text{Ш}_{1/a}(\sin\theta/\lambda)].$$

The shape of the image of a monochromatic line is changed. Instead of $\text{sinc}^2[\pi Na(\sin\theta/\lambda)]$, it becomes $\text{sinc}^4[(\pi Na/2)(\sin\theta/\lambda)]$. The sinc^4-function is nearly twice as wide as the sinc^2-function and the peak intensity of the light is reduced by a factor of 4, but the intensities of the 'side-lobes' are reduced from 1.6×10^{-3} to 2.56×10^{-6} of the main peak intensity. This reduction is important if faint satellite lines are to be identified – for example in studies of fine structure or Raman-scattered lines, where the satellite intensities are 10^{-6} of the parent or less. The process, which is widely used in optics and radioastronomy, is called *apodizing*.[6]

---

[5] By 'width' we mean here the full width at half maximum intensity of the spectrum line, usually denoted by 'FWHM'.

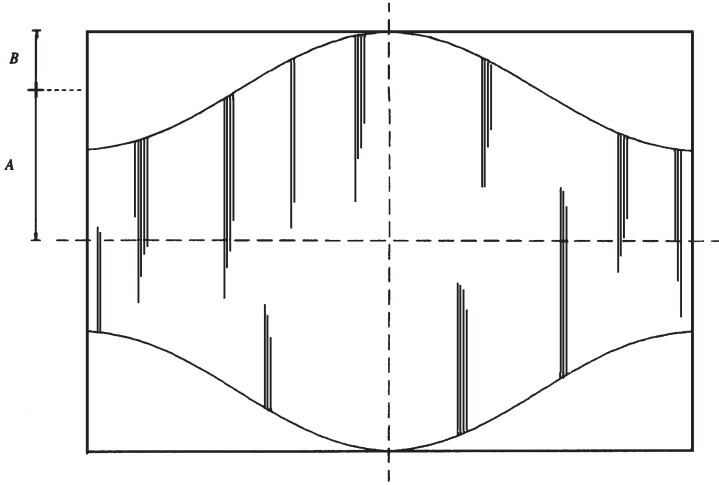[6] From the Greek 'without feet', implying that the side-lobes are reduced or removed.

Fig. 3.11. An $A + B\cos(2\pi x/(Na))$ apodizing mask for a grating.

There are more subtle ways of reducing the side-lobe intensities by masking the grating. For example, a mask as in Fig. 3.11 allows the amplitude transmitted to vary sinusoidally across the aperture according to

$$\Pi_{Na}(x)[A + B\cos(2\pi x/(Na))].$$

The Fourier transform of this is

$$\overline{E}(\theta) = Na\operatorname{sinc}(\pi pNa) * \{A\delta(p) + (B/2)[\delta(p - 1/(Na)) + \delta(p + 1/(Na))]\}$$

and this is the sum of three sinc-functions, suitably displaced. Figure 3.12 illustrates the effect.

Even more complicated masking is possible and in general what happens is that the power in the side-lobes is redistributed according to the particular problem that is faced. The nearer side-lobes can be suppressed almost completely, for example, and the power absorbed into the main peak or pushed out into the 'wings' of the line. Favourite values for A and B are $A = 0.35H$ and $B = 0.15H$, where H is the length of the grating rulings (*not* the ruled width of the grating).

3.2.6 Apertures with phase-changes instead of amplitude changes

The aperture function may be (indeed *must* be) bounded by a mask edge of finite size and it is possible – for example by introducing refracting elements – to change the phase as a function of x. A prism or lens would do this.
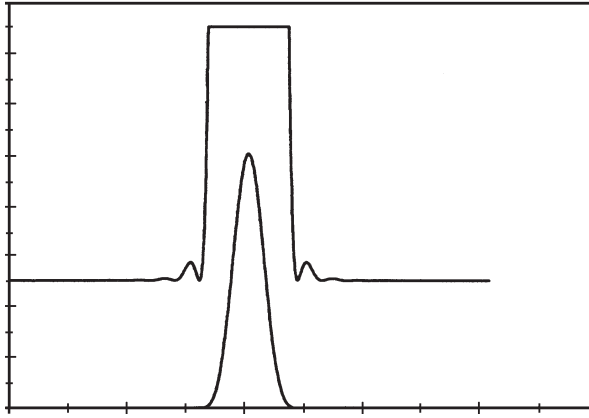
Fig. 3.12. The intensity-profile of a spectrum line from a grating with a sinusoidal apodizing mask. The upper curve is the lower curve multiplied by 1000 to show the low level of the secondary maxima.

3.2.7 Diffraction at an aperture with a prism

Because the 'optical' path is n times the geometrical path, the passage of light through a distance x in a medium of refractive index n introduces an *extra* 'path' $(n - 1)x$ compared with the same length of path in air or vacuum. Consequently there is a phase change $(2\pi/\lambda)(n - 1)x$.

There is thus (Fig. 3.13) a variation of *phase* instead of transmission across the aperture, so that the aperture function is complex. If the prism angle is ϕ and the aperture width is a, the thickness of the prism at its base is $a \tan \phi$ and, when parallel wavefronts coming from $-\infty$ have passed through the prism, the phases at the apex and the base of the prism are 0 and $(2\pi/\lambda)(n - 1)a \tan \phi$.

However, we can choose the phase to be zero at the centre of the aperture, and this is usually a good idea because it saves unnecessary algebra later on.

Then the phase at any point x in the aperture is $\zeta(x) = (2\pi/\lambda)x(n - 1)\tan \phi$ and the aperture function describing the Huygens wavelets is

$$A(x) = \Pi_a(x)e^{(2\pi i/\lambda)x(n-1)\tan \phi}.$$

The Fourier transform of this, with $p = \sin \theta/\lambda$ as usual, is

$$\overline{E}(\theta) = A \int_{-a/2}^{a/2} e^{(2\pi i/\lambda)x(n-1)\tan \phi}e^{2\pi ipx}\, dx$$

so that, after integrating and multiplying the amplitude distribution by its complex conjugate, we get

$$I(\theta) = A^2a^2 \operatorname{sinc}^2\{a\pi[p + (n - 1)\tan \phi/\lambda]\}.$$
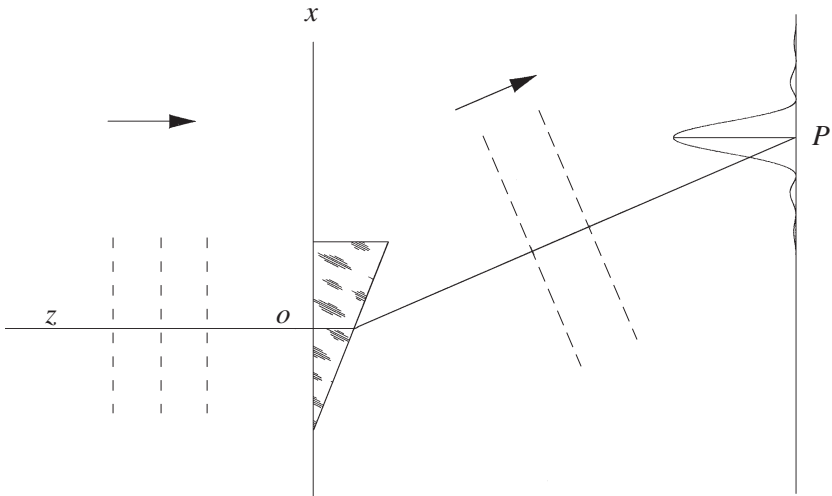
Fig. 3.13. A single-slit aperture with a prism and its displaced diffraction pattern.

Notice that if $n = 1$ we have the same expression as in equation (3.1). Here we see that the shape of the diffraction function is identical, but that the principal maximum is shifted to the direction $p = \sin\theta/\lambda = -(n-1)\tan\phi/\lambda$ or to the diffraction angle $\theta = \sin^{-1}[(n-1)\tan\phi]$. This is what would be expected from elementary geometrical optics when θ and ϕ are small.

3.2.8 The blazed diffraction grating

It is only a small step to the description of the diffraction produced by a grating which comprises, instead of alternating opaque and transparent strips, a grid of parallel prisms. There are two advantages in such a construction. Firstly the aperture is completely transparent and no light is lost; and secondly the prism arrangement means that, for one wavelength at least, all the incident light is diffracted into one order of the spectrum.

The aperture function is, as before, the convolution of the function for a single slit with a Dirac comb, the whole being multiplied by a broad $\Pi_{Na}(x)$ representing the whole width of the grating.

The diffracted intensity is then the same shifted sinc^2-function as above, but multiplied by the convolution of a Dirac comb with a narrow sinc-function, the Fourier pair of $\Pi_{Na}(x)$, which represents the shape of a single spectrum line. Now, there is a difference, because the broad sinc-function produced by a single slit has the same width as the spacing of the teeth in the Dirac comb. The zeros

of this broad sinc-function are adjusted accordingly, and for one wavelength the first order of diffraction falls on its maximum, while all the other orders fall on its zeros. For this wavelength, *all* the transmitted light is diffracted into the first order. For adjacent wavelengths the efficiency is similarly high, and in general the efficiency remains usefully high for wavelengths between 2/3 and 3/2 of this wavelength.

This is the 'blaze wavelength' of the grating and the corresponding angle θ is the 'blaze-angle'.

Reflection gratings are made by ruling lines on an aluminium surface with a diamond scribing tip, held at an angle to the surface so as to produce a series of long thin mirrors, one for each ruling. The angle is the 'blaze-angle' that the grating will have, and a similar analysis will show easily that the phase-change across one slit is $(2\pi/\lambda)2a \tan \beta$, where β is the 'blaze-angle' and a the width of one ruling (and the separation of adjacent rulings). In practice, gratings are usually used with light incident normally or near-normally on the ruling facets, that is at an incidence angle β to the surface of the grating. There is then a phase-change of zero across one ruling, but a delay $(2\pi/\lambda)2a \sin \theta$ between reflections from adjacent rulings. If this phase-change equals 2π then there is a principal maximum in the diffraction pattern.

Transmission gratings, generally found in undergraduate teaching laboratories, are usually blazed, and the effect can easily be seen by holding one up to the eye and looking at a fluorescent lamp through it. The diffracted images in various colours are much brighter on one side than on the other.

3.3 Babinet's principle

This is a neglected but useful corollary of Fraunhofer diffraction theory. It says, in effect, that the Fraunhofer diffraction pattern from any aperture is the same as that from the *complementary obstruction*. In other words, if the screen is removed and an opaque object of the same shape as the screen aperture is put in the same place, the same diffraction pattern will be seen. The reasoning is simple: if there were no screen, the amplitude scattered at an angle θ would be zero. If there is a screen with an aperture, there is a (complex) scattering amplitude $A(\theta)$. It follows then that if the screen is removed an amplitude $-A(\theta)$ has been added to cancel out the first. That amplitude must have come from the obstructing part of the screen, and if that alone is diffracting it will have an amplitude $-A(\theta)$ and an intensity AA^* – in other words the same as that from the original aperture.

(Babinet's principle fails on the axis, i.e. at zero diffraction angle. Why is this?)

Its practical application was originally in Young's *eriometer*, a device which measures the size of blood cells. In modern times its application is in nuclear physics. Fraunhofer diffraction theory is not confined to light or to electromagnetic radiation generally, but holds true for sound or any other kind of wave motion. Electron diffraction is well understood. The de Broglie waves of an electron, neutron or ion beam may be scattered from a particular species of atomic nucleus to give information, via the differential scattering amplitude, about the shape and structure of the scattering centres.

3.4 Dipole arrays

There is an obvious analogy between the diffraction grating and a linear array of equally-spaced dipole aerials. A diffraction grating reflects or transmits coherent plane wavefronts and the dipole array, fed from a common radio-frequency oscillator by properly matched transmission lines (in which the speed of transmission is a considerable fraction, $1/10$ to $3/4$, of the speed of light, depending on the type of line, dielectric constants etc.), is in effect an array of coherent point sources, at least at large distances from the array.

There are differences which make the aerial array interesting. These are chiefly that the spacing of the individual dipoles is changeable, and that phase delays can be introduced in the feeds to the individual aerials. We can represent the aerial array by a shah-function corresponding to the aperture function in optics:

$$A(x) = III_a(x)\Pi_{Na}(x),$$

where N is the number of dipoles in the array and a is the spacing.

The output beam amplitude is the Fourier transform of this:

$$\overline{A}(p) = \frac{1}{a}III_a(p) * \text{sinc}(N\pi pa),$$

where p as before is $\sin\theta/\lambda$ and the narrow sinc-function determines the width of the transmitted beam.

Now here is an opportunity to experiment – on paper at least – with various arrangements of dipoles, to calculate their behaviour. We have the advantage over the spectroscopists that we can change the phases at the dipoles. The shah-function $III_a(x)$ may be written, for example, as the sum of two shah-functions, each with twice the spacing but with one of them displaced sideways by a distance a:

$$A(x) = [III_{2a}(x) + III_{2a}(x) * \delta(x - a)] \cdot \Pi_a(Nx)$$

but now we can introduce a phase-shift ϕ into alternate members of the array, so that the aperture function looks like

$$A(x) = [III_{2a}(x)e^{i\phi} + III_{2a}(x) * \delta(x-a)] \cdot \Pi_a(Nx)$$

and we can try various values of ϕ to see what happens.

The output beam amplitude is

$$\overline{A}(p) = \left[\frac{1}{2a}III_{1/(2a)}(p)e^{i\phi} + \frac{1}{(2a)}III_{1/(2a)}(p)e^{2\pi ipa} \right] * \mathrm{sinc}(N\pi pa)$$

$$= \frac{1}{(2a)}III_{1/(2a)}(p)[e^{i\phi} + e^{2\pi ipa}] * \mathrm{sinc}(N\pi pa).$$

At this point we put in some interesting values for a and δ.

3.4.1 $a = \lambda$ and $\phi = \pi$

Let $a = \lambda$ so that the dipoles are one wavelength apart:

$$\overline{A}(\theta) = 2\lambda III_{1/(2\lambda)}(\sin\theta/\lambda)[e^{i\phi} + e^{2\pi i \sin\theta}] * \mathrm{sinc}(N\pi)\sin\theta.$$

If $\phi = \pi$ the dipoles alternate in phase.

The shah-function tells us that there is a 'tooth' in the (radiated) Dirac comb at $\sin\theta = 1/2$, i.e. at $\theta = 30°$. In the square brackets $e^{i\delta}$ and $e^{2\pi i \sin\theta}$ are both equal to -1 so that power will be emitted at this angle *on both sides* of the array-normal, with the beam-width being governed by the sinc-function, which in turn depends on the number N of dipoles in the array. There will likewise be emission at $\theta = 150°$, where $\sin\theta = 1/2$ once more (as might be expected anyway, simply on grounds of symmetry).

3.4.2 $a = \lambda/2$ and $\phi = \pi$

The amplitude function is now given by

$$\overline{A}(\theta) = \frac{1}{2\lambda}III_{1/\lambda}(\sin\theta/\lambda)[e^{i\phi} + e^{\pi i \sin\theta}] * \mathrm{sinc}(N/(2\pi))\sin\theta.$$

The shah-function here requires $\sin\theta = 1$ for a tooth, and the phases agree within the square bracket. Emission will be along the line of the dipoles and the beam width will be determined by $\sin\theta = 2/N$.

There is a hint here of how the Yagi aerial works; but it is no more than a hint. A word of caution is appropriate: although the basic idea of Fraunhofer diffraction may guide antenna design, and indeed allows proper calculation for so-called 'broadside arrays', there are considerable complications when describing 'end-fire' arrays, or 'Yagi' aerials (the sort once used for radar

transmission and television reception). The broadside array, which comprises a number of dipoles (each dipole consisting of two rods, lying along the same line, each $\lambda/4$ long and with an alternating voltage applied in the middle), behaves like a row of point sources of radiation, and the amplitude at distances large compared with a wavelength can be calculated. Both the amplitude and the relative phase radiated by each dipole can be controlled[7] so that the shape of the radiation pattern and the strengths of the side-lobes are under control.

End-fire antennae, on the other hand, have one dipole driven by an oscillator and rely on resonant oscillation of the other 'passive' dipoles to interfere with the radiation pattern and direct the output power in one direction. The nearest optical analogue is probably the Fabry–Pérot étalon or, which is practically the same thing, the interference filter. The phase re-radiated by a passive dipole depends on whether it is really half a wavelength long, on its conductivity, which is not perfect, and on the dielectric constant of any sheath which may surround it. Consequently, aerial design tends to be based on experience, experiment and computation, rather than on strict Fraunhofer theory. The passive elements may be $\lambda/3$ apart, for example, and their lengths will taper along the direction of the aerial, being slightly shorter on the transmission side and longer on the reflecting side of the excited dipole. Spacings are non-uniform, sometimes with the spacing changing logarithmically or exponentially, with some elements of peculiar shape, some 'folded', some 'batwinged' – and so it goes.[8] Such modifications allow a broader band of radiation to be transmitted or received along a narrow cone possibly only a few degrees wide. Aerial design is a black art, a path bestrewn with empiricism, with Christmas-tree designs of weird complexity and with patent-infringement law-suits.

3.4.3 To continue ...

At this point the reader's curiosity may take up the challenge. For instance the amplitude function may be split into three or more components. For example,

$$A(x) = \left[III_{3a}(x)e^{i\phi_1} + III_{3a}(x)e^{i\phi_2} * \delta(x-a) \right.$$
$$\left. + III_{3a}(x)e^{i\phi_3} * \delta(x-2a) \right] \cdot \Pi_a(Nx)$$

so that a different phase shift is applied to every third aerial.

So far we have considered Dirac combs with uniform spacing between the teeth. The door is wide open for the exploration of the convolution algebra of

---

[7] This is equivalent to apodizing in optics, but with more flexibility.
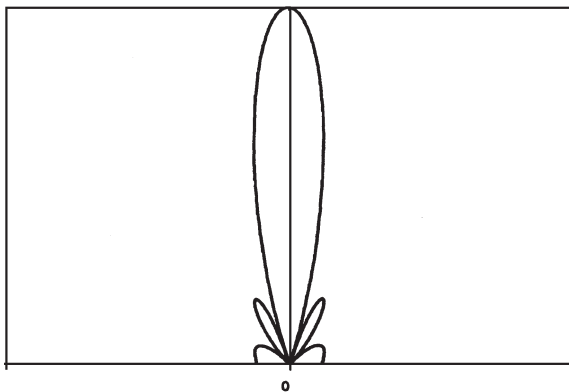[8] To paraphrase Vonnegut.

Fig. 3.14. The polar diagram of a sinc^2-function.

delta-function combs with unequal spacing, which may be logarithmic, arithmetic, exponential, Fibonacci and so on, all possibly yielding deeper insights into the black art mentioned above.

3.5 Polar diagrams

Since the important feature of Fraunhofer theory is the angle of diffraction, it is sometimes more useful, especially in antenna theory, to draw the intensity pattern on a polar diagram, with intensity as r, the length of the radius vector, and θ as the azimuth angle. The sinc^2-function then appears as in Fig. 3.14. Sometimes the logarithm of the intensity is plotted instead, to give the *gain* of the antenna as a function of angle.

3.6 Phase and coherence

Coherence is an important concept, not only in optics, but whenever oscillators are compared.

No natural light source is exactly monochromatic, and there are small variations in period and hence wavelength from time to time. Two sources are said to be coherent when any small variation in one is matched by a similar variation in the other, so that, for example, if a crest of a wave from one arrives at a given point at the same instant as the trough of a wave from the other, then at all subsequent times troughs and crests will arrive together and there is always destructive interference between the two.

In practice the variations of wavelength and phase in a quasi-monochromatic source are slow and if the wave train is divided – for example by a beam-splitter, then one wave train will be almost coherent with the other which has been delayed by a few wavelengths, as happens in an interferometer. As the path-difference is increased, by moving one of the interferometer mirrors, the fringes become less and less distinct and if the path-difference is great enough they vanish. We have reached the limit of coherence and can refer to the *coherence length* of the wave train. In 'allowed' (i.e. dipole) atomic transitions, for example, each individual wave train has a coherence length of a few metres, corresponding to the time taken for the atom to emit its light. In a laser, where the emitted light is in phase with the stimulating light, the coherence length may be anything up to a hundred times as long as the laser cavity,[9] the length depending on the reflectivity of the laser mirrors. The line width is correspondingly narrow, much narrower than the 'natural' width of the light emitted by the gas in the cavity. Similarly one can imagine the coherence of light from a distant extended source, where no source element is coherent with any other element. In this case, when light passes through a narrow slit, the wave trains arriving at one edge of the slit will sum to a complicated function of time, but, if the paths to the other edge of the slit all differ from the first set by less than a few wavelengths, the function of time there will be almost the same as for the first set and all the wave trains passing through the slit will interfere as if the source were coherent. You can hold close to your eye a spectroscope slit open a few microns, and look at a distant bright extended source such as a frosted light-bulb: it will show the secondary maxima of the sinc^2-function which would be produced if all the source-elements in the bulb were coherent. If the slit is opened slowly, the secondary maxima will crowd in to the principal maximum and eventually disappear.

In this case we refer to the slit width as the coherence *width* of the source – it is a property of the source, not of the equipment used to view it. If the experiment is done in two orthogonal directions the coherence *area* of the source can be measured.

The coherence width of the sun in green ($\lambda = 550\,\text{nm}$) light, for example, is about $60\,\mu\text{m}$, and with a narrow-band interference filter over the slit (to avoid eye-damage!) the familiar sinc^2 pattern can be seen with the slit opened to about this width. It is no coincidence of course that plane monochromatic wavefronts incident on and diffracted through the same slit will show a principal maximum in their diffraction pattern of the same angular width as the extended source.

---

[9] Sometimes much greater. See J. L. Hall's 2005 Nobel Prize lecture, J. L. Hall, *Rev. Mod. Phys.* **78** (2006), 1279–1295.
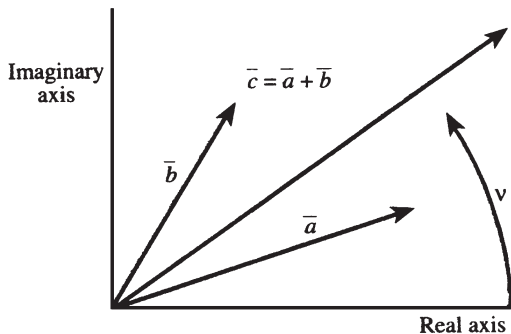
Fig. 3.15. The vector addition of two analytic wave-vectors representing two coherent sources. All three vectors are rotating at the same frequency v. The three vectors are described by complex numbers of the form $Ae^{2\pi i v t}$, the so-called 'analytic signal', but it is the real part of each, the horizontal component in the graph, which represents the instantaneous value of the electric field of the light-wave.

A star, on the other hand, has a coherence width of many – perhaps tens or hundreds – of metres and a Young's-slit interferometer with the apertures spaced by this sort of distance will show interference fringes, with the fringe visibility falling slowly as the distance between the apertures is increased. Michelson used this effect to measure the coherence width and hence the angular diameter of several stars.

3.7 Fringe visibility

An alternative way of describing coherence is by considering the *analytic* wave-vectors on the Argand plane, which rotate at about 6×10^{14} Hz for green light, but which, for two coherent sources, are rigidly linked by the phase-difference between them. If we abandon the time variation, the vector diagram looks like Fig. 3.15 and the resultant amplitude is the vector sum of the components. The resultant amplitude may be zero if the two sources are perfectly coherent, of equal amplitude and opposite in phase. Otherwise the resultant intensity is proportional to the square of the length of this vector.

If the sources are only partially coherent (Fig. 3.16) it means that the amplitude and phase angles are varying randomly over angles small compared with 2π. Interference fringes from such a pair of sources will show an intensity pattern on a screen given by

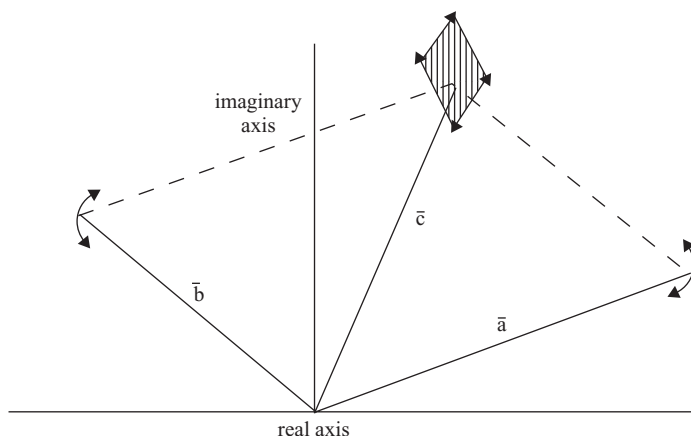$$I = I_1 + I_2 + 2\Gamma_{12}\sqrt{I_1 I_2} \cos \phi,$$

Fig. 3.16. The analytic vector diagram for two quasi-coherent sources. The two vectors here are varying randomly only in *phase*. Nevertheless, the resultant vector varies both in phase and in amplitude, and wanders randomly within the general area of the quadrilateral. Even if the amplitudes were the same and the phases opposed, there would not be complete cancellation.

where Γ_{12} is known as the *degree of coherence*, the *coherence factor* or the *coefficient of coherence*. Γ_{12} is always ≤ 1.

As usual, ϕ is the phase difference, which varies from place to place on the diffraction pattern.

The maximum intensity I_{max} in the pattern is at places where $\phi = 2n\pi$ and is given by $I_{max} = I_1 + I_2 + \Gamma_{12}$. The minimum intensity, where $\phi = (2n + 1)\pi$, is $I_{min} = I_1 + I_2 - \Gamma_{12}$.

We can now define the *visibility*, V, of the fringe pattern by

$$V = (I_{max} - I_{min})/(I_{max} + I_{min})$$

and clearly, provided that the two sources are of equal intensity, $V = \Gamma_{12}$.

3.8 The Michelson stellar interferometer

This is essentially a Young's-slit interferometer on an heroic scale. The apertures are two mirrors mounted on carriages which run along a beam fixed to the upper end of an astronomical reflecting telescope and they reflect light from a bright star to two more mirrors fixed near the centre of the beam, which in turn direct the light to the telescope objective and hence to the focus. At high magnification, interference fringes can be seen in the eyepiece, superimposed on the
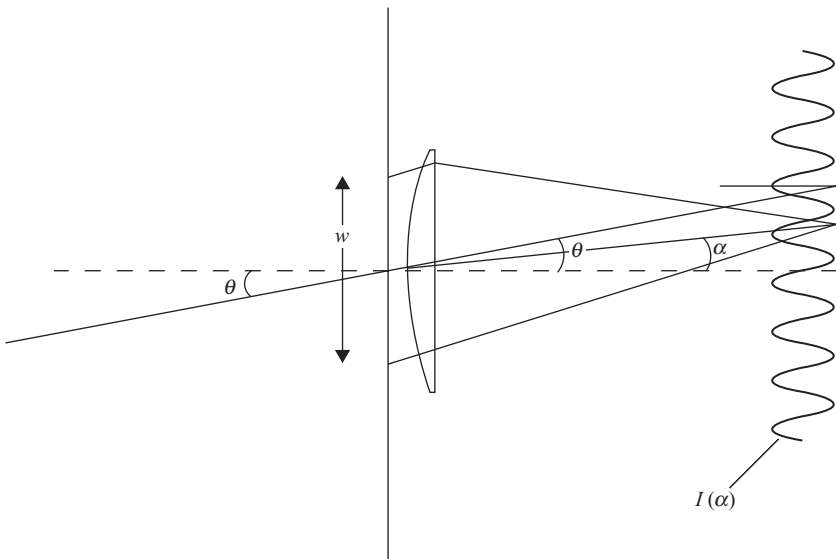
Fig. 3.17. Young's-slit interferometry with a distant extended source. An element of the source coming from a direction making an angle θ with the optic axis will produce its own infinitesimal fringe pattern displaced by this angle θ. All these fringe patterns, incoherent with each other, have their intensities added to form the resultant fringe pattern of lower visibility.

(large!) diffraction-limited image of the star. Atmospheric turbulence causes the image to move and shimmer, but the fringes move with the stellar image and remain visible to the observer. The visibility of the fringes diminishes as the mirror separation increases and may fall to zero at some point.

We now demonstrate that the fringe visibility, measured as a function of the mirror separation, is the modular Fourier transform of the intensity distribution across the source.

In Fig. 3.17, a distant, monochromatic point source of intensity $S(0)$ lying on the optic axis will give fringes and the intensity will vary sinusoidally according to

$$I(\alpha) = S(0)\left[1 + \cos\left(\frac{2\pi}{\lambda}w\cos\alpha\right)\right],$$

where λ is the wavelength, w the slit separation and α the angular variable describing the fringe pattern. The period of the pattern is λ/w, and depends on the slit separation, w.

This, of course, is a standard result in physical optics.

Another such source, situated at an angle θ to the optic axis, similarly produces perfect[10] fringes but displaced sideways by the same angle θ on the fringe pattern. The two sources are incoherent, so if they are both present their *intensities* are added.

If instead there is an extended distant source with intensity varying as $S(\theta)$, an element of infinitesimal intensity $S(\theta)d\theta$ will produce its own infinitesimal fringe pattern in the interferometer, displaced sideways by θ.

All these separate fringe patterns must be summed, so that the resultant intensity emerging at angle α to form the fringe pattern will be

$$I(\alpha) = \int_{-\infty}^{\infty} S(\theta)d\theta \left[1 + \cos\left(\frac{2\pi}{\lambda} w(\alpha - \theta) \right) \right],$$

which separates to

$$I(\alpha) = \int_{-\infty}^{\infty} S(\theta)d\theta + \int_{-\infty}^{\infty} S(\theta) \left[\cos\left(\frac{2\pi}{\lambda} w(\alpha - \theta) \right) \right] d\theta,$$

where the sines of the small angles α and θ have been replaced by the angles themselves.

The first term represents the total intensity coming from the extended source. The second term is the convolution of the source intensity distribution $S(\theta)$ with the cosine, which we write as $C(\alpha)$,

$$C(\alpha) = S(\theta) * \cos(2\pi p\theta),$$

and the variable p, conjugate to α, is w/λ.

The convolution integral, nominally from $-\infty$ to $+\infty$, is in practice over the angular width of the source.

The result of the convolution, as we saw[11] in Chapter 2, is a sinusoid with period $1/p$, determined by the wavelength λ and the (adjustable) distance w between the two apertures. It has an amplitude $A(p)$, the amplitude of the corresponding Fourier component in the transform of the source intensity distribution. (Bear in mind that in the Fourier transform the variable conjugate to α is p, and $A(p) \rightleftharpoons S(\alpha)$.) The intensity maxima of the resultant fringe pattern are $S + A$ and the minima are $S - A$ so that the fringe visibility, as a function of p, that is, of w/λ, is

$$V = \frac{A(w/\lambda)}{S} \tag{3.3}$$

and $A(w/\lambda)$ is the Fourier transform of $S(\theta)$. This is demonstrated in Fig. 3.18.

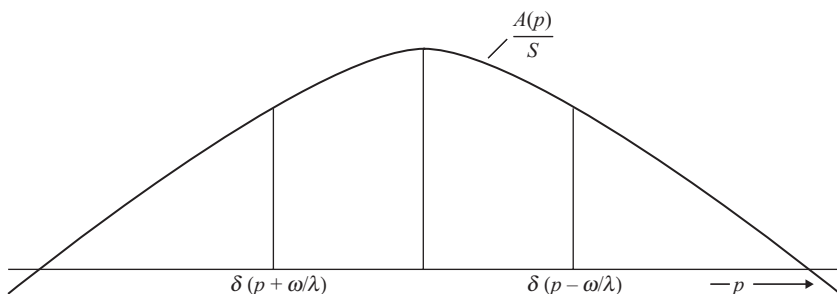
[10] That is, of visibility $V = 1$.   [11] On p. 38.

Fig. 3.18. The fringe visibility as a function of w/λ.

The fringe visibility thus decreases as w increases. When stellar diameters were measured it was a reasonable assumption that $S(\theta)$ was symmetrical so that its Fourier transform was real and symmetrical.

Otherwise $A(w/\lambda)$ was the *modular* transform, as for example when observing a double-star with components of unequal intensity, but in practice the point was academic, since phase-shifts in the fringe pattern would anyway be lost in the atmospheric disturbance, and it is simply the minima or vanishing of the fringes that were observed at particular values of w. If, for example, a double star with two equal components were observed, $S(\theta)$ would be a pair of δ-functions and the fringe visibility as a function of w/λ would decrease sinusoidally to zero, then increase again in inverse phase. The value of w at zero visibility would be observable but the phase inversion would not.

3.9 The van Cittert–Zernike theorem

The original Michelson stellar interferometer[12] comprised two 150-mm-diameter plane mirrors mounted with their normals at 45° to the optic axis of the 100″ Hooker telescope at the Mount Wilson observatory. To vary w, they could be moved on trolleys along a 6-m-long girder fixed to the top of the telescope tube, and the light from them was directed to two fixed mirrors also at 45°, whence the light was passed through to the telescope objective and hence to the focus. The Young 'slits' were thus the two moveable mirrors on the girder, which reflected starlight[13] from a star or perhaps a double star. The point of this description is that the orientation of the two apertures could have been altered and, if the star had had an ellipsoidal shape, for example,

[12] A. A. Michelson and F. G. Pease, *Astrophys. J.* **53** (1921), 249.
[13] In fact they began with the red giant Betelgeuse, also known as α-Orionis.

the coherence width would have been greater when the apertures were aligned with the star's minor axis. The fringe visibility would measure the degree of coherence for that particular separation and that particular orientation. A shape, called the 'coherence area' of the star, could in principle be mapped out, and the van Cittert–Zernike theorem, in its crudest form, states that the fringe visibility, i.e. the degree of coherence, as a function of w and the orientation angle ξ, is the two-dimensional Fourier transform of the intensity distribution on the sky as a function of α and ξ.

Thus, in its most elementary – and practical – form, the van Cittert–Zernike theorem is described by equation (3.3) above.

This is not the place for a full rigorous derivation and proof of the theorem which considers the complex degree of coherence (as exemplified by the phase-shift of the fringes) and which occupies two pages in Born & Wolf's *Principles of Optics*.[14] The idea of a 'coherence area' is the important thing. It is not fixed in space (the telescope is moving both with Earth's orbital speed and with the diurnal rotational speed of the Mount Wilson observatory) but is measured by the separation of the two apertures. It is the 'area over which some degree of coherence can be observed'.

To put it another way: if there were a circular coherent source of monochromatic light of the diameter and at the distance of Betelgeuse its 'Airy disc' here on Earth would have a diameter of about 6 m.

---

[14] M. Born and E. Wolf, *Principles of Optics*, Cambridge University Press, Cambridge, 7th edn, 1999, pp. 572–574.

4

Applications 2: signal analysis and communication theory

4.1 Communication channels

Although the concepts involved in communication theory are general enough to include bush-telegraph drums, alpine yodelling or a ship's semaphore flags, by 'communication channel' is usually meant a single electrical conductor, a waveguide, a fibre-optic cable or a radio-frequency carrier wave. Communication theory covers the same general ground as information theory, which discusses the 'coding' of messages (such as Morse code, not to be confused with encryption, which is what spies do) so that they can be transmitted efficiently. Here we are concerned with the physical transmission, by electric currents or radio waves, of the signal or message that has already been encoded. The distinction is that communication is essentially an analogue process, whereas information coding is essentially digital.

For the sake of argument, consider an electrical conductor along which is sent a varying current, sufficient to produce a potential difference $V(t)$ across a terminating impedance of one ohm (1Ω).

The mean level or time-average of this potential is denoted by the symbol $\langle V(t) \rangle$ defined by the equation:

$$\langle V(t) \rangle = \frac{1}{2T} \int_{-T}^{T} V(t)dt.$$

The power delivered by the signal varies from moment to moment, and it too has a mean value:

$$\langle V^2(t) \rangle = \frac{1}{2T} \int_{-T}^{T} V^2(t)dt.$$

For convenience, signals are represented by functions like sinusoids which, in general, disobey one of the Dirichlet conditions described at the beginning of

Chapter 2: they are not square-integrable:

$$\lim_{T \to \infty} \int_{-T}^{T} V^2(t)dt \to \infty.$$

However, in practice, the signal begins and ends at finite times and we regard the signal as the product of $V(t)$ with a very broad top-hat function. Its Fourier transform – which tells us about its frequency content – is then the convolution of the true frequency content with a sinc-function so narrow that it can for most purposes be ignored. We thus assume that $V(t) \to 0$ at $|t| > T$ and that

$$\int_{-\infty}^{\infty} V^2(t)dt = \int_{-T}^{T} V^2(t)dt.$$

We now define a function $C(v)$ such that $C(v) \rightleftharpoons V(t)$, and Rayleigh's theorem gives

$$\int_{-\infty}^{\infty} |C(v)|^2 \, dv = \int_{-\infty}^{\infty} V^2(t)dt = \int_{-T}^{T} V^2(t)dt.$$

The mean power level in the signal is then

$$\frac{1}{2T} \int_{-T}^{T} |V(t)|^2 \, dt$$

since $V^2(t)$ is the power delivered into unit impedance; and then

$$\frac{1}{2T} \int_{-T}^{T} |V(t)|^2 \, dt = \int_{-\infty}^{\infty} \frac{|C(v)|^2}{2T} \, dv$$

and we *define* $|C(v)|^2/(2T) = G(v)$ to be the spectral power density (SPD) of the signal.

4.1.1 The Wiener–Khinchine theorem

The autocorrelation function of $V(t)$ is defined to be

$$\lim_{T \to \infty} \frac{1}{2T} \int_{-T}^{T} V(t)V(t + \tau)dt = \langle V(t)V(t + \tau) \rangle.$$

Again the integral on the left-hand side diverges and we use the shift theorem and Parseval's theorem to give

$$\int_{-T}^{T} V(t)V(t + \tau)dt = \int_{-\infty}^{\infty} C^*(v)C(v)e^{2\pi i v \tau} \, dv.$$

Then

$$\frac{1}{2T} \int_{-T}^{T} V(t)V(t+\tau)dt = \int_{-\infty}^{\infty} \frac{|C(v)|^2}{2T} e^{2\pi iv\tau} \, dv = R(\tau)$$

so that, with the definition of $G(v)$ above,

$$R(\tau) = \int_{-\infty}^{\infty} G(v)e^{2\pi iv\tau} \, dv$$

and finally

$$R(\tau) \rightleftharpoons G(v).$$

In other words,

> **the spectral power density is the Fourier transform of the autocorrelation function of the signal.**

This is the Wiener–Khinchine theorem.

4.2 Noise

The term originally meant the random fluctuation of signal voltage which was heard as a hissing sound in early telephone receivers, and which is still heard in radio receivers which are not tuned to a transmitting frequency. Now it is taken to mean any randomly fluctuating signal which carries no message or 'information'. If it has equal power density at all frequencies it is called 'white' noise.[1] Its autocorrelation function is always zero since at any time the signal $n(t)$, being random, is as likely to be negative as to be positive. The only exception is at zero delay, $\tau = 0$, where the integral diverges. The autocorrelation function is therefore a δ-function and its Fourier transform is unity, in accordance with the Wiener–Khinchine theorem and with this definition of 'white'.

In practice the band of frequencies which is received is always finite, so that the noise power is always finite. There are other types of noise, for example:

- Electron shot noise, or 'Johnson noise', in a resistor, giving a random fluctuation of voltage across it: $\langle V^2(t) \rangle = 4\pi RkT \, \Delta v$, where Δv is the bandwidth, R the resistance, k Boltzmann's constant and T the absolute temperature.[2]

---

[1] This is a rebarbative use of 'white', which really defines a rough surface which reflects all the radiation incident upon it. It is used, less compellingly, to describe the colour of the light emitted by the Sun or, even less compellingly, to describe light of constant spectral power density in which all wavelengths (or frequencies; take your pick) contribute equal power.

[2] $\langle V^2 \rangle = 1.3 \times 10^{-10}(R \, \Delta v)^{1/2}$ volts in practice.

- Photo-electron shot noise, which has a normal (Gaussian) distribution of count-rate[3] at frequencies low compared with the average generation-rate and, more accurately, a Poisson distribution when equal time-samples are taken. This kind of noise is met chiefly in fibre optics when light is used for communication, and only then when the light is weak. Typically, a laser beam delivers 10^{18} photons s^{-1}, so that even at $100\,\text{MHz}$ there are 10^{10} photons/sample, or an S/N ratio of $10^5 : 1$.
- Semiconductor noise, which gives a time-varying voltage with a spectral power density which varies as $1/\nu$ – which is why many semiconductor detectors of radiation are best operated at high frequency with a 'chopper' to switch the radiation on and off. There is usually an optimum frequency, since the number of photons in a short sample may be small enough to increase photon shot noise to the level of the semiconductor noise.

4.3 Filters

By 'filter' we mean an electrical impedance which depends on the frequency of the signal current trying to pass. The exact structure of the filter, namely the arrangement of resistors, capacitors and inductances, is immaterial. What matters is the effect that the filter has on a signal of fixed frequency and unit amplitude. The filter does two things: it attenuates the amplitude and it shifts the phase. This is all that it does.[4] The frequency-dependence of its impedance is described by its filter function $Z(\nu)$. This is defined to be the ratio of the output voltage divided by the input voltage, as a function of frequency:

$$Z(\nu) = V_\text{o}/V_\text{i} = A(\nu)e^{i\phi(\nu)},$$

where V_i and V_o are 'analytic' representations of the input and output voltages, i.e. they include the phase as well as the amplitude. The impedance is complex since both the amplitude and the phase of V_o may be different from those of V_i. The filter impedance, Z, is usually shown graphically by plotting a polar diagram of the attenuation, A, radially against the angle of phase-shift, eliminating ν as a variable. The result is called a *Nyquist diagram* (Fig. 4.1). This is the same figure as that which is used to describe a feedback loop in servo-mechanism theory, with the difference that the amplitude A is always less than unity in a passive filter, so that there is no fear of the curve encompassing the point $(-1, 0)$, the criterion for oscillation in a servo-mechanism.

---

[3] Which may be converted into a time-varying voltage by a rate-meter.
[4] Unless it is 'active'. Active filters can do other things, such as doubling the frequency of the input signal.
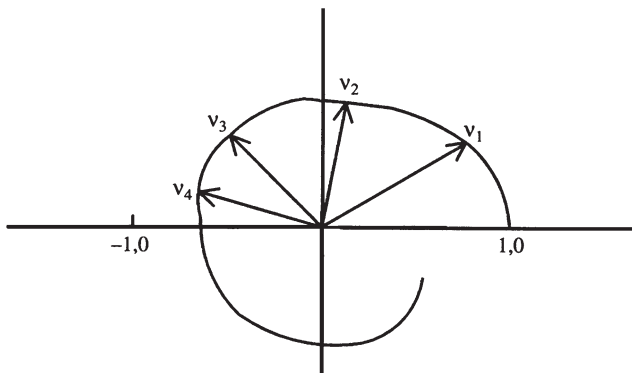
Fig. 4.1. The Nyquist diagram of a typical filter.

4.4 The matched filter theorem

Suppose that a signal $V(t)$ has a frequency spectrum $C(\nu)$ and a spectral power density $S(\nu) = |C(\nu)|^2/(2T)$. The signal emerging from the filter then has a frequency spectrum $C(\nu)Z(\nu)$ and the spectral power density is $G(\nu)$, given by

$$G(\nu) = \frac{|C(\nu)Z(\nu)|^2}{2T}.$$

If there is white noise passing through the system, with spectral power density $|N(\nu)|^2/(2T)$, the total signal power and noise power are

$$\frac{1}{2T} \int_{-\infty}^{\infty} |C(\nu)Z(\nu)|^2 \, d\nu$$

and

$$\frac{1}{2T} \int_{-\infty}^{\infty} |N(\nu)Z(\nu)|^2 \, d\nu.$$

For white noise $|N(\nu)|^2$ is a constant, equal to A, say, so that the transmitted noise power is

$$\frac{A}{2T} \int_{-\infty}^{\infty} |Z(\nu)|^2 \, d\nu$$

and the ratio of signal power to noise power is the ratio

$$(S/N)_{\text{power}} = \int_{-\infty}^{\infty} |C(\nu)Z(\nu)|^2 \, d\nu \bigg/ A \int_{-\infty}^{\infty} |Z(\nu)|^2 \, d\nu.$$

Here we use Schwartz's inequality[5]

$$\left[\int_{-\infty}^{\infty} |C(\nu)Z(\nu)|^2 \, d\nu\right]^2 \leq \int_{-\infty}^{\infty} |C(\nu)|^2 \, d\nu \int_{-\infty}^{\infty} |Z(\nu)|^2 \, d\nu$$

so that the S/N power ratio is always $\leq A \int_{-\infty}^{\infty} |C(\nu)|^2 \, d\nu$ and the equality sign holds if and only if $C(\nu)$ is a multiple of $Z(\nu)$. Hence

the S/N power ratio will always be greatest if the filter characteristic function $Z(\nu)$ has the same shape as the frequency content of the signal to be received.

This is the matched filter theorem. In words, it means that the best signal-to-noise ratio is obtained if the filter transmission function has the same shape as the signal power spectrum.

It has a surprisingly wide application, in spatial as well as temporal data transmission. The tuned circuit of a radio receiver is an obvious example of a matched filter: it passes only those frequencies containing the information in the programme, and rejects the rest of the electromagnetic spectrum. The tone-control knob does the same for the accoustic output. A monochromator does the same thing with light. The 'radial velocity spectrometer' used by astronomers[6] is an example of a spatial matched filter. The negative of a stellar spectrum is placed in the focal plane of a spectrograph, and its position is adjusted sideways – perpendicular to the slit-images – until there is a minimum of total transmitted light. The movement of the mask necessary for this measures the Doppler-effect produced by the line-of-sight velocity on the spectrum of a star.

4.5 Modulations

When a communication channel is a wireless telegraphy channel (a term which comprises everything from a modulated laser beam to an extremely low-frequency (ELF) transmitter used to communicate with submerged submarines) it is usual for it to consist of a 'carrier' frequency on which is superimposed a 'modulation'. If there is no modulating signal, the voltage at the receiver varies with time according to

$$V(t) = V e^{2\pi i (\nu_c t + \phi)},$$

[5] See, for example, D. C. Champeney, *Fourier Transforms and their Physical Applications*, Academic Press, New York, 1973, Appendix F.
[6] Particularly by R. F. Griffin. See R. F. Griffin, *Astrophys. J.* **148** (1967), 465.
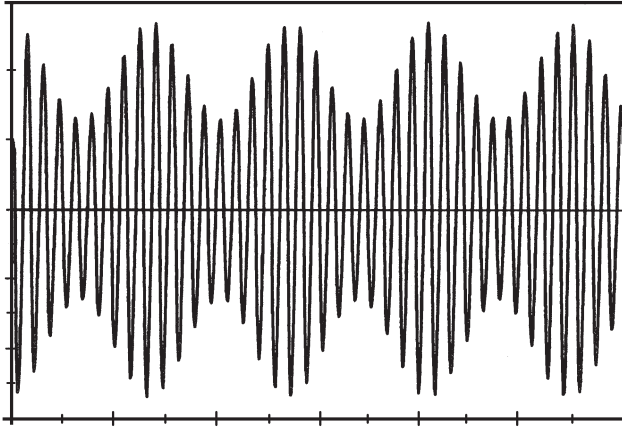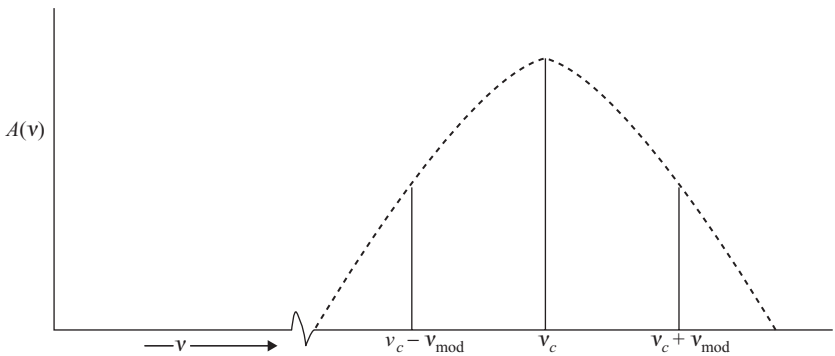
Fig. 4.2. A carrier wave with amplitude modulation.

Fig. 4.3. Various modulating frequencies occupy a band of the spectrum. The time function is $A + B \cos(2\pi \nu_{mod} t)$ and in frequency space the spectrum becomes the convolution of $\delta(\nu - \nu_c)$ with $A\delta(\nu) + B[(\delta(\nu - \nu_{mod}) + \delta(\nu + \nu_{mod})]/2$.

where ν_c is the carrier frequency; and the modulation may be carried out by making V, ν_c or ϕ a function of time.

- Amplitude modulation (Fig. 4.3). If V varies with a modulating frequency ν_{mod}, then $V = A + B \cos(2\pi \nu_{mod} t)$ and the resulting frequency distribution will be as in Fig. 4.2 and, as various modulating frequencies from $0 \rightarrow \nu_{max}$ are transmitted, the frequency spectrum will occupy a band of the spectrum from $\nu_c - \nu_{max}$ to $\nu_c + \nu_{max}$. If low modulating frequencies predominate in the signal, the band of frequencies occupied by the channel will have the appearance of Fig. 4.3 and the filter in the receiver should have this profile too.
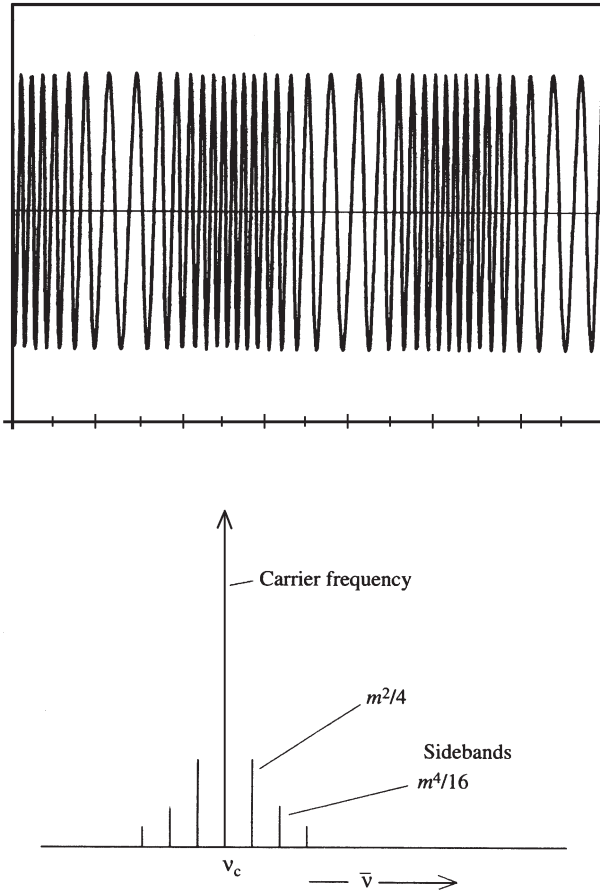
Fig. 4.4. Frequency modulation of the carrier. Many sidebands are present, with their amplitudes given by the Jacobi expansion.

The power transmitted by the carrier is wasted unless very low frequencies are present in the signal. The power required from the transmitter can be reduced by filtering its output so that only the range from ν_c to ν_{max} is transmitted. The receiver is doctored in like fashion. The result is single-sideband transmission.

- Frequency modulation (Fig. 4.4). This is important because it is possible to increase the bandwidth used by the channel. (By 'channel' is meant here perhaps the radio-frequency link used by a spacecraft approaching Neptune and its receiver on Earth, some 4×10^9 km away.) The signal now is

$$V(t) = A \cos(2\pi \nu(t)t)$$

and $v(t)$ itself is varying according to $v(t) = v_{\text{carrier}} + \mu \cos(2\pi v_{\text{mod}}(t)t)$. The parameter μ can be made very large so that, for example, a voice telephone signal normally requiring about 3×10^3 Hz bandwidth can be made to occupy several MHz if necessary. The advantage in doing this is found in the Hartley–Shannon theorem of information theory, which states that the 'channel capacity', the rate at which a noisy channel can transmit information in bits s^{-1} ('bauds'), is given by

$$dB/dt \leq 2\Omega \log_e(1 + S/N),$$

where Ω is the channel bandwidth, S/N is the *power* signal-to-noise ratio and dB/dt is the 'baud-rate' or bit-transmission rate.

So, to get a high data transmission rate, you need not slave to improve the S/N ratio because only the logarithm of that is involved: instead you increase the bandwidth of the transmission. In this way the low power available to the spacecraft transmitter near Neptune is used more effectively than would be possible in an amplitude-modulated transmitter. Theorems in information theory, like those in thermodynamics, tend to tell you what is possible, without telling you how to do it.

To see how the power is distributed in a frequency-modulated carrier, the message-signal, $a(t)$, can be written in terms of the phase of the carrier signal, bearing in mind that frequency can be defined as rate of change of phase. If the phase is taken to be zero at time $t = 0$, then the phase at time t can be written as

$$\phi = \int_0^t \frac{\partial \phi}{\partial t} \, dt$$

and $\partial \phi / \partial t = v_c + \int_0^t a(t)dt$ and the transmitted signal is

$$V(t) = a e^{2\pi i \left[v_c + \int_0^t a(t)dt \right] t}.$$

Consider a single modulating frequency v_{mod}, such that $a(t) = k \cos(2\pi v_{\text{mod}}t)$. Then

$$2\pi i \int_0^t a(t)dt = \frac{2\pi i k}{2\pi v_{\text{mod}}} \sin(2\pi v_{\text{mod}}t),$$

where k is the depth of modulation, and k/v_{mod} is called the *modulation index*, m. Then

$$V(t) = A e^{2\pi i v_c t} e^{im \sin(2\pi v_{\text{mod}}t)}.$$

It is a cardinal rule in applied mathematics that, when you see an exponential function with a sine or cosine in the exponent, there is a Bessel function

lurking somewhere. This is no exception. The second factor in the expression for $V(t)$ can be expanded in a series of Bessel functions by the Jacobi expansion[7]

$$e^{im\sin(2\pi\nu_{\mathrm{mod}}t)} = \sum_{n=-\infty}^{\infty} J_n(m)e^{2\pi in\nu_{\mathrm{mod}}t}$$

and this is easily Fourier transformable to

$$\chi(\nu) = \sum_{n=-\infty}^{\infty} J_n(m)\delta(\nu - n\nu_{\mathrm{mod}}).$$

The spectrum of the transmitted signal is the convolution of $\chi(\nu)$ with $\delta(\nu - \nu_c)$. In other words, $\chi(\nu)$ is shifted sideways so that the $n = 0$ tooth of the Dirac comb is at $\nu = \nu_c$.

The amplitudes of the Bessel functions must be computed or looked up in a table[8] and for small values of the argument m are $J_0(m) = 1$, $J_1(m) = m/2$, $J_2(m) = m^2/4$ etc. Each of these Bessel functions multiplies a corresponding tooth in the Dirac comb of period ν_{mod} to give the spectrum of the modulated carrier. Bearing in mind that $m = k/\nu_{\mathrm{mod}}$, we see that the channel is not uniformly filled and there is less power in higher frequencies.

As an example of the cross-fertilizing effect of Fourier transforms, the theory above can equally be applied to the diffraction produced by a grating in which there is a periodic error in the rulings. In Chapter 3 there was an expression for the 'aperture function' of a grating, which was

$$A(x) = \Pi_{Na}(x)[\Pi_a(x) * \amalg_a(x)],$$

and if there is a periodic error in the ruling, it is $\amalg_a(x)$ that must be replaced. The rulings, which should have been at $x = 0, a, 2a, 3a, \ldots$, will be at $0, a + \alpha\sin(2\pi\beta \cdot a), 2a + \alpha\sin(2\pi\beta \cdot 2a), \ldots$ etc. and the $\amalg$-function is replaced by

$$G(x) = \sum_{-\infty}^{\infty} \delta[x - na - \alpha\sin(2\pi\beta na)],$$

where α is the amplitude of the periodic error and $1/\beta$ is its 'pitch'. This has a Fourier transform

$$\overline{G}(p) = \sum_{-\infty}^{\infty} e^{2\pi i[na + \alpha\sin(2\pi\beta na)]}$$

[7] See, for example, H. Jeffreys & B. Jeffreys, *Methods of Mathematical Physics*, 3rd edn, Cambridge University Press, Cambridge, 1999, p. 589.
[8] For example, in Jahnke & Emde or Abramowitz & Stegun (see the bibliography).
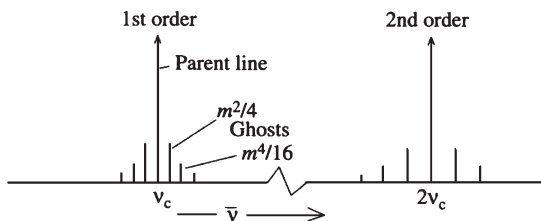
Fig. 4.5. Rowland ghosts in the spectrum produced by a diffraction grating with a period error in its rulings. The spacing of the ghost from its parent line depends on the period of the error, and the intensity depends on the square of the amplitude of the error.

with $p = \sin\theta/\lambda$ as in Chapter 3. There is a clear analogy with $V(t)$ above. The diffraction pattern then contains what are called 'ghost' lines[9] around each genuine spectrum line as in Fig. 4.5.

The analysis is not quite as simple as in the case of a frequency-modulated radio wave because the simple sinusoids are replaced by δ-functions. What happens is that the infinite sum $\overline{G}(p)$ can be analysed into a whole set of Dirac combs, of periods slightly above and below the true error-free period, and with amplitudes decreasing rapidly according to the amplitude of the Bessel function which multiplies them. The Rowland ghosts are then separated from the parent line by distances which depend on the pitch $1/\beta$ of the lead-screw of the grating ruling engine and have amplitudes which depend on the square[10] of the amplitude α of the periodic error.

These satellites on either side of a spectrum line with intensity $\pi^2 p^2 \alpha^2$ times the height of the parent and separated from it by $\Delta\lambda = \pm a\beta\lambda$ are the first-order Rowland ghosts. The next ones, of height $\pi^4 p^4 \alpha^4$ times the parent intensity, are the second-order ghosts, and so on. The analogy with the channel occupation of a frequency-modulated carrier is exact.

There are, of course, many other ways of modulating a carrier, such as *phase* modulation, *pulse-width* modulation, *pulse-position* modulation, *pulse-height* modulation and so on, quite apart from digital encoding, which is a quite separate way of conveying information. Several different kinds of modulation can be applied simultaneously to the same carrier, each requiring a different type of demodulating circuit at the receiver. The design of communications channels includes the art of combining and separating these modulators

[9] Rowland ghosts, after H. A. Rowland, the inventor of the first effective grating-ruling engine.
[10] Because $\overline{G}(p)$ gives the diffraction *amplitude*.

and ensuring that they do not influence each other with various kinds of 'cross-talk'.

4.6 Multiplex transmission along a channel

There are two ways of sending a number of independent signals along the same communication channel. They are known as *time-multiplexing* and *frequency-multiplexing*. Frequency multiplexing is the more commonly used. The signals to be sent are used to modulate[11] a *sub-carrier*, which then modulates the main carrier. A filter at the receiving end demodulates the main carrier and transmits only the sub-carrier and its sidebands (which contain the message). Different sub-carriers require different filters and it is usual to leave a small gap in the frequency spectrum between sub-carriers in order to guard against 'cross-talk', that is one signal spreading into the pass-band of another signal.

Time-multiplexing involves the 'sampling' of the carrier at regular time intervals. If, for example, there are ten separate signals to be sent, the sampling rate must be twenty times the highest frequency present in each band. The samples are sent in sequence and switched to ten different channels for decoding, and there must be some way of collating each message channel at the transmitting end with its counterpart at the receiving end so that the right message goes to the right recipient. The 'serial link' between a computer and a peripheral, which uses only one wire, is an example of this, with about eight channels,[12] one for each bit-position in each byte of data.

4.7 The passage of some signals through simple filters

This is not a comprehensive treatment of the subject, but illustrates the methods used to solve problems. Firstly we need to know about the Heaviside step-function.

4.7.1 The Heaviside step-function

When a switch is closed in an electric circuit there is a virtually instantaneous change of voltage on one side. This can be represented by a 'Heaviside

---

[11] 'Modulate' here means that the main carrier signal is multiplied by the message-bearing sub-carrier. Demodulation is the reverse process, in which the sub-carrier and its message are extracted from the transmitted signal by one of various electronic tricks.

[12] Anything between five and eleven channels in practice, so long as the transmitter and receiver have agreed beforehand about the number.
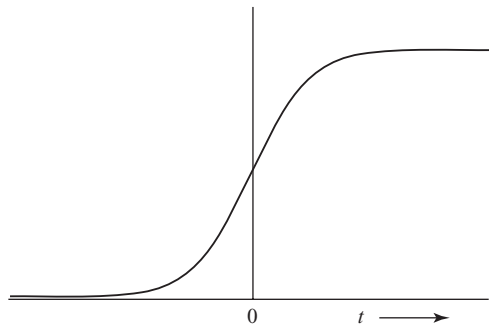
Fig. 4.6. An analytic function approximating to a Heaviside step-function in the
limit $a \to 0$.

step-function', $H(t)$. It has the property that $H(t) = 0$ for $t < 0$ and $H(t) = 1$
for $t > 0$.[13] Like the delta-function, it can be represented as the limit of an
analytic function (Fig. 4.6), for example

$$H(t) = \lim_{a \to 0} \left[\frac{1}{1 + e^{-2t/a}} \right],$$

which tends to unity as t tends to ∞, tends to zero as t tends to $-\infty$ and
automatically takes the value $1/2$ at $t = 0$.

However, this function is not Fourier-transformable because it does not
satisfy the Dirichlet condition of being square-integrable.

Instead we construct a function as follows.

We begin with the so-called 'sgn'-function (Fig. 4.7), defined by

$$\text{sgn}(t) = \begin{cases} -1, & -\infty < t < 0, \\ +1, & 0 < t < \infty \end{cases}$$

and we divide it by 2 and add $1/2$ to give a Heaviside step of unit height.

The function $\text{sgn}(t)/2$ likewise does not obey the Dirichlet conditions but
can be approximated in several ways. It may be regarded, for example, as the
limiting case of a pair of 'ramp' functions, defined by

$$f(t) = \begin{cases} \lim_{a \to 0} \dfrac{-(at + 1)}{2}, & -1/a < x < 0, \\ \lim_{a \to 0} \dfrac{(1 - at)}{2}, & 0 < x < 1/a \end{cases}$$

and the functions of this pair obey the Dirichlet conditions (at least before we go
to the limit!), and together form an antisymmetrical function which, as $a \to 0$,

---

[13] Its value *at x* = 0 is the subject of debate, but is usually taken as $H(0) = 1/2$.
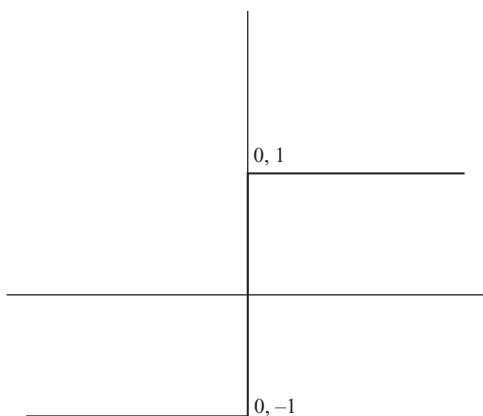
Fig. 4.7. The sgn function sgn(t).
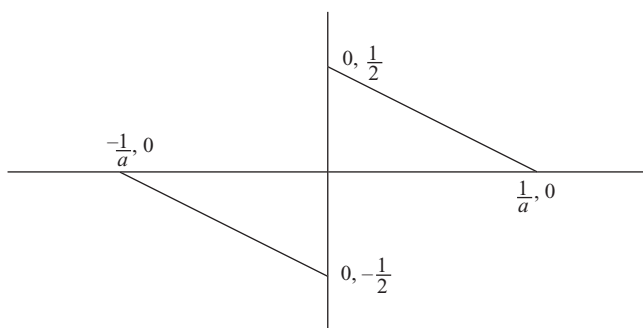
Fig. 4.8. Representation of a Heaviside step-function by two functions which obey the Dirichlet conditions.

approaches sgn(t)/2. As it does so those parts of its Fourier transform which have a factor a all vanish, leaving us with the Fourier transform of sgn(t)/2. Adding 1/2 to give the step function means that we add $\delta(v)/2$ to the Fourier transform of sgn(t)/2. (See Fig. 4.8.)

The sum of the Fourier transforms[14] of these three components in the limit as $a \to 0$ is

$$\phi(v) = \frac{\delta(v)}{2} + \frac{1}{2\pi i v}.$$

For all practical purposes we can ignore the δ-function since it cancels itself out when any finite limits appear in the Fourier transform.

---

[14] Remember to do the *inverse* transform, with $-2\pi i v t$ in the exponent, when integrating with respect to t.

Alternatively, and this is worth doing as an exercise, we can get the same result using a pair of exponentials:[15]

$$
H(t) = \begin{cases}
\dfrac{1}{2} + \lim_{a \to 0} \dfrac{1}{2} \left(e^{at} - 1 \right), & -\infty < t < 0, \\[3mm]
\dfrac{1}{2} + \lim_{a \to 0} \dfrac{1}{2} \left(1 + e^{-at} \right), & 0 < t < \infty.
\end{cases}
$$

4.7.2 The passage of a voltage step through a 'perfect' low-pass filter

Suppose that the filter is a 'low-pass' filter with no attenuation or phase-shift up to a critical frequency ν_c and zero transmission thereafter.[16] If the height of the step is V volts, the voltage as a function of time is a Heaviside step-function, $V H(t)$. Its frequency content is then $V/(2\pi i \nu)$ and the output frequency spectrum is the product of this with the filter profile: that is, $\overline{V}(\nu) = V/(2\pi i \nu) \cdot \Pi_{\nu_c}(\nu)$. The output signal, as a function of time, is the Fourier transform of this, which is

$$
f_0(t) = V \int_{-\nu_c}^{\nu_c} \frac{e^{2\pi i \nu t}}{2\pi i \nu} \, d\nu,
$$

where the top-hat has been replaced by finite limits on the integral.

The function to be transformed is antisymmetrical and so there is only a sine-transform:

$$
f_0(t) = iV \int_{-\nu_c}^{\nu_c} \frac{\sin(2\pi \nu t)}{2\pi i \nu} \, d\nu = Vt \int_{-\nu_c}^{\nu_c} \mathrm{sinc}(2\pi \nu t) d\nu
$$

$$
= 2Vt \int_{0}^{\nu_c} \mathrm{sinc}(2\pi \nu t) d\nu = \frac{1}{\pi} \int_{0}^{2\pi \nu_c t} \mathrm{sinc}(x) dx
$$

with the obvious substitution $x = 2\pi \nu t$.

The integral is a function of t, obviously, and must be computed since sinc-functions are not directly integrable. The result is shown graphically in Fig. 4.9.

The rise-time depends on the filter bandwidth. People who use oscilloscopes on the fastest time-base settings to look at edges will recognize this curve.

---

[15] This pair was pointed out to me by an unknown referee who took me to task for a glaring error in previous editions of this book: I gave the Fourier transform as a pure imaginary function, despite the fact that $H(t)$ is not antisymmetrical. *Mea culpa.*

[16] Such a filter, known colloquially as a 'brick-wall' filter, is impossible practically and there are inevitably phase-shifts tied to the attenuation or 'roll-off' rates: nevertheless, various approximations abound in the world of electronics.
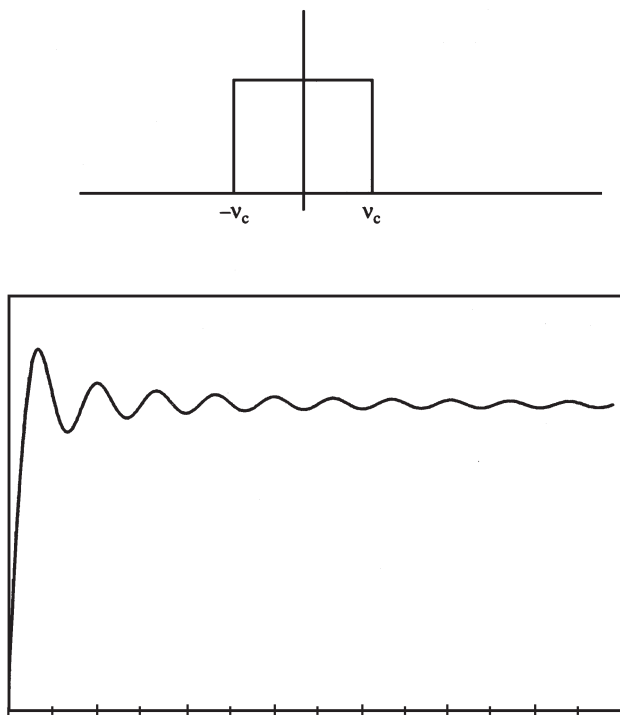
Fig. 4.9. Passage of a Heaviside step-function through a perfect low-pass filter. The pass band is a top-hat function in frequency space, and this sets the limits on the integral of the Heaviside step's transform.

4.8 The Gibbs phenomenon

When you display a square-wave on an oscilloscope, the edges are never quite sharp (unless they are made so by some subtle and deliberate electronic trick) but show small oscillations which increase in amplitude as the corner is approached. They may be quite small in a high-bandwidth oscilloscope.

The reason is to be found in the finite bandwidth of the oscilloscope. The square-wave, regarded as the convolution of a top-hat with a Dirac comb, is synthesized from a Dirac comb with tooth-heights modulated by an enveloping sinc-function. To give a *perfect* square-wave, an infinite number of teeth is required, that is to say, the series expansion for $F(t)$ must have an infinite number of terms: sharp corners need high frequencies. Since there is an upper limit to the available frequencies, only a finite number of terms can, in practice, be included. This is equivalent to multiplying the sinc-modulated Dirac comb in frequency-space by a top-hat function of width $2\nu_{max}$, and in t-space, which

is what the oscilloscope displays, you see the convolution of the square-wave with a very narrow sinc-function $\text{sinc}(2\pi \nu_{\max})$. Convolution with the leading edge of the displayed square-wave (effectively with a Heaviside step-function) replaces the sharp edge by the integral of the sinc-function between $-\infty$ and t, and the result is shown in Fig. 4.9.

The phenomenon was discovered experimentally by A. A. Michelson and Stratton. They designed a mechanical Fourier synthesizer, in which a pen position was controlled by eighty springs pulling together against a master-spring, each controlled by eighty gear-wheels which turned at relative rates of $1/80, 2/80, 3/80, \ldots, 79/80$ and $80/80$ turns per turn of a crank-handle. The synthesizer could have the spring tensions set to represent the eighty amplitudes of the Fourier coefficients and the pen position gave the sum of the series. As the operator turned the crank-handle a strip of paper moved uniformly beneath the pen and the pen drew the graph on it, reproducing, to Michelson's mystification, a square-wave as planned, but showing the Gibbs phenomenon. Michelson assumed, wrongly, that mechanical shortcomings were the cause: Gibbs gave the true explanation in a letter to *Nature*.[17]

The machine itself, a marvel of its period, was constructed by Gaertner & Co. of Chicago in 1898. It now languishes in the archives of the South Kensington Science Museum.

4.8.1 The passage of a train of pulses through a low-pass filter

Suppose that we represent the pulse train by a III-function. If the pulse repetition frequency is ν_0 the train is described by $\text{III}_a(t)$, where $a = 1/\nu_0$. Suppose that the filter, as before, transmits perfectly all frequencies below a certain limit and nothing above that limit. In other words, the filter's frequency profile or 'filter function' is the same top-hat function Π_{ν_f}. The Fourier transforms of the signal and the filter function are $(1/a)\text{III}_{\nu_0}(\nu)$ and $\Pi_{\nu_f}(\nu)$, respectively. The frequency spectrum of the output signal is then the product of the input spectrum and the filter function, $(1/a)\text{III}_{\nu_0}(\nu) \cdot \Pi_{\nu_f}(\nu)$, and the output signal is the Fourier transform of this, namely the convolution of the original train of pulses with $\text{sinc}(2\pi \nu_f t)$. If the filter bandwidth is wide compared with the pulse repetition frequency, $1/a$, the sinc-function is narrow compared with the separation of individual pulses, and each pulse is replaced, in effect, by this narrow sinc-function. On the other hand, if the filter bandwidth is small and contains only a few harmonics of this fundamental frequency, the pulse-train will resemble a sinusoidal wave. An interesting sidelight is that if the transmission function

---

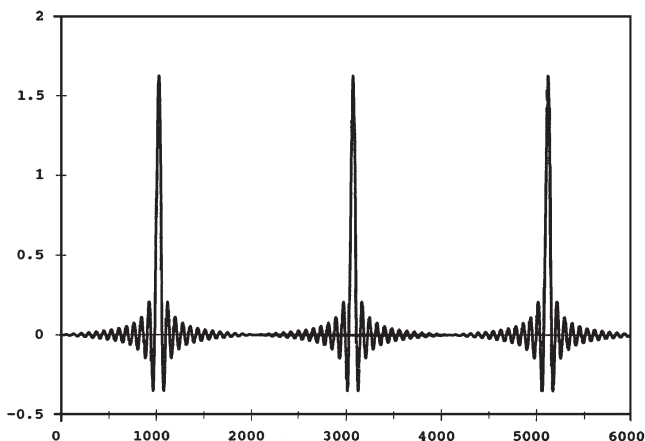[17] J. W. Gibbs, *Nature* **59** (1899), 606.

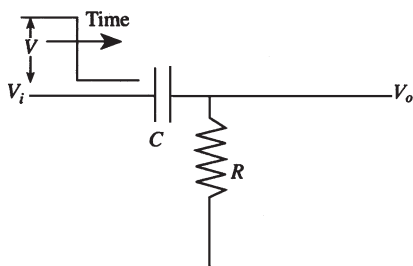Fig. 4.10. Attenuation of a pulse train by a narrow-band low-pass filter.

Fig. 4.11. A simple high-pass filter passing a voltage step.

of the filter is a decaying exponential,[18] $Z(v) = e^{-k|v|}$, then the wave train is the convolution of $III_a(t)$ with $(k/(2\pi^2))/[t^2 + (k/(2\pi))^2]$. The square of the resulting function may be familiar to students of the Fabry–Pérot étalon as the 'Airy' profile. (See Fig. 4.10.)

4.8.2 Passage of a voltage step through a simple high-pass filter

This is an example which shows that contour integration has simple practical uses occasionally.

By Ohm's law (Fig. 4.11):

$$V_o = V_i \frac{R}{R + 1/(2\pi i v C)} = V_i \frac{2\pi i v R C}{2\pi i v R C + 1} = V_i \frac{2\pi i v}{2\pi i v + \alpha},$$

where R is the resistance, C the capacitance in the circuit and $\alpha = 1/(RC)$.

---

[18] Do the Fourier transform of this in two parts: $-\infty \to 0$ and $0 \to \infty$.

Let the input step have height V so that it is described by the Heaviside step-function $\overline{V}_i(t) = V H(t)$. Its frequency content is then $V/(2\pi i \nu) = V_i(\nu)$ and

$$V_o(\nu) = \frac{V}{2\pi i \nu} \cdot \frac{2\pi i \nu}{2\pi i \nu + \alpha} = \frac{V}{2\pi i \nu + \alpha}.$$

The time-variation of the output voltage is the Fourier transform of this:

$$\overline{V}_o(t) = V \int_{-\infty}^{\infty} \frac{e^{2\pi i \nu t}}{2\pi i \nu + \alpha} \, d\nu.$$

Replace $2\pi \nu$ by z:

$$\overline{V}_o(t) = \frac{V}{2\pi} \int_{-\infty}^{\infty} \frac{e^{izt}}{iz + \alpha} \, dz$$

and multiply top and bottom by $-i$ to clear z of any coefficient:

$$\overline{V}_o(t) = \frac{-iV}{2\pi} \int_{-\infty}^{\infty} \frac{e^{izt}}{z - i\alpha} \, dz.$$

This integral will not yield to elementary methods ('quadrature'). So we use Cauchy's integral formula:[19] if z is complex, the integral of $f(z)/(z - a)$ anti-clockwise round a closed loop in the Argand plane containing the point a is equal to $2\pi i f(a)$. The quantity $f(a)$ is the *residue* of $f(z)/(z - a)$ at the 'pole', a. Written formally, it is

$$\oint \frac{f(z)}{z - a} \, dx = 2\pi i f(a).$$

Here the pole is at $z = i\alpha$, so $e^{izt} = e^{-\alpha t}$ and

$$\frac{-iV}{2\pi} \int_C \frac{e^{izt}}{z - i\alpha} \, dz = -2\pi i \frac{iV}{2\pi} e^{-\alpha t} = V e^{-\alpha t}$$

and the loop ('contour') comprises (a) the real axis, to give the desired integral with $dz = dx$, and (b) the positive semicircle at infinite radius where the integrand vanishes. Along the real axis the integral is

$$\lim_{r \to \infty} \frac{-iV}{2\pi} \int_{-r}^{r} \frac{e^{ixt}}{x - i\alpha} \, dx,$$

which is the integral we want. Along the semicircle at large r, z is complex and so can be written $z = e^{i\theta}$ or as $r(\cos\theta + i\sin\theta)$ so that e^{izt} becomes $e^{ir(\cos\theta + i\sin\theta)t}$. The real part of this is $e^{-rt\sin\theta}$, which, for positive values of t,

---

[19] Which is of fundamental importance and to be found in any book dealing with the functions of a complex variable.
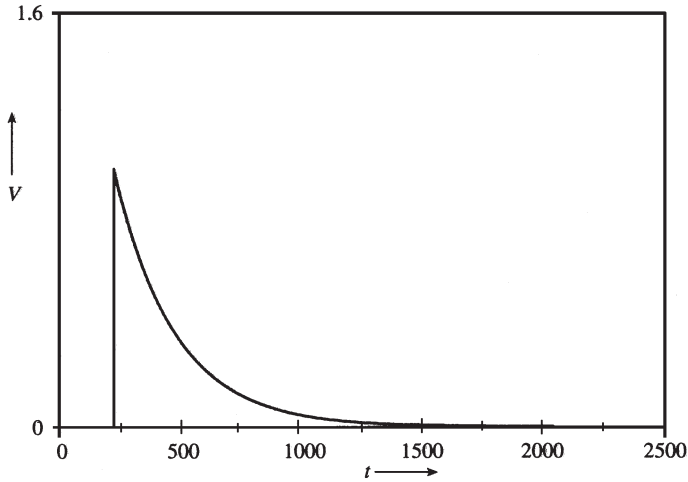
Fig. 4.12. V_o as a function of time after passing through a simple high-pass filter when the input is a Heaviside step-function.

vanishes as r tends to infinity (this is why we choose the positive semicircle – $\sin\theta$ is positive). The integral around the positive semicircle then contributes nothing to the total.

Thus, for $t > 0$, the time variation $V_o(t)$ of the output voltage is

$$V_o(t) = Ve^{-\alpha t}.$$

For negative values of t, the negative semicircle must be used for integration in order to make the integral vanish. The negative semicircle contains no pole, so the real axis integral is also zero. So the complete picture of the response is that shown in Fig. 4.12.

5

Applications 3: interference spectroscopy and spectral line shapes

5.1 Interference spectrometry

One of the fundamental formulae of interferometry is the equation giving the condition for maxima and minima in an optical interference pattern:

$$2\mu d \cos\theta = m\lambda,$$

where m must be integer for a maximum and half-integer for a minimum.

There are five possible variables in this equation, and by holding three constant, allowing one to be the independent variable and calculating the other, many different types of fringe can be described, sufficient for nearly all interferometers; and nearly all the types of interference fringe referred to in optics textbooks,[1] such as 'localized' fringes, fringes of constant inclination, Tolansky fringes, Edser–Butler fringes etc. are included.

5.2 The Michelson multiplex spectrometer

The Michelson interferometer (Fig. 5.1) dates from about 1887. In the original version, a lens collimates light from a source and transmits it through a so-called beam-splitter, a half-silvered reflector which transmits and reflects equal amplitudes of the incident light. (It also absorbs a considerable fraction.) The two separated beams are coherent and are reflected from two flat mirrors, or possibly two reflecting cube-corners, and returned to the beam-splitter. There the two beams recombine and equal fractions are again transmitted and reflected. The transmitted fractions are the ones of interest. Because of the coherence the combined amplitudes may be added, and the addition is vectorial because,

---

[1] For example, M. Born & E. Wolf, *Principles of Optics*, 7th edn, Cambridge University Press, Cambridge, 2002; or E. Hecht & A. Zajac, *Optics*, 4th edn, Addison Wesley, New York, 2003.
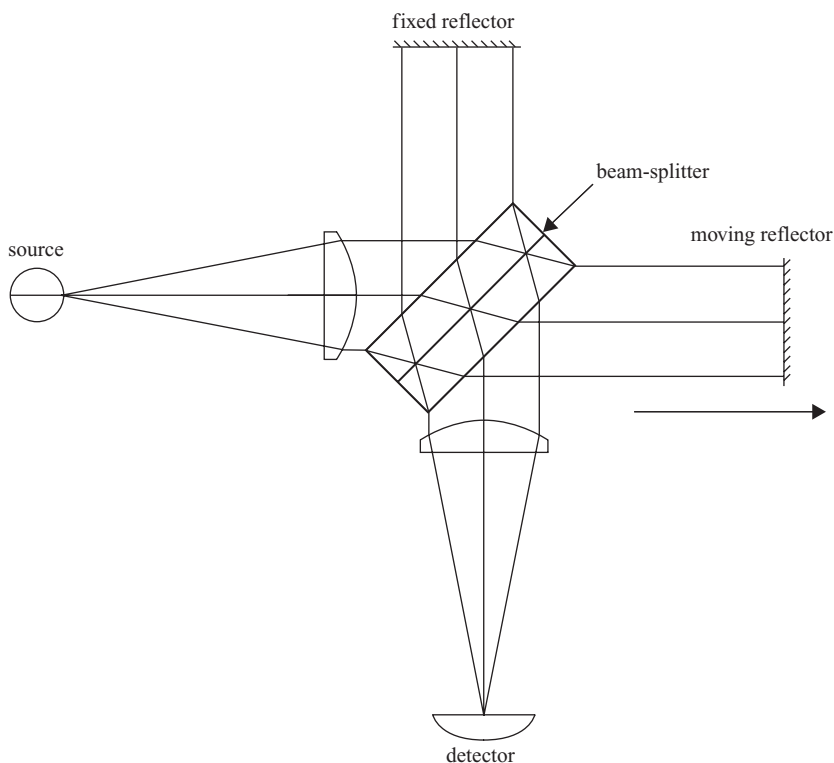
Fig. 5.1. The Michelson interferometer: optical arrangement. The moving reflector must be displaced in steps which are accurately $\lambda/4$, where λ is the shortest wavelength in the spectrum, and the alignment of its surface must be maintained constant to within $\pm\lambda/8$ or better.

unless the two arms are of exactly equal length, there is a phase-difference between the two components and they may reinforce or cancel each other out if the path-difference is an integer or half-integer number of wavelengths. If the light is monochromatic the transmitted intensity varies sinusoidally as one of the reflectors is moved uniformly to change the path-difference. Michelson originally used this fact to measure wavelengths and ultimately to calibrate measuring-rods by tediously counting the number of fringes passing when moving a mirror by a known, measured distance.

When several wavelengths are present the output signal contains a range of frequencies with amplitudes corresponding to the intensities of the various spectral components. Fourier analysis of the signal can thus recover the spectrum of the source.

It was Lord Rayleigh who, in a letter[2] to Michelson, pointed out that the intensity of the light in the fringe system is the Fourier transform of the spectrum of the transmitted light, although there were no means at the time of measuring the intensity, let alone computing its Fourier transform.

With improvements in technology in the latter half of the twentieth century both light intensity and reflector positions became measurable with the necessary accuracy. Fourier transforms became computable via the FFT,[3] and high-resolution Fourier spectrometry became possible. The reasons for doing spectroscopy in this way were two-fold.

(1) The 'throughput' or 'light-grasp' of an interferometer is greater by a factor of several hundred than that of a grating spectrometer of the same aperture.
(2) There is a substantial gain in signal-to-noise ratio in infra-red spectroscopy, where electronic noise in the detector is the chief source of noise, since the whole spectrum is being observed at once instead of having small wavelength intervals selected and measured sequentially by a monochromator. This gain is generally known as the *multiplex advantage* or the *Fellgett advantage* after its discoverer.[4]

All this allows the analysis of very faint astrophysical or aeronomic sources, or the very rapid measurement of infra-red absorption spectra, sometimes in 'real-time' as gaseous fractions come successively through from a gas-chromatograph column to an absorption cell.

There were formidable technical problems to be overcome, since the device is mechanically equivalent to a grating-ruling engine with a new grating ruled every time a spectrum is measured, and a similar precision is needed.

5.2.1 The theory of the Michelson–Fourier spectrometer

In normal adjustment, the focusing lens produces a series of concentric fringes at its focal plane, and there is an aperture through which light from one fringe can pass through to the detector. This aperture is equivalent to the slit of a grating spectrometer. Light of wavenumber ν arriving at the beam splitter can be described[5] by

$$A = A_0 e^{2\pi i \nu t}$$

---

[2] Lord Rayleigh, *Phil. Mag.* **34** (1892), 407.   [3] See Chapter 9.
[4] P. B. Fellgett, *Proc. Phys. Soc.* B **62** (1949), 529.
[5] It is more convenient to consider wave*number* rather than wave*length* in this type of spectroscopy.

and immediately after the beam-splitter the two emerging wavefronts, ignoring absorption, are

$$A_1 = A_2 = \frac{A_0}{\sqrt{2}} e^{2\pi i v t}.$$

If the two beams travel distances d_1 and d_2 in the two arms of the interferometer, then on recombining they emerge in the transmitted direction as

$$A_{\text{trans}} = \left[\frac{A(0)}{2} e^{2\pi i v d_1} + \frac{A_0}{2} e^{2\pi i v d_2} \right] e^{2\pi i v t}.$$

Notice, incidentally, that even if the transmitted and reflected amplitudes are not equal, each beam experiences one transmission and one reflection and the two finally transmitted amplitudes are (or ought to be) the same.

The transmitted intensity, which is what the detector sees, is then

$$I = \frac{|A_0|^2}{2} [1 + \cos(2\pi v(d_1 - d_2))]$$

and from here on we shall refer to $(d_1 - d_2)$ as the path-difference Δ.

So much for monochromatic light. In reality a monochromatic beam would convey no power, since power is proportional to bandwidth, and the intensity received by the detector from a source of infinitesimal bandwidth, dv, can be described by

$$I(v)dv = \frac{I_0(v)dv}{2} [1 + \cos(2\pi v \Delta)],$$

again neglecting losses in the beam-splitter, scattering and other practical matters.

Now, if a real source of light of spectral power density $S(v)$ is sent through the instrument the power received at the detector is

$$I(\Delta) = \int_0^\infty \frac{S(v)dv}{2} [1 + \cos(2\pi v \Delta)]$$

$$= \frac{S}{2} + \frac{1}{2} \int_0^\infty S(v)dv \cos(2\pi v \Delta)$$

and we generally write this expression as

$$2I(\Delta) - S = J(\Delta) = \int_0^\infty S(v)dv \cos(2\pi v \Delta),$$

where S represents the total power delivered to the detector. $J(\Delta)$, by its definition, may well be negative when the path-difference is such as to send half the incident power back to the source.

More succinctly, we write

$$J(\Delta) \rightleftharpoons S(\nu).$$

The 'interferogram', $J(\Delta)$, which is what is recorded, is the Fourier cosine transform of $S(\nu)$, the spectral power density.

Various practical matters intervene. Before the days of the digital computer and even then only after the discovery or invention of the fast Fourier transform (q.v.), there was no real possibility of doing serious Fourier spectroscopy despite the display of much ingenuity in the invention of analogue devices for carrying out the transform. In modern practice the interferogram is recorded digitally, either as the path-difference is changed continuously by a smooth motion of one of the reflectors, or by a step-by-step change of path-difference, a 'sample' being taken at each step. Here the sampling theorem intervenes and, in principle, the interferogram should be sampled at intervals of path-difference not greater than the reciprocal of twice the highest wavenumber in the spectrum. In practice this may be wasteful if the source occupies less than an octave of the electromagnetic spectrum and an analysis of the complete interferogram would only show that large parts of the spectrum are empty. With suitable optical filtering, step-lengths can be made larger and the spectrum recovered from a higher alias of the true spectrum.

Again, in practice, optical and mechanical shortcomings make it difficult to find the exact position of zero path-difference and there may be wave-length dispersion in the optics, so that the position of zero path-difference is wavenumber-dependent. Various techniques are in use to correct for these instrumental defects, for example by using the interpolation theorem to find the 'true' sample magnitudes (what they would have been if the samples had been taken exactly from zero path-difference) and by computing the power transform.

The similarity to the mechanism of a grating-ruling engine extends to similar errors of measurement. If, for example, there is a cyclic variation in the step length, there will be spurious satellite lines.

The technique generally is valuable only where detector noise predominates. In the visible and ultra-violet, photo-electric detectors are chiefly used and photo-electron shot noise from the incoming signal is the chief noise source. Then not only is there no multiplex advantage, but there is actually a multiplex *dis*advantage, since photo-electron shot noise from a dominant emission line appears throughout the recovered spectrum and can swamp all the other faint emission lines which may be present.

Other Fourier-transform-related processes are involved in the analysis of the interferogram. If, for example, the path-difference has been changed smoothly instead of step-wise, each sample recorded for the interferogram is accumulated

over a small change of path-difference and so is the convolution of the true sample with a top-hat function of width equal to one sample interval. The spectrum coming from the transformer has been multiplied by a very broad sinc-function with zero-crossing points at $2\nu_f$ and the computed spectrum must be divided by this sinc-function to recover the true spectrum.

The instrumental profile of a Fourier spectrometer is a sinc-function, rather than the sinc^2-function of a grating spectrograph. This has the disadvantage of enormous side-lobes, or secondary maxima, which are 22% of the height of the principal maximum so that apodization is essential. This is done by multiplying the interferogram by some suitable function, so that the output line profile is the convolution of the sinc-profile with the apodizing function.

The process is exactly analogous to the covering of a diffraction grating with an apodizing mask as outlined in Chapter 3. There was much experimentation with functions of different proportions, and the function discovered by Janine Connes[6] has found much favour. It requires that the nth sample of an interferogram with N samples be multiplied by $[1 - (n/N)^2]^2$. It is illustrated in Fig. 5.2.

5.3 The shapes of spectrum lines

When an electrical charge is accelerated it loses energy to the radiation field around it. In uniform motion it produces a magnetic field proportional to the current, that is, to $\mathbf{e}\,\partial x/\partial t$; and if the charge is accelerated the changing magnetic field produces an electric field proportional to $\mathbf{e}\,\partial^2 x/\partial t^2$. This in turn induces a magnetic field (via Maxwell's equations), which is also proportional to $\mathbf{e}\,\partial^2 x/\partial t^2$.

If the charge is oscillating, so are the fields induced around it and these are seen as electromagnetic radiation – in other words, light or radio waves. The power radiated is proportional to the squares of the field strengths $\frac{1}{2}(\epsilon_0\mathbf{E}^2 + \mu_0\mathbf{H}^2)$, which are proportional to $\mathbf{e}(\partial^2 x/\partial t^2)^2$. The total power radiated is $[2/(3c^2)]|\ddot{\mathbf{X}}|^2$, where $\mathbf{X}$ is the maximum value of the dipole moment $\mathbf{ex}$ generated by the oscillating charge. A dipole losing energy in this way is a damped oscillator, and one of Planck's early successes[7] was to show that the damping constant γ is given (in SI units) by

$$\gamma = \frac{1}{4\pi\epsilon_0}\frac{8\pi^2}{3}\frac{\mathbf{e}^2}{mc}\frac{1}{\lambda^2}.$$

[6] J. Connes, *Aspen Conference on Multiplex Fourier Spectroscopy*, G. A. Vanasse, A. T. Stair & D. J. Baker, (eds). AFCRL-71-0019. 1971, p. 83.
[7] M. Planck, *Ann. Phys.* **60** (1897), 577.
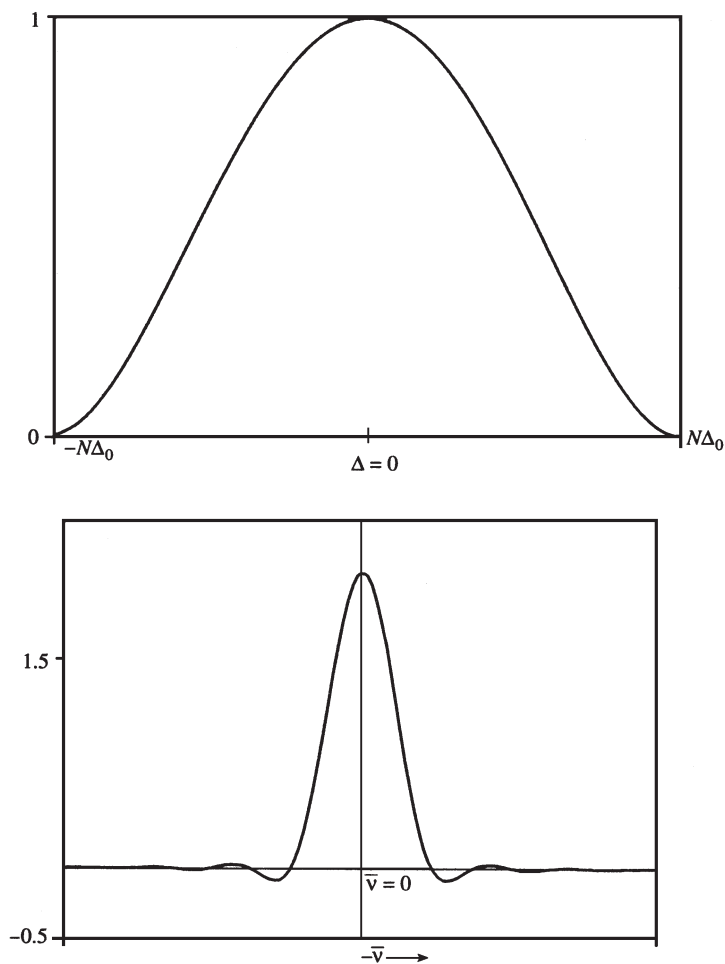
Fig. 5.2. The Connes apodizing function for infra-red Fourier spectroscopy and its effect on the instrumental profile. Without it each emission line in the spectrum would be represented by a sinc-function with secondary maxima −22% of the principal maximum in height.

The equation of motion for an oscillating dipole is then the usual damped harmonic oscillator equation:

$$\ddot{x} + \gamma \dot{x} + Cx = 0,$$

where C is the 'elastic' coefficient, which depends on the particular dipole, and which describes its stiffness and the frequency of the oscillation. Here γ is of course the damping coefficient which determines the rate of loss of energy.

The solution of the equation is well known, being

$$f(t) = e^{-\frac{\gamma}{2}t}\left(Ae^{2\pi i\bar{\nu}_0 t} + Be^{-2\pi i\bar{\nu}_0 t}\right),$$

and it is convenient to put $A = 0$ here so that the amplitude, as a function of time, is

$$f(t) = e^{-\frac{\gamma}{2}t} Be^{-2\pi i\bar{\nu}_0 t}.$$

The Fourier transform of this gives the spectral distribution of amplitude and, when multiplied by its complex conjugate, gives the spectral power density:

$$\phi(\bar{\nu}) = \int_0^\infty e^{-\frac{\gamma}{2}t} Be^{2\pi i\bar{\nu}_0 t} e^{-2\pi i\bar{\nu}t}\, dt$$

(the lower limit of integration is 0 because the oscillation is deemed to begin then). On integrating we get

$$\phi(\bar{\nu}) = e^{-\frac{\gamma}{2}t}\left[\frac{e^{2\pi i(\bar{\nu}_0 - \bar{\nu})t}}{2\pi i(\bar{\nu}_0 - \bar{\nu}) - \gamma/2}\right]_0^\infty = \frac{1}{2\pi i(\bar{\nu}_0 - \bar{\nu}) - \gamma/2}.$$

The spectral power density is then

$$I(\bar{\nu}) = \frac{1}{4\pi^2(\bar{\nu}_0 - \bar{\nu})^2 + (\gamma/2)^2}$$

and the line profile is the Lorentz profile discussed in Chapter 1. See Fig. 5.3.

The same equation can be derived quantum mechanically[8] for the radiation of an excited atom. The constant $\gamma/2$ is now the 'transition probability', the reciprocal of the 'lifetime of the excited state' if only one downward transition is possible. The FWHM of a spectrum line emitted by an 'allowed' or 'dipole' atomic transition of this sort is usually called the 'natural' width of the line. The shape occurs yet again in nuclear physics, this time called the 'Breit–Wigner formula', and describing in the same way the energy spread in radioactive-decay energy spectra. The underlying physics is obviously the same as in the other cases.

There is thus a direct link between the transition probability and the breadth of a spectrum line, and in principle it is possible to measure transition probabilities by measuring this breadth. With typical 'allowed' or 'dipole' transitions – the sort usually seen in spectral discharge lamps – the transition probabilities are in the region of 10^8 s^{-1} and the breadth of a spectrum line at 5000 Å – in the green – is about 0.003 Å. This requires high resolution, a Fabry–Pérot étalon for instance, to resolve it. The measurement is quite difficult since atoms in a

[8] See, for example, N. F. Mott & I. N. Sneddon, *Wave Mechanics and its Applications*, Oxford University Press, Oxford, 1948, Chapter 10, Section 48.
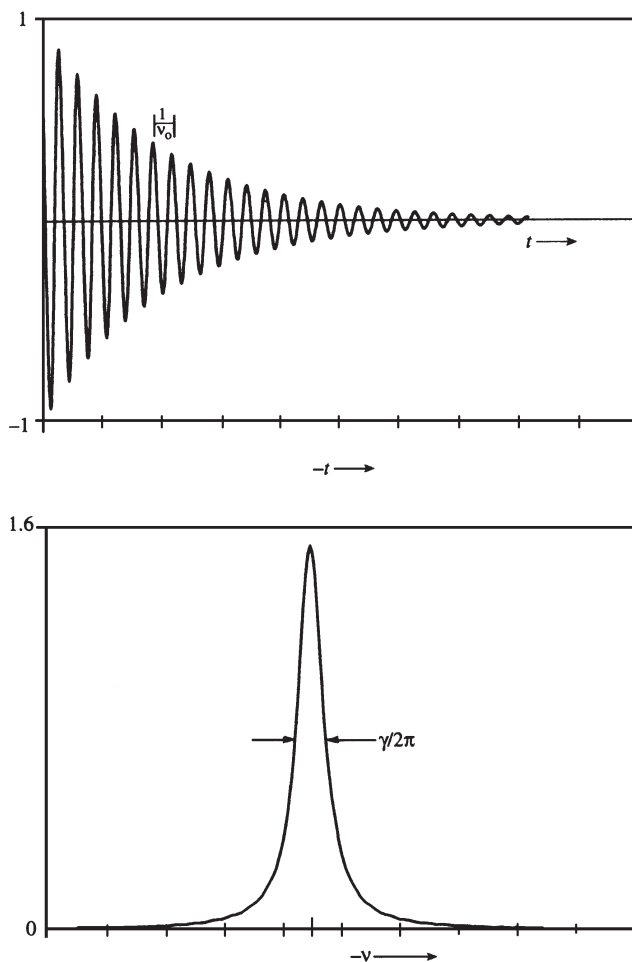
Fig. 5.3. The amplitude of a damped harmonic oscillator and the corresponding spectrum line profile: a Lorentz function with FWHM $\gamma/(2\pi)$. This would be the shape of a spectrum line emitted by an atomic transition if the atoms were held perfectly still during their emission.

gas are in violent motion, and a collimated beam of excited atoms is required in order to see the natural decay by this means.

The violent motion of atoms or molecules in a gas is described by the Maxwellian distribution of velocities. The kinetic energy has a Boltzmann distribution, and the fraction of atoms with velocity v in the observer's line-of-sight has a Gaussian distribution:

$$n(v) = n_0 e^{-mv^2/(2kT)}$$

with a proportionate Doppler shift, giving a Gaussian profile to what otherwise would be a monochromatic line:

$$I(\lambda) = I_0 e^{-(\lambda - \lambda_0)^2/a^2}.$$

The width parameter, a, comes from the Maxwell velocity distribution and $a^2 = 2\lambda_0^2 kT/(mc^2)$, where k is Boltzmann's constant, T the temperature, m the mass of the emitting species and c the speed of light.

When we substitute numbers into this formula we find that the intensity profile is a Gaussian with FWHM proportional to wavelength, and with $\Delta\lambda/\lambda = 7.16 \times 10^{-7}\sqrt{T/M}$, where M is the molecular weight of the emitting species.

This Doppler broadening, or temperature broadening, by itself would give a different line shape from that caused by radiation damping: a Gaussian profile rather than a Lorentz profile. Unless the emitter has a fairly high molecular weight or the temperature is low, the Doppler width is much greater than the natural width. However, the line shape that is really observed, after making allowance for the instrumental function, is the convolution of the two into what is called a 'Voigt' profile,

$$V(\lambda) = G(\lambda) * L(\lambda).$$

The Fourier transform will be the product of another Gaussian shape and the Fourier transform of the Lorentz shape. This Lorentz shape is a spectral power density and its Fourier transform is, according to the Wiener–Khinchine theorem, the autocorrelation of the truncated exponential function representing the decay of the damped oscillator. This autocorrelation is easily calculated. Let s be the variable paired with λ. Then $L(\lambda) \rightleftharpoons l(s)$, where

$$l(s) = \int_s^\infty e^{-\frac{\gamma}{2}s'} e^{-\frac{\gamma}{2}(s'-s)} \, ds'$$

$$= \begin{cases} \dfrac{1}{\gamma} e^{-\frac{\gamma}{2}s} & \gamma > 0, \\[2mm] \dfrac{1}{\gamma} e^{\frac{\gamma}{2}s} & \gamma < 0. \end{cases}$$

Autocorrelations are necessarily symmetrical and so we can write

$$l(s) = \frac{2}{\gamma} e^{\frac{\gamma}{2}|s|}.$$

For positive values of s, the Fourier transform of the Voigt line profile is the product

$$v(s) = e^{-\pi^2 s^2 a^2} e^{-\frac{\gamma}{2}s}$$

and a graph of $\log_e v(s)$ versus s is a parabola. From this parabola the two quantities γ and a can be extracted by elementary methods, and the two components of the convolution are separated.

Voigt profiles occur fairly frequently in spectroscopy. Not only is the line profile of a damped oscillator a Lorentz curve, but the instrumental profile of a Fabry–Pérot étalon is the convolution of a Lorentz profile[9] with a Dirac comb. Fabry–Pérot fringes, when used to measure the temperature of a gas or a plasma, therefore show Voigt profiles and if the instrument is used properly – that is with the appropriate spacing between the plates for the given experiment – the Lorentz half-width will be similar to the Gaussian half-width.

Other causes of spectral line shapes can easily be imagined. If the pressure is high, atoms will collide with each other before they have had time to finish their transition. The decaying exponential is then cut short, and the resulting line shape is the convolution of the Lorentz profile with a sinc-function. The width of the sinc-function will be different for every decay, with a Poisson distribution about some average value. The resulting spectrum line then shows 'pressure-broadening', which increases as the intercollision time diminishes, i.e. as the pressure increases. This is a phenomenon which can be used, for example, to diagnose conditions in remote plasmas.

---

[9] Because where the transmitted intensity is non-trivial the sine of the phase-angle in the Airy formula can be replaced by the angle itself.

6

Two-dimensional Fourier transforms

6.1 Cartesian coordinates

The extension of the basic ideas to two dimensions is simple and direct. As before, we assume that the function $F(x, y)$ obeys the Dirichlet conditions and we can write

$$A(p, q) = \int_{y=-\infty}^{\infty} \int_{x=-\infty}^{\infty} F(x, y)e^{2\pi i(px+qy)} \, dx \, dy,$$

$$F(x, y) = \int_{q=-\infty}^{\infty} \int_{p=-\infty}^{\infty} A(p, q)e^{-2\pi i(px+qy)} \, dp \, dq.$$

The space of the transformed function is of course two-dimensional, like the original space. The extension to three or more dimensions is obvious.

It sometimes happens that the function $F(x, y)$ is separable into a product $f_1(x)f_2(y)$. In this case the Fourier pair, $A(p, q)$, is separable into $\phi_1(p)\phi_2(q)$ and we find separately that

$$f_1(x) \rightleftharpoons \phi_1(p); \qquad f_2(y) \rightleftharpoons \phi_2(q).$$

If $F(x, y)$ is not separable in this way then the transform must be done in two stages:

$$A(p, q) = \int_{-\infty}^{\infty} e^{2\pi iqy} \left\{ \int_{-\infty}^{\infty} F(x, y)e^{2\pi ipx} \, dx \right\} dy,$$

and whether the x-integral or the y-integral is done first may depend on the particular function, F.

6.2 Polar coordinates

Sometimes – often – there is circular symmetry and polar coordinates can be used. The transform space is also defined by polar coordinates, ρ and ϕ, and the substitutions are

$$x = r\cos\theta; \qquad y = r\sin\theta;$$
$$p = \rho\cos\phi; \qquad q = \rho\sin\phi.$$

Then

$$A(\rho,\phi) = \int_{r=0}^{\infty}\int_{\theta=0}^{2\pi} F(r,\theta)e^{2\pi i(\rho\cos\phi\cdot r\cos\theta + \rho\sin\phi\cdot r\sin\theta)} r\,dr\,d\theta,$$

where $r\,dr\,d\theta$ is now the element of area in the integration, as can be seen directly or from the Jacobian $\partial(x,y)/\partial(r,\theta)$.

This shortens to

$$A(\rho,\phi) = \int_{r=0}^{\infty}\int_{\theta=0}^{2\pi} F(r,\theta)e^{2\pi i\rho r\cos(\theta-\phi)} r\,dr\,d\theta$$

and, if the function F is separable into $P(r)\Theta(\theta)$, the integrals separate into

$$\int_{r=0}^{\infty} P(r)\left\{\int_{\theta=0}^{2\pi}\Theta(\theta)e^{2\pi i\rho r\cos(\theta-\phi)}\,d\theta\right\} r\,dr.$$

If there is circular symmetry A is a function of r only, and $\Theta(\theta) = 1$. We can write

$$A(\rho,\phi) = \int_{r=0}^{\infty} P(r)\left[\int_{\theta=0}^{2\pi} e^{2\pi i\rho r\cos(\theta-\phi)}\,d\theta\right] r\,dr.$$

We now put $\theta - \phi = \alpha$, a new independent variable, with $d\alpha = d\phi$ (the integral, being taken around 2π, does not depend on the value of θ).

Then the θ-integral becomes

$$\int_{0}^{2\pi} e^{2\pi i\rho r\cos\alpha}\,d\alpha$$

and this (see Appendix A.2) is equal to $2\pi J_0(2\pi\rho r)$, where J_0 denotes the zeroth-order Bessel function.

Then

$$A(\rho) = 2\pi\int_{0}^{\infty} P(r)r\,J_0(2\pi\rho r)dr,$$

which is known as a Hankel transform. It is a close relative of the Fourier transform.

The Bessel functions of any order n, $J_n(x)$, have the property that when they are multiplied by $x^{1/2}$ they form an orthogonal set[1] like the trigonometric functions:

$$\int_0^\infty x J_n(x) J_m(x) dx = \delta_m^n,$$

where δ_m^n is the usual Kronecker-delta ($\delta_m^n = 0$ if $m \neq n$ and $\delta_m^m = 1$).

Consequently there is an inversion formula as in the Fourier transform, so that $P(r)$ can be recovered from

$$P(r) = 2\pi \int_0^\infty A(\rho)\rho J_0(2\pi\rho r) d\rho$$

and the two functions are symbolically linked by

$$P(r) \Leftrightarrow A(\rho).$$

6.3 Theorems

Some, but not all, of the theorems derived in Chapter 2 carry over into two dimensions. As above, assume that $P(r) \Leftrightarrow A(\rho)$; then we have the following.

- The similarity theorem: $P(kr) \Leftrightarrow (1/k^2)A(\rho/k)$.
- The addition theorem: $P_1(r) + P_2(r) \Leftrightarrow A_1(\rho) + A_2(\rho)$.
- Rayleigh's theorem:

$$\int_0^\infty |P(r)|^2 r\, dr = \int_0^\infty |\Phi(\rho)|^2 \rho\, d\rho.$$

- The convolution theorem. There is a convolution theorem like that in one dimension but one of the functions has to explore the whole plane in two dimensions instead of just sliding over the other. The product integral is done at each point in the plane to obtain the convolution:

$$C(r') = P_1(r) * * P_2(r) = \int_{r=0}^\infty \int_{\theta=0}^{2\pi} P_1(r) P_2(R) r\, dr\, d\theta,$$

where $R^2 = r^2 + r'^2 - 2rr' \cos\theta$ and the symbol $**$ is used to denote a two-dimensional convolution. Then

$$C(r) \Leftrightarrow A_1(\rho) A_2(\rho).$$

---

[1] A proof of the orthogonality is given by Bracewell (see the bibliography).

6.4 Examples of two-dimensional Fourier transforms with circular symmetry

- The top-hat function, also known as 'circ' or 'disk':

$$P(r) = \begin{cases} h, & 0 < r < a, \\ 0, & a < r < \infty, \end{cases}$$

$$A(\rho) = 2\pi h \int_0^a r \cdot J_0(2\pi\rho r)dr.$$

We use the property (see Appendix A.2)

$$\frac{d}{dx}(x J_1(x)) = x J_0(x).$$

Let

$$2\pi\rho r = x; \qquad 2\pi\rho \, dr = dx.$$

Then

$$A(\rho) = 2\pi h \int_0^{2\pi a\rho} \frac{x}{2\pi\rho} J_0(x)\frac{dx}{2\pi\rho}$$

$$= \frac{h}{2\pi\rho^2} \int_0^{2\pi a\rho} x J_0(x)dx = \frac{h}{2\pi\rho^2} [x J_1(x)]_0^{2\pi a\rho}$$

$$= \frac{ah}{\rho} J_1(2\pi a\rho) = \pi a^2 h \left\{ \frac{2J_1(2\pi a\rho)}{2\pi a\rho} \right\}$$

and finally

$$A(\rho) = \pi a^2 h \, \text{Jinc}(2\pi a\rho), \quad \text{where Jinc}(x) = \frac{2J_1(x)}{x}.$$

Jinc contains the factor of 2 in order that $\text{Jinc}(0) = 1$.

This, with a as the aperture radius and ρ as $\sin\theta/\lambda$, gives the amplitude of diffraction of light or radio waves at a circular aperture. The intensity distribution, which is the square modulus of this, is the famous 'Airy disc' familiar to students of the telescope and other optical imaging instruments.

- The thin annulus. $P(r)$ is a circle of radius a. In optics, for a very thin ring transmitting light,

$$P(r) = h\delta(r - a).$$

Then

$$A(\rho) = 2\pi h \int_0^\infty r\delta(r - a) J_0(2\pi\rho r)dr$$

$$= 2\pi ah J_0(2\pi a\rho).$$

6.5 Applications

6.5.1 Fraunhofer diffraction by a rectangular slot

The simple two-dimensional Fraunhofer theory of Chapter 3 can now be elaborated. There, we assumed that the element dS on the surface S was equal *in area* to dx, the width of a slit × unit length perpendicular to the diagram.

Now we can use $dS = dx\,dy$, a small rectangle in the diffracting aperture, perpendicular to the direction of propagation, and we can calculate the diffracted amplitude in a direction specified by direction cosines l, m, n. From this we can calculate the intensity at a point on a plane at a distance z from the aperture. If the amplitude at the element of area $dx\,dy$ at $Q(x, y)$ is $K\,dx\,dy$, then at P, on the distant screen, it will be $K\,dx\,dy\,e^{\frac{2\pi i}{\lambda}R'}$ and, from elementary coordinate geometry, $R' = R - lx - my$, where l and m are the direction cosines of the line OP and R is the distance from the origin to the point P on the distant screen. See Fig. 6.1.

The total disturbance at P is then the sum of all the elementary disturbances from the $z = 0$ plane, so that we can write

$$A(p, q) = \int\int_{\text{aperture}} K\,dx\,dy\,e^{2\pi i\left(\frac{R}{\lambda} - \frac{lx}{\lambda} - \frac{my}{\lambda}\right)}$$

$$= C \int\int_{\text{aperture}} e^{-2\pi i(px + qy)}\,dx\,dy,$$
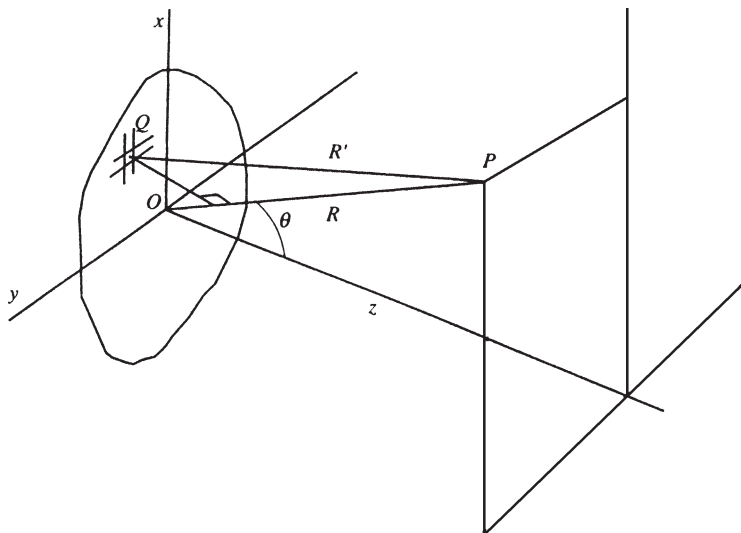
Fig. 6.1. The two-dimensional diffracting aperture, in Cartesian coordinates.

where $p = l/\lambda$, $q = m/\lambda$ and C is a constant which depends on the area of the aperture, and contains the constant phase factors and any other things which do not affect the relative intensity in the diffraction pattern.

If the aperture is a rectangle of sides $2a$ and $2b$, the integrals separate:

$$A(p, q) = C \int_{-a}^{a} e^{-2\pi i p x} \, dx \int_{-b}^{b} e^{-2\pi i q y} \, dy,$$

and the intensity diffracted in the direction whose direction cosines are $p\lambda$ and $q\lambda$ is the square-modulus of this:

$$I(p, q) = I_0 \, \mathrm{sinc}^2(2\pi a p) \mathrm{sinc}^2(2\pi b q).$$

Notice that, perhaps surprisingly, the intensity at the central peak is proportional to the *square* of the area of the aperture.

6.5.2 Fraunhofer diffraction by a circular aperture

If the aperture is circular and of radius a, the Hankel transform is used, with $x = r \cos\theta$, $y = r \sin\theta$ as before and with $p = l/\lambda = \rho \cos\phi$, $q = m/\lambda = \rho \sin\phi$ and $\rho^2 = p^2 + q^2$.

The third direction cosine, n, is given by

$$n^2 = 1 - l^2 - m^2 = 1 - (p\lambda)^2 - (q\lambda)^2$$

so that

$$\rho^2 = \frac{1}{\lambda^2}(l^2 + m^2) = \frac{1 - n^2}{\lambda^2}$$

or $\rho = \sin\theta/\lambda$, where θ is the angle between OP and the z-axis.

Then, immediately, we have

$$A(\theta) = A(0) \frac{J_1(2\pi a \sin\theta/\lambda)}{2\pi a \sin\theta/\lambda}$$

and

$$I(\theta) = I(0) \left[\frac{J_1(2\pi a \sin\theta/\lambda)}{2\pi a \sin\theta/\lambda} \right]^2,$$

which is the formal equation for the intensity in the Airy disc. Again notice that $I(0)$ is proportional to the square of the area of the aperture. The total power in the pattern is of course proportional to the area of the aperture, but as the radius of the diffracting aperture doubles, for example, the pattern on a distant screen has half the radius and one-quarter the area, out to the first zero-intensity ring.

As an exercise, the calculation of the intensity distribution in the diffraction pattern made by an annular aperture can be done. If the inner and outer radii of the annulus are a and b, the amplitude function is

$$A(\theta) = K \left[a^2 \frac{J_1(2\pi a \sin\theta/\lambda)}{2\pi a \sin\theta/\lambda} - b^2 \frac{J_1(2\pi b \sin\theta/\lambda)}{2\pi b \sin\theta/\lambda} \right]$$

and the intensity distribution is the square of this.

A graph of this function shows that the central maximum is narrower than that of the Airy disc for the same outer radius. A telescope with an annular aperture apparently beats the 'Rayleigh criterion' for spatial resolution. However, it does so at the expense of putting a lot of intensity into the ring around the central maximum, and the gain is usually more illusory than real.

6.6 Solutions without circular symmetry

In general, provided that the aperture function can be separated into $P(r)$ and $\Theta(\theta)$, then, as we saw earlier,

$$A(\rho, \phi) = \int_{r=0}^{\infty} P(r) \left\{ \int_{\theta=0}^{2\pi} \Theta(\theta) e^{2\pi i \rho r \cos(\theta - \phi)} \, d\theta \right\} r \, dr.$$

Consider the interference pattern of a set of apertures – or antennae – equally spaced around the circumference of a circle. If there are N of them, the θ-dependent function is

$$\Theta(\theta) = \sum_{0}^{N-1} \delta(\theta - 2\pi n/N)$$

and the r-dependent part is

$$P(r) = \delta(r - a).$$

In other words, the sources are equally spaced at angles $2\pi/N$ around the circle of radius a

Then

$$A(\rho, \phi) = \int_0^{\infty} r\delta(r - a) \sum_{0}^{N-1} e^{2\pi i \rho r \cos(2\pi n/N - \phi)} \, dr$$

$$= a \sum_{0}^{N-1} e^{2\pi i \rho a \cos(2\pi n/N - \phi)}.$$

This is as far as the analysis can be taken. The pattern, $I(\rho, \phi)$, can be computed without difficulty from this expression, and is a typical example of a problem
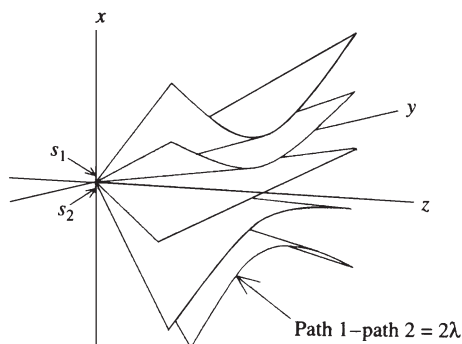
Fig. 6.2. The cones of maximum intensity in a two-beam interference pattern. The two interfering sources are on the x-axis, above and below the origin.

solved by computer after analysis fails. The particular case of $N = 2$ yields the familiar pattern of two-beam interference, including the hyperbolic shapes of the fringes on a distant plane surface:

$$A(\rho, \phi) = a[e^{2\pi i a\rho \cos \phi} + e^{2\pi i a\rho \cos(\pi - \phi)}]$$
$$= 2a \cos(2\pi a\rho \cos \phi),$$

and the intensity pattern is given by

$$I(\rho, \phi) = 4a^2 \cos^2(2\pi a\rho \cos \phi),$$

which has maxima when $2a\rho \cos \phi$ is integer. Since $\rho = \sin \alpha/\lambda$, the maxima occur when $\phi = n\lambda/2a \sin \alpha$. Here α is the angle between the z-axis and the direction of diffraction, and ϕ is the *azimuth* (angle in the p, q-plane), so that interference fringes, the maxima of $I(\rho, \phi)$, emerge along directions defined by the condition $(2a/\lambda)\sin \alpha \cos \phi = $ constant, that is to say, on cones of semi-angle ϕ about the $\phi = 0$-axis (see Fig. 6.2). If they are received on a plane perpendicular to the z-axis they show hyperbolic shapes, but on a plane perpendicular to the x-axis (the $\phi = 0$-axis: the axis containing the two sources) the shapes would be concentric circles.

Other cases, such as $N = 4$, yield to analysis as well. But in general, to parody Clausewitz, it is best to regard computation as the continuation of analysis by other means.

7

Multi-dimensional Fourier transforms

The physical world seems to comprise four dimensions of space and time, and other dimensions, such as electrical potential or temperature, are used occasionally for drawing graphs. For this reason Fourier transforms in three or more dimensions can be useful sometimes. The extension is not difficult and can sometimes give greater insight into what is happening in Nature than can mere geometry. This chapter describes some of the functions and ideas which are helpful in manipulating multi-dimensional Fourier transforms.

7.1 The Dirac wall

This is described by

$$f(x, y) = \delta(x - a)$$

and is zero everywhere except on the line $x = a$, where it is infinite. Despite this infinity, it may be envisaged as a wall, parallel to the y-axis, of unit height, as in Fig. 7.1.

Its two-dimensional Fourier transform (Fig. 7.2) is given by

$$\phi(p, q) = \int_{x=-\infty}^{\infty} \int_{y=-\infty}^{\infty} \delta(x - a)e^{2\pi i p x} e^{2\pi i q y} \, dx \, dy$$

$$= \int_{y=-\infty}^{\infty} e^{2\pi i p a} e^{2\pi i q y} \, dy$$

$$= e^{2\pi i p a} \delta(q),$$

which has a complex amplitude[1] and is zero except on the line $q = 0$.

---

[1] In the sense mentioned in Chapter 1, namely that a δ-function is infinite at each point but its integral, which we consider to be its 'amplitude', is unity.
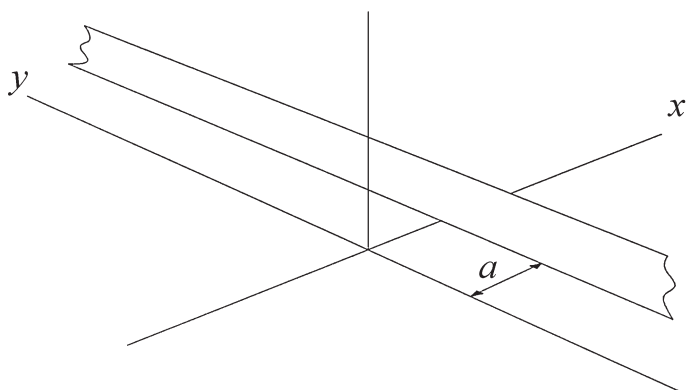
Fig. 7.1. A simple Dirac wall, $f(x, y) = \delta(x - a)$.
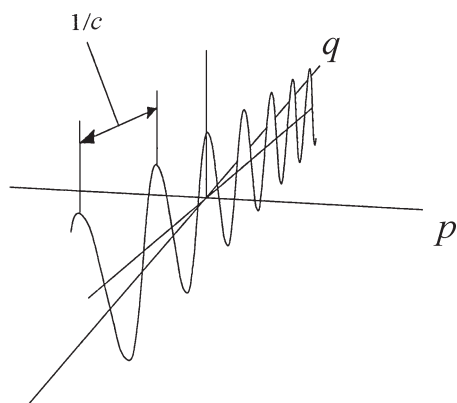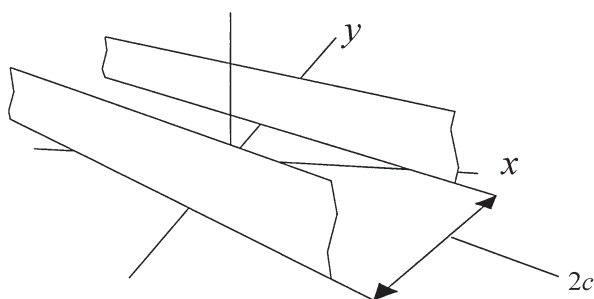
Fig. 7.2. The Fourier tranform of a pair of Dirac walls.

A pair of these Dirac walls, equally disposed about the y-axis, has a Fourier transform given by

$$\phi(p, q) = 2\delta(q)\cos(2\pi pa).$$

A wall standing on a line inclined to the y-axis at an angle θ is described by $f(x, y) = \delta(lx + my - c)$, where $l = \cos\theta$, $m = \sin\theta$ and c is the length of the perpendicular from the origin to the line. The δ-function is zero everywhere on the x, y-plane except on the line and its two-dimensional Fourier transform is

$$\phi(p, q) = \int_{x=-\infty}^{\infty} \int_{y=-\infty}^{\infty} \delta(lx + my - c)e^{2\pi ipx}e^{2\pi iqy} \, dx \, dy.$$

Do the y-integration first,[2]

$$\phi(p, q) = \frac{1}{m} \int_{x=-\infty}^{\infty} e^{2\pi ipx}e^{2\pi iq(c-lx)/m} \, dx,$$

and notice that 'integration' here is a simple replacement of the variable in the exponential by the argument of the δ-function.

Then, rearranging the exponents,

$$\phi(p, q) = \frac{1}{m}e^{2\pi iqc/m} \int_{x=-\infty}^{\infty} e^{2\pi ix(p-lq/m)} \, dx$$
$$= e^{2\pi iqc/m}\delta(mp - lq),$$

which is zero except on the line $mp - lq = 0$ in the p, q-plane.

Equally, the y-integration could have been done first, in which case the Fourier transform would have been

$$e^{2\pi ipc/l}\delta(mp - lq).$$

The period in the phase-factor is $1/c$ and it is measured along the direction of the line $mp - lq = 0$ in p, q-space. As we shall see later, it is possible to envisage a one-dimensional variable $u = p/l$ or q/m, conjugate to c, along that line, and then the above function describes a complex sinusoid of period $1/c$ along the Dirac wall. Its one-dimensional Fourier transform *along that line* would then be a δ-function at a distance c from the origin, situated at the point lc, mc in x, y-space. This δ-function would lie on the line $mx - ly = 0$.

This is the place to mention that much insight can be gained by superposing the two planes so that the p- and q-axes of one coincide with the x- and y-axes

---

[2] Bearing in mind from Chapter 1 that $\delta(lx + my - c) = (1/m)\delta(y - (c - lx)/m)$.

of the other. In this example, the Fourier transform of the Dirac wall lies on a line in the p, q-plane perpendicular to the wall in the x, y-plane.

A pair of Dirac walls, equally disposed on either side of the origin, has a two-dimensional Fourier transform given by

$$\delta(lx + my - c) + \delta(lx + my + c) \rightleftharpoons \delta(mp - lq) \cdot 2\cos(2\pi qc/m),$$

that is to say, a Dirac wall with a sinusoidally-varying amplitude and lying on the line $mp - lq = 0$.

Notice particularly that, with this superposition of the two planes, the function and its transform are related in spatial position, *irrespective of the orientation*[3] *of the coordinate systems chosen.* In this example they lie on perpendicular Dirac walls.

7.2 Computerized axial tomography

A particularly useful application of these ideas is to be found in computerized transverse axial scanning tomography, vulgarly known as CAT-scanning or C-T scanning. Imagine a Dirac wall taking a vertical slice through a two-dimensional function $F(x, y)$ lying on the x, y-plane (Fig. 7.3(a)). If the wall stands on the line $lx + my - c = 0$ the product is zero everywhere except on the line. On the line stands a Dirac wall (Fig. 7.3(b)) with amplitude varying as $F(x, (c - lx)/m)$. The line-integral (Fig. 7.3(c))

$$P_l(c) = \int_{-\infty}^{\infty} F(x, y)\delta(lx + my - c)ds \qquad (7.1)$$

(where ds is the line element along the direction defined by l) depends only on l and c. Incidentally, $P_l(c)$ is known as the *Radon transform*[4] of $F(x, y)$. It can be imagined, as in the previous section, as a δ-function of amplitude $P_l(c)$ standing on the line $mx - ly = 0$ at a distance c from the origin. With c as variable it becomes a function of c along the line and this function is called the *projection* of $F(x, y)$ in the direction θ where $\cos\theta = l$.

Now, as the direction θ rotates from 0 to π, the various functions $P_l(c)$ sweep out a two-dimensional function $Q(x, y)$ on the x, y-plane.

What is more interesting, however, is the function which results from first taking the *one-dimensional* Fourier transform of $P_l(c)$ along the line $mx - ly = 0$, with c as variable on the x, y-plane and u as its conjugate on the p, q-plane.

---

[3] But not of the position of the origin.
[4] *Vide* e.g. S. R. Deans, *The Radon Transform and Some of its Applications*, John Wiley, New York, 1983.
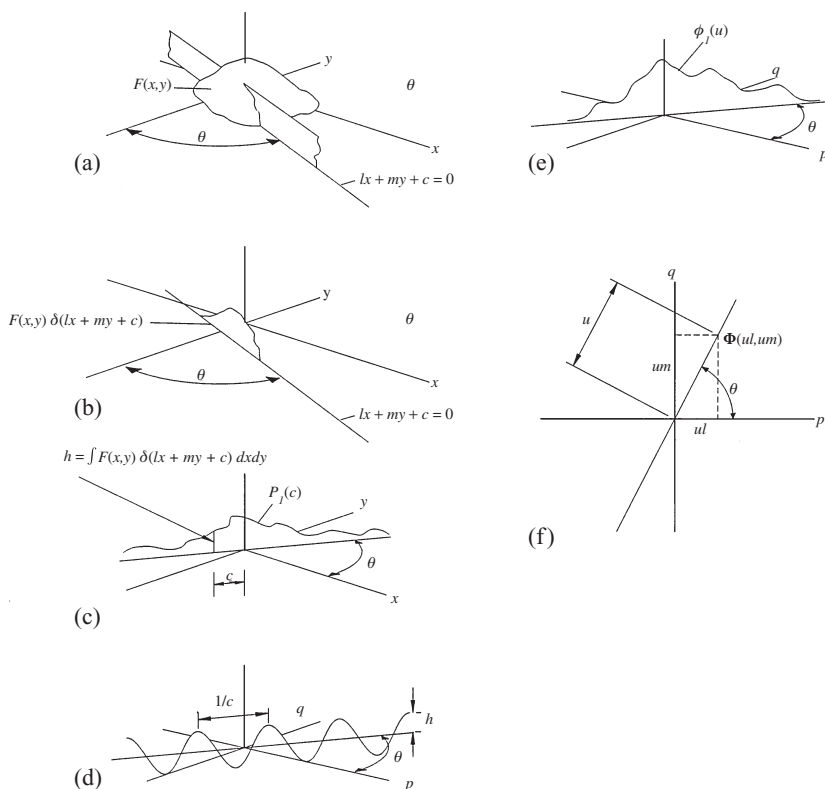
Fig. 7.3. The steps in computerized axial tomography. (a) A Dirac wall through the function $F(x, y)$. (b) The slice to be integrated along the line $lx + my + c = 0$. (c) The integral of the slice along the line, making one point of the function $P(c)$, the Radon transform of $F(x, y)$. (d) The one-dimensional Fourier transform of that point with c as variable, lying on the line in conjugate p, q-space perpendicular to the Dirac wall. (e) The complete one-dimensional Fourier transform, $\phi(u)$, of $P(c)$ in p, q-space. (f) The point on this function which defines one point of the two-dimensional function $\Phi(ul, um)$ which is shown to be the two-dimensional Fourier transform of the original $F(x, y)$.

In the p, q-plane this Fourier transform, $\phi_l(u)$, will lie on the line $mp - lq = 0$ which is superimposed on $mx - ly = 0$ on the x, y-plane. This set of Fourier transforms, too, sweeps out a two-dimensional function $\Phi(p, q)$ (the function $\phi_l(u)$ in Fig. 7.3(e)) as the direction of the projection changes from 0 to π.

We now demonstrate the remarkable fact that $\Phi(p, q)$ is the two-dimensional Fourier transform of $F(x, y)$.

To do this we first of all write $\delta(lx + my - c)$ as a one-dimensional Fourier integral, using c as the variable and u as its conjugate:

$$\delta(lx + my - c) = \int_{u=-\infty}^{\infty} e^{2\pi i(lx+my-c)u} \, du$$

$$= \int_{u=-\infty}^{\infty} e^{2\pi iu(lx+my)} e^{-2\pi icu} \, du,$$

and if we insert this into the equation for $P_l(c)$ (equation (7.1)) we find

$$P_l(c) = \int_{x=-\infty}^{\infty} \int_{y=-\infty}^{\infty} F(x, y) \int_{u=-\infty}^{\infty} e^{2\pi iu(lx+my)} e^{-2\pi icu} \, du \, dx \, dy$$

and, on changing the order of integration,

$$P_l(c) = \int_{u=-\infty}^{\infty} \left(\int_{x=-\infty}^{\infty} \int_{y=-\infty}^{\infty} F(x, y) e^{2\pi iu(lx+my)} \, dx \, dy \right) e^{-2\pi icu} \, du.$$

Within the brackets is $\Phi(ul, um)$, the two-dimensional Fourier transform of $F(x, y)$, and notice (Fig. 7.3(e)) that on the p, q-plane $ul = p$ and $um = q$.
Thus

$$P_l(c) = \int_{-\infty}^{\infty} \Phi(ul, um) e^{-2\pi icu} \, du,$$

whence, for a fixed direction θ,

$$\Phi(ul, um) = \Phi(p, q) = \int_{-\infty}^{\infty} P_l(c) e^{2\pi icu} \, dc.$$

This is still a one-dimensional transform and it defines $\Phi(p, q)$ along the line $mp - lq = 0$. In Radon transform theory it is called the *projection slice theorem*.

Thus, if we know $P_l(c)$ for all azimuths θ, from 0 to π, and do the complete set of one-dimensional transforms, the two-dimensional function $\Phi(p, q)$ is known. The original function $F(x, y)$ is then obtained from

$$F(x, y) = \int_{-\infty}^{\infty} \int_{-\infty}^{\infty} \Phi(p, q) e^{-2\pi i(px+qy)} \, dp \, dq.$$

If a three-dimensional object is partially transparent to radiation such as X-rays, visible light or a particle beam, it is possible to make a two-dimensional map of the absorption coefficient (α) on a plane section through it. When monochromatic radiation is transmitted through the object it is attenuated

according to *Beer's law*, which states that the intensity of the radiation trans-
mitted in the x-direction falls according to

$$\frac{\partial I}{\partial x} = -I\alpha,$$

where I is the intensity at the point x along the direction of transmission, and
α is the absorption coefficient for that wavelength or frequency. The coefficient
depends on the nature of the absorbing material and, if the absorption is constant
along the path, Beer's law in one dimension takes the form

$$I(x) = I_0 e^{-\alpha x}.$$

If α varies from point to point, then the integral along the transmission path
(the 'line-integral') must be taken and

$$I(x) = I_0 e^{-\int_0^x \alpha(x) \cdot dx}.$$

From this the following useful equation emerges:

$$\int_0^x \alpha(x) \cdot dx = \ln(I_0/I(x)).$$

The function of computer-aided tomography is to make a two-dimensional
plot – the map – of α in a plane slice through the object. Notice that if the
source and the detector are both outside the object then the line-integral of α is
identical with

$$\int_{-\infty}^{\infty} \alpha(x) \cdot dx = \ln(I_0/I(x)).$$

Consider an absorbing object – a skull, for example – through which a
narrow beam of X-rays can be transmitted from a source to a detector. The
line-integral of the absorption coefficient α follows from the logarithm of the
ratio of the intensity at the source to the intensity at the detector.

We now use this narrow beam as a saw-blade to 'cut' a plane section through
the object.

In Fig. 7.3 the z-axis is used to depict the absorption coefficient, $\alpha(x, y)$, in
the section and the radiation beam is directed along the line $lx + my - c = 0$.
We replace the $F(x, y)$ by $\alpha(x, y)$ in equation (7.1):

$$P_l(c) = \int_{-\infty}^{\infty} \alpha(x, y) \cdot \delta(lx + my - c) ds.$$

As the source and detector move together in the x, y-plane in a direction
perpendicular to the transmission direction, c is changing while l is constant.

The beam, as it moves, takes a slice through the absorbing object (hence the word 'tomography') and there will be a measurement of the line-integral $P_l(c)$ as a function of c (Fig. 7.3(c)).

The one-dimensional Fourier transform, $\phi_l(u)$, of $P_l(c)$ maps out, as the direction θ of the projection changes, the two-dimensional function $\Phi(p, q)$, the aggregate of these ϕ-functions over all azimuths and this, as we have seen, is the two-dimensional Fourier transform of $\alpha(x, y)$.

This is the central idea in computerized axial tomography.

The inevitable conclusion is that, provided that $P_l(c)$ is measured for every azimuth $\theta(\theta = \cos^{-1} l)$ from $\theta = 0$ to $\theta = 180°$, and the one-dimensional Fourier transforms are taken, then the function $\Phi(ul, um)$ is known over the whole p, q-plane[5] and the inverse transform of $\Phi(ul, um)$ is $\alpha(x, y)$, the original desired function:

$$\alpha(x, y) = \int_{-\infty}^{\infty} \int_{-\infty}^{\infty} \Phi(q, p) \cdot e^{-2\pi i q x} e^{-2\pi i p y} \, dq \cdot dp.$$

The function $\alpha(x, y)$ then represents the two-dimensional distribution of density, or absorption cross-section, of X-rays or other exploring radiation beams by the material through which the radiation passes.

The practical implementations[6] of the idea have been manifold and to the universal public good. This brief description ignores the extraordinary extensions of the idea[7] in areas as diverse as cosmology and geophysics, and it must also be mentioned that other methods than Fourier transforms may be used to recover the required data. There can have been few inventions more deserving of a Nobel prize than this one.

7.3 A 'spike' or 'nail'

This is described by a two-dimensional δ-function, $\delta(x - a)\delta(y - b)$, and is zero everywhere in the x, y-plane except at the point (a, b). Being the product of a function of x and a function of y, it is separable and its Fourier transform is $e^{2\pi i p a} e^{2\pi i q b}$.

---

[5] Or as much of it as the resolution of the source and detector will permit. Instrumental considerations limit the spatial frequencies accessible to a CAT-scanner and only a limited area – about $2 \, \text{mm}^{-2}$ – of frequency-space (the p, q-plane) is useable in practice with X-ray tomography.

[6] The 1979 Nobel prize for physiology and medicine was awarded to G. N. Hounsfield and A. Cormack for the invention of CAT-scanning. The prototype CAT-scanner, constructed by EMI, went into service at the Atkinson Morley Hospital, Wimbledon, in 1971.

[7] Described, for example, by Herman (see the bibliography).
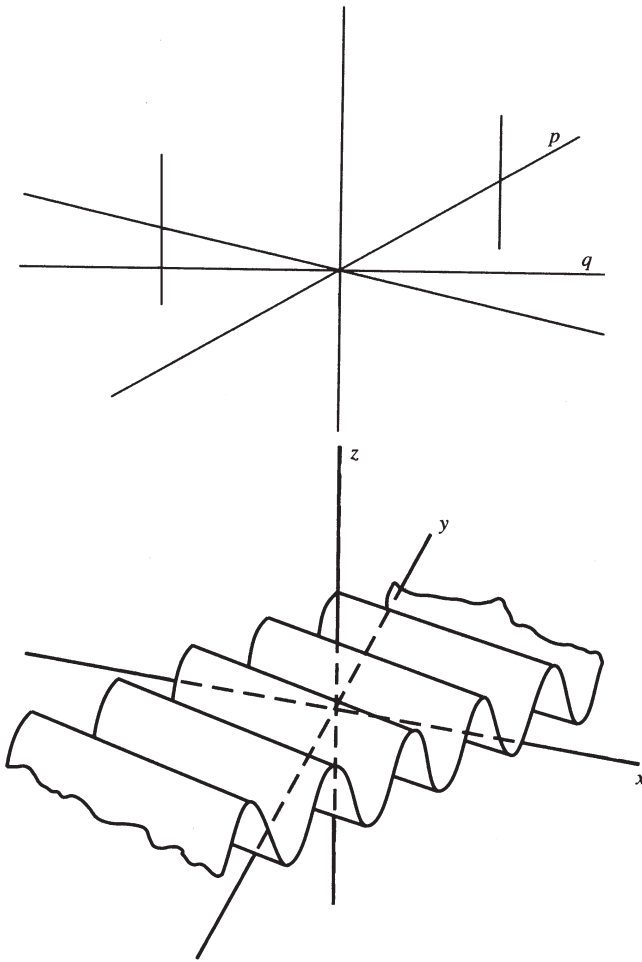
Fig. 7.4. The Fourier transform of a pair of nails at $\pm(x, y)$.

A pair of such nails equally disposed about the origin is described by

$$f(x, y) = \delta(x - a)\delta(y - b) + \delta(x + a)\delta(y + b)$$

and its Fourier transform is

$$\phi(p, q) = 2\cos[2\pi(pa + qb)].$$

This is a corrugated sheet. Lines of constant phase (wave crests) lie on the lines $pa + qb = $ integer, and are illustrated in Fig. 7.4 and again, on superposition, the line joining the nails on the x, y-plane is perpendicular to the wave crests on the p, q-plane.

7.4 The Dirac fence

This is an infinite row of equally-spaced δ-functions (the fence-posts) along a line. When it runs along the x-axis and the spacing of the posts is a, the fence is described by

$$f(x, y) = \left[\sum_{n=-\infty}^{\infty} \delta(x - na) \right] \delta(y) = III_a(x)\delta(y).$$

Its Fourier transform follows from the Fourier transform of a III-function mentioned in Chapter 1 and is $(1/a)III_{1/a}(p)$, a parallel set of walls, all parallel to the q-axis, with spacing $1/a$.

If the fence is inclined to the x-axis at an angle θ, then $l = \sin\theta$ and $m = \cos\theta$ define the direction of the line of the fence, and the fence is described by

$$f(x, y) = \left[\sum_{n=-\infty}^{\infty} \delta(lx + my - na) \right] \delta(mx - ly).$$

The first factor requires the function to be zero except when $lx + my = na$ (thus defining a set of parallel walls) and the second requires that it be zero except on a line perpendicular to the first set, passing through the origin. This can also be written as

$$f(x, y) = III_a(lx + my)\delta(mx - ly).$$

The Fourier transform can be seen graphically as the convolution of the two separate transforms. The transform of the first factor is

$$\phi_1(p, q) = \int_{-\infty}^{\infty} \int_{-\infty}^{\infty} \sum_{n=-\infty}^{\infty} \delta(lx + my - na)e^{2\pi ipx}e^{2\pi iqy} \, dx \, dy$$

and once more the simple rule for integrating a product which includes a δ-function applies:

$$\phi_1(p, q) = \frac{1}{l} \int_{-\infty}^{\infty} \sum_{n=-\infty}^{\infty} e^{2\pi ip(na-my))/l}e^{2\pi iqy} \, dy$$

$$= \frac{1}{l} \sum_{n=-\infty}^{\infty} e^{2\pi ipna/l} \int_{-\infty}^{\infty} e^{2\pi iy(q-pm/l)} \, dy$$

$$= \delta(ql - pm) \sum_{n=-\infty}^{\infty} e^{2\pi ipna/l},$$
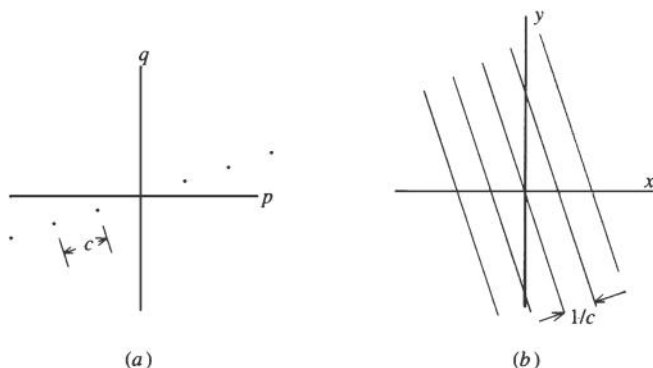
Fig. 7.5. (a) A line of fence-posts of spacing c and (b) its Fourier transform, a series of parallel walls a distance $1/c$ apart.

which is a row of fence-posts spaced $1/a$ apart[8] lying on the line $lq = mp$.

The second factor transforms similarly:

$$\phi_2(p, q) = \int_{-\infty}^{\infty} \int_{-\infty}^{\infty} \delta(mx - ly) e^{2\pi i px} e^{2\pi i qy} \, dx \, dy$$

$$= \frac{1}{m} \int_{-\infty}^{\infty} e^{2\pi i p(ly/m)} e^{2\pi i qy} \, dy$$

$$= \delta(lp + mq),$$

which is a wall passing through the origin, lying on the line $lp = -mq$, that is, perpendicular to the fence-post of the first factor when the p, q-plane is superimposed on the x, y-plane.

The convolution of these two factors, $\phi_1(p, q) ** \phi_2(p, q) = w(p, q)$, is an infinite series of parallel walls, spaced $1/a$ apart, lying on lines parallel to the line $lp = -mq$. On superposition of the two spaces, these walls are perpendicular to the original fence line. See Fig. 7.5.

7.5 The 'bed of nails'

Now consider the convolution of two fences, f_1 and f_2. Let each lie on a line through the origin, at angles θ_1 and θ_2 and with spacings a_1 and a_2. The convolution, $f_1 ** f_2$, will be a two-dimensional array of δ-functions – a 'bed of nails' (Fig. 7.6).

---

[8] Actually the product of a wall lying on the line $ql = pm$ and an infinite set of walls of spacing a/l lying perpendicular to the p-axis.
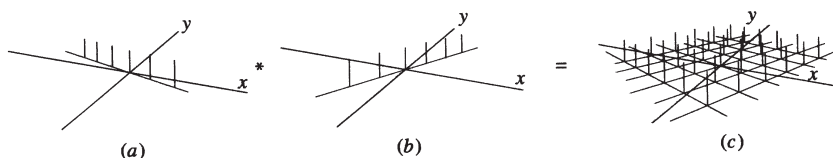
Fig. 7.6. The convolution of two lines of fence-posts, (a) and (b), to give a 'bed of nails', (c).

The Fourier transform of this convolution is the product $w_1 w_2$ of the two transforms, each one a series of parallel walls, and differs from zero only when both factors are different from zero. This gives another 'bed of nails'.

The interesting thing is that the route to $w_1 w_2$ from $f_1 * * f_2$ is not unique. The two-dimensional array $w_1 w_2$ could have been composed from two different factors, both again parallel sets of walls, but transformed from different fences f_1' and f_2' with different spacings a_1' and a_2' and different angles θ_1' and θ_2'. But the convolution of this new pair will necessarily yield the same function $f_1 * * f_2$ as before.

The correspondence between the two beds of nails is this: corresponding to *any* set of parallel lines that can be drawn through points in one plane there is a point[9] in the other. In Fig. 7.7, parallel lines separated by $1/a$ in one plane are matched by a point distance a in the other; another set separated by $1/b$ correspond to the point distance b, and so on. The whole thing is the two-dimensional analogue of the 'reciprocal lattice' idea in crystallography.

There is a familiar illustration: seats in a theatre or cinema are arranged regularly, often staggered so that people do not sit directly behind someone. Alignments of seat-backs can be seen in different directions, and these correspond to the lines that can be drawn through beds of nails.

7.6 Parallel-plane delta-functions

In three dimensions the function $\delta(lx + my + nz)$ describes a function of unit amplitude which is zero except on the plane $lx + my + nz = 0$.

Its three-dimensional Fourier transform is

$$\phi(p, q, r) = \int_{-\infty}^{\infty} \int_{-\infty}^{\infty} \int_{-\infty}^{\infty} \delta(lx + my + nz)e^{2\pi ipx}e^{2\pi iqy}e^{2\pi irz}\, dx\, dy\, dz$$

[9] Actually a pair of points – one on either side of the origin.
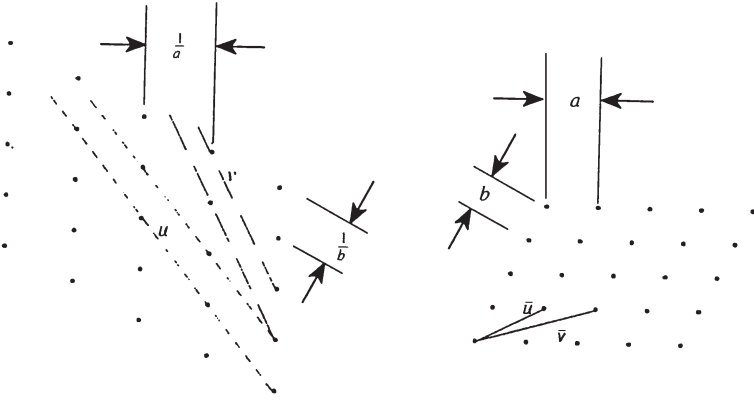
Fig. 7.7. Reciprocal lattices: the correspondence between a bed of nails and its Fourier pair. The pair are not unique: dashed lines show other possible Dirac walls, with different spacings, and the letters u and v show the corresponding directions of the Dirac fences which are their Fourier transforms. In the diagram on the right, $\bar{u}$ and $\bar{v}$ are the reciprocals of u and v: the narrow spacing of the walls implies a greater spacing between the fence-posts.

and, after the x-integration,

$$\phi(p, q, r) = \frac{1}{l} \int_{-\infty}^{\infty} \int_{-\infty}^{\infty} e^{2\pi i (p/l)(-my-nz)} e^{2\pi iqy} e^{2\pi irz} \, dy \, dz$$

$$= \frac{1}{l} \int_{-\infty}^{\infty} \int_{-\infty}^{\infty} e^{2\pi iy(q-mp/l)} e^{2\pi iz(r-np/l)} \, dy \, dz,$$

which is separable into

$$\frac{1}{l} \int_{-\infty}^{\infty} e^{2\pi iy(q-mp/l)} \, dy \int_{-\infty}^{\infty} e^{2\pi iz(r-np/l)} \, dz$$

so that

$$\phi(p, q, r) = l\delta(lq - mp)\delta(lr - np),$$

a δ-function which, when the coordinate systems are superimposed, is zero except on the line $p/l = q/m = r/n$, a line through the origin, perpendicular to the original plane in the x, y, z frame.

The extension is intuitive: a pair of parallel planes equally disposed about the origin and each at a distance a from the origin will have as a Fourier transform a line along which the amplitude varies sinusoidally with period $1/a$. An infinite sequence of equally separated parallel planes will transform to a row of equally-spaced points along a line passing through the origin and

perpendicular to the planes. It is the three-dimensional version of a Dirac comb but the function differs from zero at isolated *points*.

7.7 Point arrays

The ideas are even more apparent when transforms are done in three dimensions, when point-arrays are defined by products of three three-dimensional III-functions. For example, $III_a(l_1 x + m_1 y + n_1 z)$ defines a set of parallel planes on which the function is not zero. The planes have equations $l_1 x + m_1 y + n_1 z - \lambda a = 0$, where l, m and n are direction cosines, λ is any integer and a is the perpendicular distance between two adjacent planes.

Two other sets of parallel planes can be defined similarly by $III_b(l_2 x + m_2 y + n_2 z)$ and $III_c(l_3 x + m_3 y + n_3 z)$ and the point array or lattice is defined by the product of these three functions.

The Fourier transform of one of these functions is simple:

$$\phi(p,q,r) = \int_{-\infty}^{\infty} \int_{-\infty}^{\infty} \int_{-\infty}^{\infty} \sum_{\lambda=-\infty}^{\infty} \delta(lx+my+nz-\lambda a)e^{2\pi i(px+qy+rz)}\, dx\, dy\, dz.$$

Do the x-integral first:

$$\phi(p,q,r) = \frac{1}{l} \sum_{\lambda=-\infty}^{\infty} \int_{-\infty}^{\infty} \int_{-\infty}^{\infty} e^{2\pi i p(\lambda a - nz - my)/l} e^{2\pi i(qy+rz)}\, dy\, dz,$$

where the λ-sum provides the III-function and the integral as before is merely the substitution of the value into the δ-function argument which makes it non-zero.

The integral is now separable:

$$\phi(p,q,r) = \frac{1}{l} \sum_{\lambda=-\infty}^{\infty} e^{2\pi i p a \lambda/l} \cdot \int_{-\infty}^{\infty} e^{-2\pi i \left(\frac{pn}{l}-r\right)z}\, dz \int_{-\infty}^{\infty} e^{-2\pi i \left(\frac{pm}{l}-q\right)y}\, dy$$

$$= \frac{1}{l} \sum_{\lambda=-\infty}^{\infty} e^{2\pi i p a \lambda/l} \cdot \frac{1}{n}\delta\left(\frac{p}{l}-\frac{r}{n}\right) \cdot \frac{1}{m}\delta\left(\frac{p}{l}-\frac{q}{m}\right).$$

The last two factors, the δ-functions, define two planes. The intersection of the planes defines a line. The sum over λ defines those points on the line where the lattice points exist in p, q, r-space.[10]

---

[10] By analogy with all the other entities to which the prefix 'Dirac' has been attached, the idea of a 'Dirac string' might be advanced to describe a spatial curve on which a three-dimensional function $f(x, y, z)$ is defined, on the understanding that it is zero everywhere except on that

Again, if the p, q, r-space is superimposed on the x, y, z-space, we find that $\phi(p, q, r)$ is a set of equispaced points along a line perpendicular to the set of planes defined by $\delta(lx + my + nz - \lambda a)$ and that the spacing between the points is $1/a$.

7.8 Lattices

A complete three-dimensional lattice, described by the product of three planar III-functions of the type $III_a(lx + my + nz)$ has as its Fourier transform the triple convolution of three lines of equispaced points. This gives a new lattice – the *reciprocal lattice*[11] in p, q, r-space, which is used in crystallography. Points on this reciprocal lattice define various planes in x, y, z-space, which contain two-dimensional arrays of lattice points. Lines from the origin to points on the reciprocal lattice define both the orientation and the separation of the corresponding planes in x, y, z-space.

This now clears up a fundamental problem in describing crystals. The three III-functions used to define the crystal lattice in x, y, z-space are not the only possible ones. Other sets of planes can be used – an infinite number of possibilities exists. The points in the reciprocal lattice define uniquely such sets of parallel planes. The lines ('vectors') from the origin to these points in p, q, r-space are normal to the lattice-planes in x, y, z-space and the length of each vector is inversely proportional to the separation of the planes in x, y, z-space. The coordinates of the lattice points in p, q, r-space, when multiplied by a factor to make them integer, are the *Miller indices*, beloved of crystallographers, of the x, y, z-planes.

---

curve. For example, $f(x, y, z)\delta(l_1x + m_1y + n_1z)\delta(l_2x + m_2y + n_2z)$ describes a function which is zero everywhere except on the line $x/(n_1m_2 - n_2m_1) = y/(l_1n_2 - l_2n_1) = z/(l_1n_2 - l_2n_1)$.

[11] *Vide* e.g. H. M. Rosenberg, *The Solid State*, 3rd edn, Oxford University Press, Oxford, 1988.

8

The formal complex Fourier transform

In physics we are usually concerned with functions of real variables, which are often experimental curves, data strings, or shapes and patterns. Generally the function is asymmetrical about the y-axis and so its Fourier transform is a complex function of a real variable; that is, for any value of p, a complex number is defined.

Any function obeying the Dirichlet conditions can be divided into a symmetrical and an antisymmetrical part. In Fig. 8.1, for example, and generally, $f_s(x) = \frac{1}{2}[f(x) + f(-x)]$ and $f_a(x) = \frac{1}{2}[f(x) - f(-x)]$. The symmetrical part is synthesized only from cosines and the antisymmetrical part only from sines. We write

$$f(x) = f_s(x) + f_a(x); \qquad f_s(x) \rightleftharpoons \phi_s(p); \qquad f_a(x) \rightleftharpoons \phi_a(p),$$

where $\phi_s(p)$, being made of cosines, is real and symmetrical and $\phi_a(p)$ is imaginary and, being made of sines, is antisymmetrical.

We can also define the following.

(a) The phase transform of $f(x)$, which is the function $\theta(p)$, where

$$\tan \theta(p) = \phi_a(p)/\phi_s(p).$$

(b) The power transform:

$$P(p) = |\phi(p)|^2 = \phi_a(p)^2 + \phi_s(p)^2.$$

(c) The modular transform:

$$M(p) = |\phi(p)| = \sqrt{\phi_a(p)^2 + \phi_s(p)^2}.$$

All these have their practical uses, although none of them has a unique inverse.
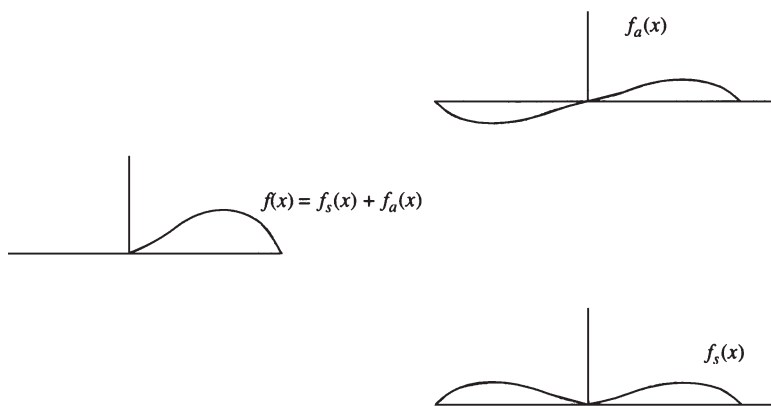
Fig. 8.1. Dividing a function into symmetrical and antisymmetrical parts.

A useful corollary of the convolution theorem is that if $C(x) = f_1(x) * f_2(x)$ and $C(x) \rightleftharpoons \Gamma(p)$ then the power transforms of C, f_1 and f_2, given by $|\Gamma|^2$, $|\phi_1|^2$ and $|\phi_2|^2$, are related by

$$|\Gamma|^2 = |\phi_1|^2 \cdot |\phi_2|^2.$$

A simple example shows the use of phase transforms. Consider for instance a displaced top-hat function (any function would do, in fact), of width a and displaced sideways by a distance b.

The function is

$$f(x) = \Pi_a(x) * \delta(x - b).$$

Its Fourier transform is

$$\phi(p) = a \operatorname{sinc}(\pi a p) \cdot e^{2\pi i b p}$$
$$= a \operatorname{sinc}(\pi a p)\big[\cos(2\pi b p) + i \sin(2\pi b p)\big]$$

and its phase transform is

$$\theta(p) = \tan^{-1}(\sin(2\pi p b)/\cos(2\pi p b))$$

so that $\theta(p) = 0$ when $p = 0$ and $\theta(p) = 2\pi$ when $p = 1/b$.

Phase transforms are useful when an experimentally measured function, which should have been symmetrical, has been displaced by an unknown amount from its axis of symmetry – for example by sampling it in the wrong places. A quick calculation of a few points on the phase transform will find the displacement and allow any adjustments to be made or the true, symmetrical samples to be computed by interpolation. It also confirms (or not!) that the

(a)
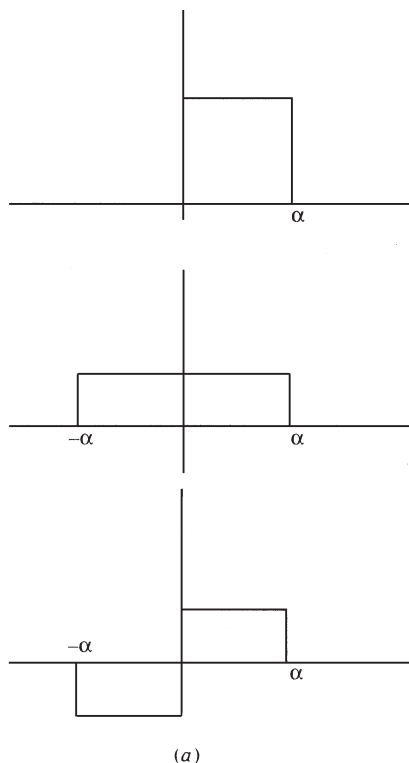
Fig. 8.2. A top-hat function displaced by half its own width. (a) The dissection of the top-hat into symmetrical and antisymmetrical parts.

function really is symmetrical, since only then is its phase transform a straight line.

It is worth including here something which will be useful later when considering computing Fourier transforms. Since it is easy to separate the real and imaginary parts of a complex function of x or p and then to divide these into their symmetrical and antisymmetrical parts, it is possible to combine two real functions of x into a complex function and then separate the combined complex Fourier transform into its constituent parts. This is a useful technique when computing digital Fourier transforms: one can do two transforms for the price of one.

Written analytically, let the two functions be $f_1(x)$ and $f_2(x)$ and separate each into its symmetrical and antisymmetrical parts:

$$f_1(x) = f_{1s}(x) + f_{1a}(x); \qquad f_2(x) = f_{2s}(x) + f_{2a}(x).$$
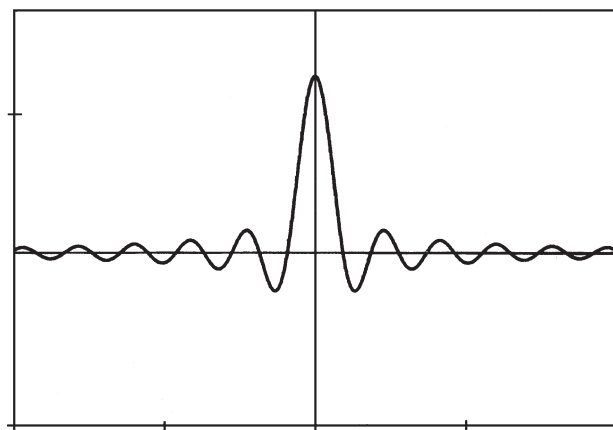
(*b*)
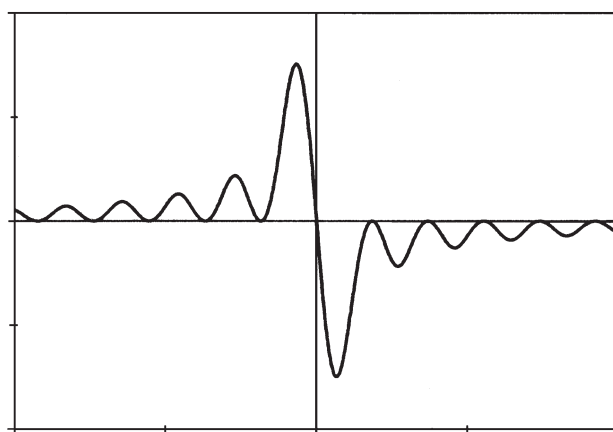
(*c*)

Fig. 8.2. (*cont.*) (b) The cosine transform. (c) The sine transform.

Let

$$F(x) = f_1(x) + if_2(x).$$

Let

$$F(x) \rightleftharpoons \Phi(p).$$

Then

$$\Phi(p) = \int_{-\infty}^{\infty} [f_1(x) + if_2(x)]e^{2\pi ipx}\, dx.$$
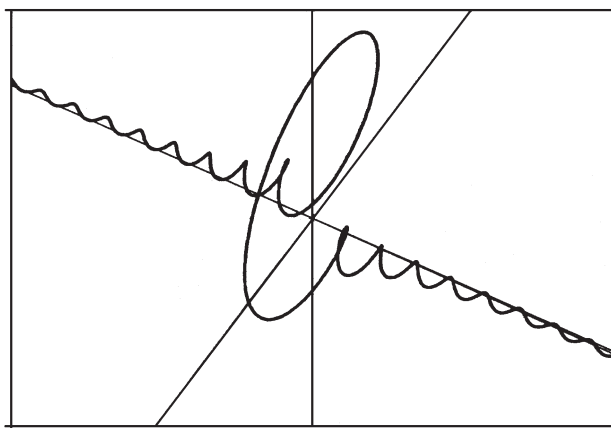
(*d*)
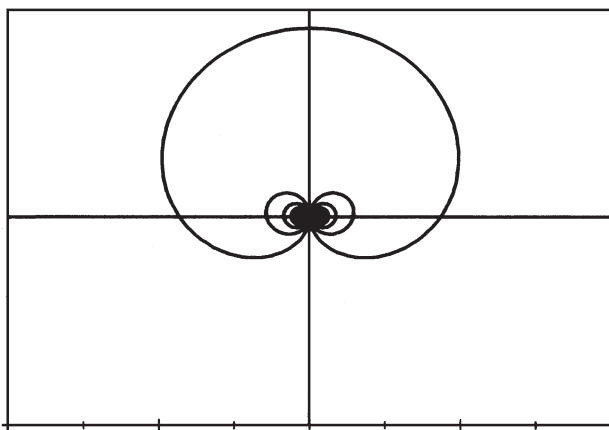
(*e*)

Fig. 8.2. (*cont.*) (d) The transform in perspective. (e) The Nyquist diagram – the view looking along the v-axis.

Remember that a symmetrical function has only a cosine transform, etc.,

$$\Phi(p) = \int f_{1s}(x)\cos(2\pi px)dx + i \int f_{1a}(x)\sin(2\pi px)dx$$
$$+ i \int f_{2s}(x)\cos(2\pi px)dx - \int f_{2a}(x)\sin(2\pi px)dx$$
$$= \phi_{1s}(p) + i\phi_{1a}(p) + i\phi_{2s}(p) - \phi_{2a}(p),$$

where the meaning of each suffix is the same as in the f-functions.

Then

$$\Phi(p) = [\phi_{1s}(p) - \phi_{2a}(p)] + i[\phi_{1a}(p) + \phi_{2s}(p)].$$

Both the real part and the imaginary part of $\Phi(p)$ now have symmetrical and antisymmetrical components. When $\Phi(p)$ has been computed, it has a real part, $\Phi_r(p)$, and an imaginary part, $\Phi_i(p)$.

The symmetrical real part is

$$\frac{1}{2}[\Phi_r(p) + \Phi_r(-p)] = \phi_{1s}(p)$$

and the antisymmetrical part is

$$\frac{1}{2}[\Phi_r(p) - \Phi_r(-p)] = -\phi_{2a}(p).$$

Similarly,

$$\frac{1}{2}[\Phi_i(p) - \Phi_i(-p)] = \phi_{1a}(p)$$

and

$$\frac{1}{2}[\Phi_i(p) + \Phi_i(-p)] = \phi_{2s}(p)$$

so that, finally,

$$f_1(x) \rightleftharpoons \frac{1}{2}[\Phi_r(p) + \Phi_r(-p)] + \left(\frac{i}{2}\right)[\Phi_i(p) - \Phi_i(-p)]$$

$$\rightleftharpoons \frac{1}{2}\phi_{1s}(p) + \left(\frac{i}{2}\right)\phi_{1a}(p)$$

and, similarly,

$$f_2(x) \rightleftharpoons \frac{1}{2}\phi_{2s}(p) + \left(\frac{i}{2}\right)\phi_{2a}(p).$$

In other words, the Fourier transform of $f_1(x)$ is $\frac{1}{2} \times$ (the symmetrical part of the real component of $\Phi(p)$ plus $i \times$ the antisymmetrical part of the imaginary component of $\Phi(p)$), and the Fourier transform of $f_2(x)$ is $\frac{1}{2} \times$ (the symmetrical part of the imaginary component plus $i \times$ the antisymmetrical part of the real component). The computer sorts these out without difficulty!

Notice that all the F's, Φ's, f's and ϕ's with suffixes are *real* quantities. This is because a computer deals ultimately in real numbers, although its program may include complex arithmetic. This level of complication is not commonly met when discussing analytic Fourier transforms. However, computing algorithms compute the complex transform whether you like it or not, and the

relations above can be used to do tricks in shortening computing time when you know that the data represent only real functions.

Diagrammatically, the process can be represented by

$$f_{1s}(x) \leftarrow \cos \rightarrow \phi_{1s}(p),$$
$$f_{1a} \leftarrow i \sin \rightarrow i\phi_{1a},$$
$$if_{2s} \leftarrow \cos \rightarrow i\phi_{2s},$$
$$if_{2a} \leftarrow i \sin \rightarrow -\phi_{2a}.$$

A function is said to be Hermitian if its real part is symmetrical and its imaginary part is antisymmetrical. So, if $f_1(x)$ is symmetrical and $f_2(x)$ is antisymmetrical, then $\phi_{1a} \equiv 0$ and $\phi_{2s} \equiv 0$. Then

$$\Phi(p) = \phi_{1s}(p) + \phi_{2a}(p)$$

and is real. Alternatively, the Fourier transform of a real but asymmetrical function is Hermitian:

$$f_1(x) \rightleftharpoons \phi_{1s}(p) + i\phi_{1a}(p).$$

9

Discrete and digital Fourier transforms

9.1 History

Fourier transformation is formally an analytic process which uses integral calculus. In experimental physics and engineering, however, the integrand may be a set of experimental data, and the integration is necessarily done artificially. Since a separate integration is needed to give each point of the transformed function, the process would become exceedingly tedious if it were to be attempted manually, and many ingenious devices have been invented for performing Fourier transforms mechanically, electrically, acoustically and optically. These are all now part of history since the arrival of the digital computer and more particularly since the discovery – or invention – of the 'fast Fourier transform' algorithm or FFT as it is generally called. Using this algorithm, the data are put ('read') into a file (or 'array', depending on the computer jargon in use), the transform is carried out, and the array then contains the points of the transformed function. It can be achieved by a software program, or by a purpose-built integrated circuit. It can be done very quickly so that vibration-sensitive instruments with Fourier transformers attached can be used for tuning pianos and motor engines, for aircraft and submarine detection and so on. It must not be forgotten that the ear is Nature's own Fourier transformer,[1] and, as used by an expert piano-tuner, for example, is probably the equal of any electronic simulator in the 20–20 000-Hz range. The diffraction grating, too, is a passive Fourier transformer device, provided that it is used as a spectrograph taking full advantage of the simultaneity of outputs.

The history of the FFT is complicated and has been researched by Brigham[2] and, as with many discoveries and inventions, it arrived before the (computer) world was ready for it. Its digital apotheosis came with the publication

---

[1] It detects the *power* transform, and is not sensitive to phase.
[2] E. O. Brigham, *The Fast Fourier Transform*, Prentice-Hall, Englewood Cliffs, NJ, 1974.

of the 'Cooley–Tukey' algorithm[3] in 1965. Since then other methods have been virtually abandoned except for certain specialized cases and this chapter is a description of the principles underlying the FFT and how to use it in practice.

9.2 The discrete Fourier transform

There is a pair of formulae by which sets of numbers $[a_n]$ and $[A_m]$, each set having N elements, can be mutually transformed:

$$A(m) = \frac{1}{N} \sum_0^{N-1} a(n)e^{2\pi i n m/N}; \qquad a(n) = \sum_0^{N-1} A(m)e^{-2\pi i n m/N}. \qquad (9.1)$$

In appearance and indeed in function, these are very similar to the formulae of the analytic Fourier transform and are generally known as a 'discrete Fourier transform' (DFT). They can be associated with the true Fourier transform by the following argument.

Suppose, as usual, that $f(x)$ and $\phi(p)$ are a Fourier pair. If $f(x)$ is multiplied by a III-function of period a then the Fourier transform becomes

$$\Phi(p) = \int_{-\infty}^{\infty} f(x)III_a(x)e^{2\pi i p x}\, dx = (1/a)[\phi(p) * III_{1/a}(p)].$$

Now suppose that $f(x)$ is negligibly small for all x outside the limits $-a/2 \rightarrow (N-1/2)a$, so that there are N teeth in the Dirac comb, and $f(x)$ extends over a range $\leq Na$. We rewrite the integral and use the properties of δ-functions so that

$$\Phi(p) = \int_{-\infty}^{\infty} \sum_{n=-\infty}^{\infty} f(x)e^{2\pi i p x}\delta(x - na)dx$$

$$= \sum_{n=-\infty}^{\infty} \int_{-\infty}^{\infty} f(x)e^{2\pi i p x}\delta(x - na)dx.$$

Because there are only N teeth in the comb, the sum is finite and the integral means substituting the argument of the δ-function as usual.

$$\Phi(p) = \sum_{n=0}^{N-1} f(na)e^{2\pi i p n a}$$

$$= (1/a)[\phi(p) * III_{1/a}(p)].$$

[3] J. W. Cooley & J. W. Tukey, 'An algorithm for the machine calculation of complex Fourier series', *Math. Computation* **19** (April 1965), 297–301.

This in turn is periodic in p with period $1/a$, and can be written

$$\Phi(p) = (1/a)\phi(p) * \text{Ш}_{1/a}(p)$$
$$= (1/a)[\phi(p) + \phi(p + 1/a) + \phi(p - 1/a)$$
$$+ \phi(p + 2/a) + \phi(p - 2/a) + \cdots],$$

and in its first period $\Phi(p)$ is the same as the analytic function $(1/a)\phi(p)$.

Now consider n small intervals of p, each of width $1/(Na)$. At the mth such interval the equation becomes

$$\Phi(m/(Na)) = \sum_{n=0}^{N-1} f(na)e^{2\pi i na(m/(Na))} = (1/a)\phi(m/(Na))$$

or, more succinctly,

$$\sum_{n=0}^{N-1} f(n)e^{2\pi i nm/N} = (1/a)\phi(m),$$

and this approximates to the analytic Fourier transform. The approximation is that in its first period the periodic $\Phi(p) = \phi(p)$. Theoretically it is not – there is bound to be some overlap since $\phi(p)$ is not zero – but practically the discrepancy can be ignored.[4]

The choice of the interval $-a/2 \rightarrow (N - 1/2)a$ for $f(x)$ is so as to have exactly N teeth in the Dirac comb without the embarrassment of having teeth at the very edge – where a top-hat function changes from 1 to 0, for example. In theory *any* interval of the same length would do.

9.3 The matrix form of the DFT

One way of looking at the formula for the discrete Fourier transform is to set it out as a matrix operation. The data set $[a(n)]$ can be written as a column matrix or 'vector' (in an N-dimensional space), to be multiplied by a square matrix containing all the exponentials and giving another column matrix with N components, $[A(m)]$, as its result:

$$
\begin{bmatrix}
A(0) \\
A(1) \\
A(2) \\
A(3) \\
\vdots \\
A(N-1)
\end{bmatrix}
=
\begin{bmatrix}
1 & 1 & 1 & \cdots & 1 \\
1 & e^{2\pi i/N} & e^{4\pi i/N} & \cdots & e^{2(N-1)\pi i/N} \\
1 & e^{4\pi i/N} & e^{8\pi i/N} & \cdots & e^{4(N-1)\pi i/N} \\
1 & e^{6\pi i/N} & e^{12\pi i/N} & \cdots & e^{6(N-1)\pi i/N} \\
\vdots & \vdots & \vdots & \vdots & \vdots \\
1 & \cdots & \cdots & \cdots & e^{(N-1)^2 2\pi i/N}
\end{bmatrix}
\begin{bmatrix}
a(0) \\
a(1) \\
a(2) \\
a(3) \\
\vdots \\
a(N-1)
\end{bmatrix}.
$$

---

[4] It is not possible for a function and its Fourier pair both to be finite in extent – one at least must extend to $\pm\infty$ – but the condition that both be small compared with the values in the region of interest is allowable.

The process of matrix multiplication requires n^2 multiplications for its completion. If large amounts of data are to be processed, this can become inordinate, even for a computer. Some people like to process columns of data with 10^6 numbers occasionally, but normally experimenters make do with 1024, although they often require the transform in a few microseconds.

The secret of the fast Fourier transform is that it reduces the number of multiplications to be done from N^2 to about $2N \log_2(N)$. A data 'vector' 10^6 numbers long then requires 4.2×10^7 multiplications instead of 10^{12}, a gain in speed by a factor of approximately 26 200. In this year of grace 2010, the computation time on a desktop computer is reduced from about 2 minutes to a few microseconds.

The way it does this is, in essence, to factorize the matrix of exponentials, but there are easier ways of looking at the process. For example, suppose that the number N of components in the vector is the product of two numbers k and l. Instead of writing the subscript of each number in the vector to denote its position $(0 \ldots N - 1)$, it can be given two subscripts s and t, and written $a(s, t)$, with $a(s, t) = a(sk + t)$, where s takes values from 0 to $(l - 1)$ and t runs from 0 to $(k - 1)$. In this way all the numbers in the vector are labelled, but now with two suffixes instead of one. There is absolutely no point in doing this except for computational purposes: it is purely a piece of computer-mathematical manipulation, and would have struck mathematicians of pre-computer days as ludicrous. However, we now write the digital transform as

$$A(u, v) = \sum_{s=0}^{l-1} \sum_{t=0}^{k-1} a(s, t) e^{2\pi i (sk+t)(ul+v)/kl},$$

where the suffix m in the transformed vector has similarly been dissected into u and v, with $m = ul + v$. The suffix u runs from 0 to $(k - 1)$ and v runs from 0 to $(l - 1)$.

The exponent is now multiplied out and gives

$$A(u, v) = \sum_{s=0}^{l-1} \sum_{t=0}^{k-1} a(s, t) e^{2\pi i su} e^{2\pi i sv/l} e^{2\pi i tu/k} e^{2\pi i vt/(kl)}.$$

The first exponential factor is unity and is discarded. The double sum can be rewritten now as

$$A(u, v) = \sum_{t=0}^{l-1} e^{2\pi i tu/k} e^{2\pi i vt/(kl)} \sum_{s=0}^{k-1} a(s, t) e^{2\pi i sv/l},$$

which is legitimate since only the last exponent contains a factor of s.

This sum over k terms gives a new set of numbers $[g(v, t)]$ and we write

$$A(u, v) = \sum_{t=0}^{l-1} [g(v, t)e^{2\pi i v t/(kl)}] e^{2\pi i t u/k}.$$

The array $[g(v, t)]$ is multiplied by $e^{2\pi i v t/(kl)}$ to give an array $[g'(v, t)]$ and finally the sum

$$g''(v, u) = \sum_{t=0}^{l-1} g'(v, t)e^{2\pi i t u/k}$$

and $g''(v, u) = A(u, v)$. (The reversing of the order of v and u is important.)

The transform has been split into two stages. There are k transforms, each of length l, followed by N multiplications by the exponential factors $e^{2\pi i v t/(kl)}$ (the 'twiddle-factors'), followed by l transforms, each of length k: a total of $kl^2 + lk^2 = N(k + l)$ multiplications, apart from the relatively small number, N, of multiplications (by $e^{2\pi i v t/(kl)}$) in the middle.

The lesson is that, provided N can be factorized, the vector $[a(n)]$ can be turned into a rectangular $k \times l$ matrix and treated column by column as a set of shorter transforms. For example, if there were a factor of 2, the even-numbered a's could be put into one vector of length $N/2$ and the odd-numbered a's into another. Then each is subjected to a Fourier transform of half the length to give two more vectors, and these, after multiplying by the 'twiddle-factors' as above, can be recombined into a vector of length N.

The same process can be repeated, provided that $N/2$ can be factorized; and if the factors are always 2, it continues until only 2×2 matrices are left, with trivially easy Fourier transforms (and a multiplicity of twiddle-factors!). The interesting thing is that each number in the transformed vector has its address in bit-reversed order. In the example given earlier the final outcome was $g''(v, u)$, so that the two indices have to be reversed – the number $g''(v, u)$ is in the wrong place in the array. This effect is multiplied until, in the 2^N transform, the transformed data appear in the wrong addresses, the true address being the bit-reversed order of the apparent address.

The fast Fourier transform is thus usually done with N a power of 2. This is not only very efficient in terms of computing time, but also ideally suited to the binary arithmetic of digital computers. The details of the way programs are written are given by Brigham[5] and a BASIC listing of an FFT routine is given at the end of this chapter. There are many such routines, the results of many hours of research, and sometimes they are very efficient. This one is not

---

[5] E. O. Brigham, *The Fast Fourier Transform*, Prentice-Hall, Englewood Cliffs, NJ, 1974.
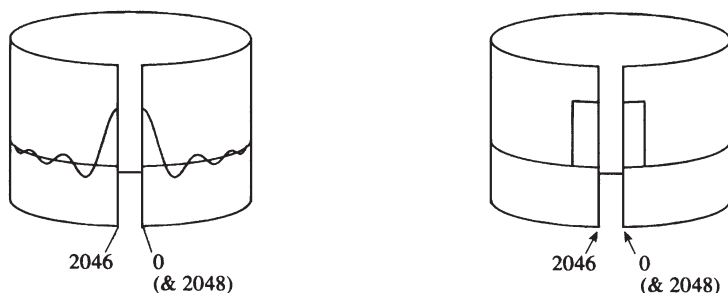
Fig. 9.1. The implementation of the FFT using a sinc-function as an example. The two cylinders, unwrapped, represent the input and output data arrays. Do not expect zero to be in the middle as in the analytic case of a Fourier transform. If the input data are symmetrical about the centre, these two halves must be exchanged (en-bloc, not mirror-imaged) before and after doing the FFT.

particularly fast but will suffice for practice and is certainly suitable for student laboratory work.

The data file for this program must be 2048 words long (1024 complex numbers, alternately real and imaginary parts), and, if only real data are to be transformed, they should go in the even-numbered elements of the array, from 0 to 2046. Some caution is needed: zero frequency is at array element 0. If you want to Fourier transform a sinc-function, for example, the positive part of the function should go at the beginning of the array and the negative part at the end. Figure 9.1 illustrates the point: the output will similarly contain the zero-frequency value in element 0, so that the top-hat appears to be split between the beginning and the end.

Alternatively, you can arrange to have zero frequency at point 1024 in the array, in which case the input and output arrays must both be transposed, by having the first and second halves interchanged (but not flipped over) before and after the FFT is done.

Attention to these details saves a lot of confusion! It helps to think of the array as wrapped around a cylinder, with the beginning of the array at zero frequency and the end at point (-1) instead of $(+1023)$.

9.3.1 Two-dimensional FFTs

Two-dimensional transforms can be done using the same routines. The data are in a rectangular array of 'pixels' which form the picture which is to be transformed. Each row should first have its right and left halves transposed. Then each column must have the top and bottom halves transposed, so that what was perhaps a circle in the middle of the picture becomes four quadrants, one in

each corner. Then each row is given the FFT treatment. Then each column in the resulting array gets the same. Then the rows and finally the columns are transposed again to give the complete FFT. At this stage periodic features, such as a TV raster, for example, will appear as Dirac nails (provided that the original picture has been sampled often enough) and can be suppressed by altering the contents of the pixels where they appear. Then the whole procedure is reversed to give the whole 'clean' picture.

Apodizing functions can similarly be applied to remove false information, to smooth edges and to improve the picture cosmetically.

Obviously far more elaborate techniques than this have been developed, but this is the basis of the whole process.

The output can be used in a straightforward way to give the power, phase or modular transforms, and the data can be presented graphically with simple routines which need no description here.

9.4 A BASIC FFT routine

FFT routines can be routinely downloaded from the Web, so that observational or experimental data can be loaded into them, the handle pulled and, like magic, out comes the Fourier transform. However, there are many people who like to enter the computational fray at a more fundamental level, to load their own FFT routine into a BASIC, FORTRAN or C++ program and experiment with it. Translation of the instructions between one and another is relatively simple and so I have resisted the urging of colleagues to delete the BASIC routine which was given in previous editions.

9.4.1 A routine for 1024 complex numbers

The listing below is of a simple BASIC routine for the fast Fourier transform of 1024 complex numbers.[6] This is a routine which can be incorporated into a program which you can write for yourself.

The data to be transformed are put in an array D(I) declared at the beginning of the program as 'DIM D(2047)'. The reals go in the even-numbered places, beginning at 0, and the imaginaries in the odd-numbered places. The transformed data are found similarly in the same array. The variable G on line 131 should be set to 1 for a direct transform and to -1 for an inverse transform. Numbers to be entered into the D(I) array should be in ASCII format. The

---

[6] But N can be changed by changing the first line of the program.

program should fill the D(I) array with data; call the FFT as a routine with a 'GOSUB 100' statement (the 'RETURN' is the last statement, on line 10), and this can be followed by instructions for displaying the data.

It is well worth your while to incorporate a routine for transposing the two halves of the D(I) array before and after doing the transform, as an aid to understanding what is happening.

```
100   N=2048              REM for 1024 complex points
      PRINT "BEGIN FFT"       transform.
      J=1
      G=1                 REM for direct transform. G=-1
      FOR I=1 TO N STEP 2   for inverse.
      IF (I-J)<0 GOTO 1
      IF I=J GOTO 2
      IF (I-J)>0 GOTO 2
1     T=D(J-1)
      S=D(J)
      D(J-1)=D(I-1)
      D(J)=D(I)
      D(I-1)=T
      D(I)=S
2     M=N/2
3     IF (J-M)<0 GOTO 5
      IF J=M GOTO 5
      IF (J-M)>0 GOTO 4
4     J=J-M
      M=M/2
      IF (M-2)<0 GOTO 5
      IF M=2 GOTO 3
      IF(M-2)>0 GOTO 3
5     J=J+M
      NEXT I
      X=2
      IF (X-N)<0 GOTO 7
6     IF X=N GOTO 8
      IF (X-N)>0 GOTO 8
7     F=2*X
      H=6.28319/(G*X)
      R=SIN(H/2)
      W=−2*R*R
```

```
      V=SIN(H)
      P=1
      Q=0
      FOR M=1 TO X STEP 2
      FOR I=M TO N STEP F
      J=I+X
      T=P*D(J-1)-Q*D(J)
      S=P*D(J)+Q*D(J-1)
      D(J-1)=D(I-1)-T
      D(J)=D(I)-S
      D(I-1)=D(I-1)+T
      D(I)=D(I)+S
      NEXT I
      T=P
      P=P*W-Q*V+P
      Q=Q*W+T*V+Q
      NEXT M
      X=F
      GOTO 6
8     CLS
      FOR I=0 TO N-1
      D(I)=D(I)/(SQR(N/2))
      NEXT I
      PRINT "FFT DONE"
10    RETURN
```

Next, here is a short program to generate a file with .DAT extension which will contain a top-hat function of any width you choose. The data are generated in ASCII and can be used directly with the FFT program above.

```
      REM Program to generate a "Top-hat" function.
      INPUT "input desired file name", A$
      INPUT 'Top-hat Half-width ?', N
      PI=3.141 592 654
      DIM B(2047)
      FOR I=1024-N TO 1024+N STEP 2
      B(I)=1/(2*N)
      NEXT I
      C$=".DAT"
      C$=A$+C$
      PRINT
```

```
OPEN C$ FOR OUTPUT AS #1
FOR I=0 TO 2047
PRINT #1,B(I)
NEXT I
CLOSE #1
```

The simple file-generating arithmetic in lines 6–8 can obviously be replaced by something else, and this sort of 'experiment' is of great help in understanding the FFT process.

The file thus generated can be read into the FFT program with the following:

```
    REM Subroutine FILELOAD
    REM To open a file and load contents into D(I)
    GOSUB 24
    (insert the next stage of the program, e.g. 'GOSUB 100', here)
    CLS:LOCATE 10,26,0
    PRINT "NAME OF DATA FILE ?"
    LOCATE 14,26,0
    INPUT A$
    ON ERROR GOTO 35
    OPEN "I",#1,A$
    FOR I=0 TO 2047
    ON ERROR GOTO 35
    INPUT #1,D(I)
    NEXT I
    CLOSE
35  RETURN
```

Appendix

A.1 Parseval's theorem and Rayleigh's theorem

Parseval's theorem states that

$$\int_{-\infty}^{\infty} f(x)g^*(x)dx = \int_{-\infty}^{\infty} F(p)G^*(p)dp.$$

This proof relies on the fact that if

$$g(x) = \int_{-\infty}^{\infty} G(p)e^{2\pi ipx}\, dp$$

then

$$g^*(x) = \int_{-\infty}^{\infty} G^*(p)e^{-2\pi ipx}\, dp$$

(simply by taking complex conjugates of everything).

Then it follows that

$$G^*(p) = \int_{-\infty}^{\infty} g^*(x)e^{2\pi ipx}\, dx.$$

The *argument* of the integral on the left-hand side of the theorem can now be written as

$$f(x)g^*(x) = \int_{-\infty}^{\infty} F(q)e^{2\pi iqx}\, dq \int_{-\infty}^{\infty} G^*(p)e^{-2\pi ipx}\, dp.$$

We integrate both sides with respect to x. If we choose the order of integration carefully, we find

$$\int_{-\infty}^{\infty} f(x)g^*(x)dx = \int_{-\infty}^{\infty} \left\{ \int_{-\infty}^{\infty} F(q) \left[\int_{-\infty}^{\infty} G^*(p)e^{-2\pi ipx}\, dp \right] e^{2\pi iqx}\, dq \right\} dx$$

and, on changing the order of integration,

$$= \int_{-\infty}^{\infty} \left\{ F(q) \int_{-\infty}^{\infty} g^*(x) e^{2\pi i q x} \, dx \right\} dq$$

$$= \int_{-\infty}^{\infty} F(q) G^*(q) dq.$$

The theorem is often seen in a simplified form, with $g(x) = f(x)$ and $G(p) = F(p)$. Then it is written

$$\int_{-\infty}^{\infty} |f(x)|^2 \, dx = \int_{-\infty}^{\infty} |F(p)|^2 \, dp.$$

This is **Rayleigh's theorem**.

Another version of Parseval's theorem involves the coefficients of a Fourier *series*. In words, it states that the average value of the square of $F(t)$ over one period is the sum of the squares of all the coefficients of the series.

The proof, using the half-range series, is simple:

$$F(t) = \frac{A_0}{2} + \sum_0^{\infty} A_n \cos\left(\frac{2\pi n t}{T}\right) + B_n \sin\left(\frac{2\pi n t}{T}\right)$$

and, since all cross-products vanish on integration and

$$\int_0^T \cos^2(2\pi n t) dt = \int_0^T \sin^2(2\pi n t) dt = \frac{1}{2},$$

we have

$$\int_0^T [F(t)]^2 \, dt = T \left[\frac{A_0^2}{4} + \sum_1^{\infty} \frac{A_n^2 + B_n^2}{2} \right].$$

A.2 Useful formulae from Bessel-function theory

The Jacobi expansion

$$e^{ix \cos y} = J_0(x) + 2 \sum_{n=1}^{\infty} i^n J_n(x) \cos(ny),$$

$$e^{ix \sin y} = \sum_{z=-\infty}^{\infty} J_z(x) e^{izy}.$$

The integral expansion

$$J_0(2\pi\rho r) = \frac{1}{2\pi} \int_0^{2\pi} e^{2\pi i \rho r \cos\theta} \, d\theta,$$

which is a particular case of the general formula

$$J_n(x) = \frac{i^{-n}}{2\pi} \int_0^{2\pi} e^{in\theta} e^{ix\cos\theta} \, d\theta,$$

$$\frac{d}{dx}\left(x^{n+1} J_{n+1}(x)\right) = x^{n+1} J_n(x).$$

The Hankel transform

This is similar to a Fourier transform, but with polar coordinates, r, θ. The Bessel functions form a set with orthogonality properties similar to those of the trigonometrical functions and there are similar inversion formulae. These are

$$F(x) = \int_0^\infty p f(p) J_n(px) dp,$$

$$f(p) = \int_0^\infty x F(x) J_n(px) dx,$$

where J_n is a Bessel function of any order.

Bessel functions are analogous in many ways to the trigonometrical functions sine and cosine. In the same way as sine and cosine are the solutions of the SHM equation $d^2 y/dx^2 + k^2 y = 0$, they are the solutions of *Bessel's equation*, which is

$$x^2 \frac{d^2 y}{dx^2} + x\frac{dy}{dx} + (x^2 - n^2)y = 0.$$

In its full glory, n need not be an integer and neither x nor n need be real. The functions are tabulated in various books[1] for real x and for integer and half-integer n, and can be calculated numerically, as are sines and cosines, by computer.

In its simpler form, as shown, the Hankel transform occurs with θ as variable when Laplace's equation is solved in cylindrical polar coordinates and variables are separated to give functions $R(r)\Theta(\theta)\Phi(\phi)$, and this is why it proves useful in Fourier transforms with circular symmetry.

---

[1] For example, in Jahnke & Emde (see the bibliography).

A.3 Conversion of Fourier-series coefficients into complex exponential form

We use de Moivre's theorem to do the conversion. Write $2\pi \nu_0 t$ as θ. Then, expressed as a half-range series, $F(t)$ becomes

$$F(t) = A_0/2 + \sum_{m=1}^{\infty} A_m \cos(m\theta) + B_m \sin(m\theta).$$

This can also be written as a full-range series:

$$F(t) = \sum_{m=-\infty}^{\infty} a_m \cos(m\theta) + b_m \sin(m\theta),$$

where $A_m = a_m + a_{-m}$ and $B_m = b_m - b_{-m}$.

Then, by virtue of de Moivre's theorem, the full-range series becomes

$$F(t) = \sum_{m=-\infty}^{\infty} \frac{a_m}{2}(e^{im\theta} + e^{-im\theta}) + \frac{b_m}{2i}(e^{im\theta} - e^{-im\theta})$$

$$= \sum_{m=-\infty}^{\infty} \frac{a_m - ib_m}{2} e^{im\theta} + \sum_{m=-\infty}^{\infty} \frac{a_m + ib_m}{2} e^{-im\theta}.$$

The two sums are independent and m is a dummy suffix, which means that it can be replaced by any other suffix not already in use. Here, we replace $m = -m$ in the second sum. Then

$$F(t) = \sum_{m=-\infty}^{\infty} \frac{a_m - ib_m}{2} e^{im\theta} + \sum_{m=-\infty}^{\infty} \frac{a_{-m} + ib_{-m}}{2} e^{im\theta}$$

$$= \sum_{m=-\infty}^{\infty} e^{im\theta} \left\{ \frac{A_m - iB_m}{2} \right\}$$

$$= \sum_{m=-\infty}^{\infty} e^{im\theta} C_m$$

and $C_{-m} = C_m^*$.

Bibliography

The most popular books on the practical applications of Fourier theory are undoubtedly those of Champeney and Bracewell, and they cover the present ground more thoroughly and in much more detail than here. E. Oran Brigham, on the fast Fourier transform (FFT), is the classic work on the subjects dealt with in Chapter 9.

Of the more theoretical works, the 'bible' is Titchmarsh, but a more readable (and entertaining) work is Körner's. Whittaker's (not to be confused with the more prolific E. T. Whittaker) is a specialized work on interpolation, but that is a subject which is getting more and more important, especially in computer graphics.

Many writers on quantum mechanics, atomic physics and electronic engineering like to include an early chapter on Fourier theory. One or two (who shall be nameless) get it wrong! They confuse ω with ν or leave out a 2π when there should be one, or something like that. The specialist books, like those below, are much to be preferred.

Abramowitz, M. & Stegun, I. A. *Handbook of Mathematical Functions*. Dover, New York. 1965
  A more up-to-date version of Jahnke & Emde, below.
Bracewell, R. N. *The Fourier Transform and its Applications*. McGraw–Hill, New York. 1965
  This is one of the two most popular books on the subject. Similar in scope to this book, but more thorough and comprehensive.
Brigham, E. O. *The Fast Fourier Transform*. Prentice Hall, New York. 1974
  The standard work on digital Fourier transforms and their implementation by various kinds of FFT program.
Champeney, D. C. *Fourier Transforms and Their Physical Applications*. Academic Press, London & New York. 1973
  Like Bracewell, one of the two most popular books on practical Fourier transforming. Covers similar ground, but with some differences in detail.

Champeney, D. C. *A Handbook of Fourier Theorems*. Cambridge University Press, Cambridge. 1987

Herman, G. T. *Image Reconstruction from Projections*. Academic Press, London & New York. 1980
   Includes details of Fourier methods (among others) for computerized tomography, including theory and applications.

Jahnke, E. & Emde, F. *Tables of Functions with Formulae and Curves*. Dover, New York. 1943
   The classic work on the functions of mathematical physics, with diagrams, charts and tables of Bessel functions, Legendre polynomials, spherical harmonics etc.

Körner, T. W. *Fourier Analysis*. Cambridge University Press, Cambridge. 1988
   One of the more thorough and entertaining works on analytic Fourier theory, but plenty of physical applications: expensive, but firmly recommended for serious students.

Titchmarsh, E. C. *An Introduction to the Theory of Fourier Integrals*. Clarendon Press, Oxford. 1962
   The theorists' standard work on Fourier theory. Unnecessarily difficult for ordinary mortals, but needs consulting occasionally.

Watson, G. N. *A Treatise of the Theory of Bessel Functions*. Cambridge University Press, Cambridge. 1962
   Another great theoretical classic: chiefly for consultation by people who have equations they can't solve, and which seem likely to involve Bessel functions.

Whittaker, J. M. *Interpolary Function Theory*. Cambridge University Press, Cambridge. 1935
   A slim volume dealing with (among other things) the sampling theorem and problems of interpolating points between samples of band-limited curves.

Wolf, E. *Introduction to the Theory of Coherence and Polarization of Light*. Cambridge University Press, Cambridge. 2007
   Gives more detail about material in Chapter 3, especially regarding coherence and the van Cittert–Zernike theorem.

Index

f refers to footnote.